

12-2013

The Role of Histone H3 and H4 in Centromere Function and Genome Integrity

Payel Chaudhuri

University of Arkansas, Fayetteville

Follow this and additional works at: <http://scholarworks.uark.edu/etd>



Part of the [Genetics Commons](#), and the [Molecular Biology Commons](#)

Recommended Citation

Chaudhuri, Payel, "The Role of Histone H3 and H4 in Centromere Function and Genome Integrity" (2013). *Theses and Dissertations*. 979.

<http://scholarworks.uark.edu/etd/979>

This Dissertation is brought to you for free and open access by ScholarWorks@UARK. It has been accepted for inclusion in Theses and Dissertations by an authorized administrator of ScholarWorks@UARK. For more information, please contact scholar@uark.edu, ccmiddle@uark.edu.

The Role of Histone H3 and H4 in Centromere Function
and Genome Integrity

The Role of Histone H3 and H4 in Centromere Function
and Genome Integrity

A dissertation submitted in partial fulfillment
of the requirements for the degree of
Doctor of Philosophy in Cell and Molecular Biology

by

Payel Chaudhuri
Bangalore University
Bachelor of Science in Biotechnology, 2004
Bangalore University
Master of Science in Biotechnology, 2006

December 2013
University of Arkansas

This dissertation is approved for recommendation to the Graduate Council.

Dr. Inés Pinto
Dissertation Director

Dr. Gisela F. Erf
Committee Member

Dr. Ralph Henry
Committee Member

Dr. Michael Lehmann
Committee Member

ABSTRACT

Histone H2A plays an important role in chromosomal segregation among parent and daughter cells during mitosis. While it is established that this histone is important in maintaining chromosome number in cell, further work is carried out to explore the role of other histones like H3 and H4 for similar effects. A systematic study is initiated by screening a library based on mutation of different amino acid residues in these histones. This detailed screening identified specific regions within H3 and H4, which are critically important for centromeric function. These histones residing near the DNA entry/exit region of nucleosome effects the functionality of cell cycle protein, Sgo1, which in turn helps maintaining error free cell cycle by sensing proper tension among sister chromatids during anaphase of mitosis. This work shows that a mutation in H3 and H4 at the DNA entry/exit region moderately effects the nucleosome structure and reduces the centromeric and pericentromeric localization of Sgo1.

ACKNOWLEDGEMENTS

I would like to thank Dr. Inés Pinto for her support, mentorship and patience. I am very lucky to have her as my advisor. She always encouraged me in times when I needed the most and given me the opportunity to work independently. I would like to thank Dr. David McNabb for his constructive criticism and thoughtful suggestions. I am also thankful to Ms. Marsha Rhoades for teaching me the lab techniques. I am grateful to all my lab members for making my research experience in this lab a memorable one.

DEDICATION

This dissertation is dedicated to my father and mother, Mr. S. S. Chaudhuri and Mrs. Debjani Chaudhuri and my husband Champak Das for their personal sacrifices and constant encouragement to achieve my goals. I also like to mention my daughter, Elina Das for her support, love and care.

TABLE OF CONTENTS

I. INTRODUCTION	1
II. LITERATURE REVIEW.....	3
A. <i>Saccharomyces cerevisiae</i> as a model genetics.....	4
B. Histone and its modification.....	4
C. Histone code and crosstalk among histone modifications.....	11
D. Distinct chromatin structure of the centromere.....	12
E. Cell cycle and chromosome segregation.....	13
III. METHODS.....	17
A. Yeast strains, genetic methods and media.....	18
B. Bacterial strains and plasmids.....	19
C. Mutant H3 and H4 library screening.....	20
D. Time point study of mutants.....	21
E. Canavanine assay of ploidy.....	21
F. Microscopy.....	22
G. Flow cytometry.....	22
H. <i>PDS1</i> stability assay.....	23
I. Chromatin Immunoprecipitation assay.....	23
J. Viability assay.....	24

IV. RESULTS.....	36
A. Strain construction and library screening.....	37
B. Characterization of the H3 and H4 mutants.....	39
C. Interaction of histone H3 and H4 mutants with Sgo1.....	42
D. Interaction of histone H3 and H4 mutants with Ipl1 and Bub1kinases.....	44
V. DISCUSSIONS.....	93
A. H3 and H4 mutants define regions of the nucleosome susceptible to chromosome segregation defects.....	94
B. Specific H3 and H4 mutations cause chromosome segregation defects.....	96
C. Sgo1 plays an important role in the DNA entry/exit point of the nucleosome.....	98
D. The H3 and H4 mutants alter the structure of histone H2A in the nucleosome....	99
E. H3 and H4 mutant effects on the nucleosome structure.....	100
F. Proposed model of the centromeric and pericentromeric structure in the histone H3 and H4 mutants.....	102
VI. REFERENCES.....	105

I. INTRODUCTION

The quest to understand the ability of cells for sustaining their normal function, to thrive and propagate leads us to genetics. It is important to understand the way genes control the cell to perform its normal cellular functions, and how these functions lead to the faithful transmission of chromosomes from mother to daughter cells. Mutations that affect the regulation of gene expression or protein function can result in detrimental effects on the genome integrity. To execute this task, it is useful to start with a simple system that provides us with the principles that govern the same process in more complex and difficult to study organisms. For this purpose, I am using the unicellular eukaryote *Saccharomyces cerevisiae*, commonly known as the budding yeast, as the model organism to understand the role of histones in the normal propagation of cells.

Histone proteins are important not only for packaging chromosomes, but also for distributing equal amount of chromosomes into the developing daughter cells. Past work from our laboratory has shown the importance of histone H2A in chromosome segregation [1]. The objective of the research presented here is to establish the role of histones H3 and H4 in this essential cellular process. A thorough protein-structure analysis was undertaken, with the goal of understanding the contribution of each amino acid residue of histones H3 and H4 to the process of chromosome segregation. This was carried out using substitution and deletion mutations present in a synthetic histone H3 and H4 library. The results not only revealed specific regions within histones H3 and H4 that are very important for maintaining chromosome number, but also the role played by other non-histone proteins to ensure equal segregation of chromosomes during cell division. Altogether, the outcome of this work has provided new and insightful information regarding the basic mechanism that histones, along with other proteins, play in securing the integrity of the genome during each round of chromosome replication and cell division.

II. LITERATURE REVIEW

***Saccharomyces cerevisiae* as a model eukaryote**

The budding yeast, *Saccharomyces cerevisiae*, is a useful unicellular eukaryote, widely being used as a model genetic system to understand conserved processes in higher eukaryotes, including humans. It is the first eukaryote whose genome has been completely sequenced, and has many genes that share functional conservation throughout metazoans [2]. *Saccharomyces cerevisiae* can be maintained both in haploid and diploid state, making it an ideal system to study recessive genes and gene complementation [3]. The haploid yeast has 16 chromosomes that are very well characterized. The high degree of homologous recombination makes the manipulation of its genes very easy and amenable for research. In addition, it has a short generation time of less than two hours (ideal growth conditions) making it a practical experimental organism. This class of fungi is non-pathogenic in nature, and therefore is appropriate for performing genetic studies in the laboratory [3, 4]. The basic mechanism of the cell cycle, where a cell grows and divides into two daughter cells, is well conserved among all eukaryotes. Any insults to the well-controlled cell cycle can lead to many life threatening diseases, like cancer and tumorigenesis [5]. *S. cerevisiae* has served as a very useful model system to understand cell cycle regulation in all eukaryotes, which in turn will help in understanding the abnormalities of the cell-cycle that affect human health [6].

Histones and its modifications

In the eukaryotic cell nucleus, the negatively charged DNA is organized by a group of small alkaline proteins called histones. They are arranged into a very compact structure called chromatin, which in turn consists of a set of a repetitive basic unit, the nucleosome. Based on crystallographic studies, the high-resolution structure of the nucleosome (2.8 Å) was first

reported by Luger *et al.* in 1996 [7]. Each nucleosome is made up of two copies of four histone proteins (H3, H4, H2A and H2B) and wrapped by 147 bp of DNA. These core proteins have a common histone fold structural motif of the following configuration: helix1-loop1-helix2-loop2-helix3. These folds are important for interaction among the histones within a nucleosome and also between the histones and DNA. The highly basic N-terminal tails of the histones protrude out of the nucleosomes [8]. The nucleosome consists of a histone octamer where two copies of H3 and H4 form a tetramer in the center surrounded by two H2A-H2B dimers [9, 10]. Another histone, H1, is reported to be present in between nucleosomes near the entry/exit point of the DNA [11]. In budding yeast histone H1 is present only after thirty seven nucleosomes [12]. This systematic level of packaging helps the chromatin achieve its highest level of compaction in its three dimensional structure; the chromosome [13]. The amino terminal tails of histones are very flexible and are subjected to various covalent post-translational modifications, such as acetylation, methylation, phosphorylation, ADP ribosylation, ubiquitylation and sumoylation [14]. These modifications are not restricted to histone tails but are also seen in the globular domain of the histone proteins. They play a major role in maintaining the chromatin structure, thereby regulating all chromosomal functions, including transcription, DNA replication, and chromosome segregation. The details of the histone modifications are discussed in the following sections.

Acetylation

This is the most well studied histone modification to date. Histone Acetyltransferases (HAT) and Histone Deacetylases (HDAC) are the enzymes that respectively add and remove acetyl groups from particular lysine residues in histones. Acetylation neutralizes the positive

charge on these residues making them less associated to the negatively charged DNA. Hypoacetylation is particularly seen in heterochromatic regions of chromosomes (chromatin structure that remains condensed throughout the major part of the cell cycle and remains transcriptionally silent), whereas hyper-acetylation is associated with euchromatin (chromatin structure that remains de-condensed throughout the major part of the cell cycle and transcriptionally active). This is particularly evident in the case of the inactive X chromosome in humans females (Barr body), where H4K5, H4K8, H4K12, H4K16 are not acetylated [15]. The open chromatin structure associated with hyper acetylation allows various regulatory proteins to access the DNA. Moreover, acetylation of H4K5, H4K12 and H3K56 are an important marker for newly synthesized histones in the cytoplasm, which later get incorporated into the replicating DNA at the S phase of the cell cycle during nucleosome assembly [16]. The acetylation of H4 tail residues is important in determining the level of compaction that a chromatin can undergo. Although acetylation of H4K16 is a euchromatin mark, it also serves as a recognition motif for the Sir proteins that lead to formation of heterochromatin both at telomeres and the silent mating type loci in yeast [17].

Histone Deacetylases, on the other hand, are important for a compact chromatin structure and cell cycle progression [18]. In *Saccharomyces cerevisiae*, histone H2A mutants with defects in chromosome segregation have shown to be genetically suppressed by a deletion of HDAC [19]. Currently, inhibitors of HDAC have become major targets of research for the treatment of abnormal cell proliferation in tumor and cancer cell [20-22].

Phosphorylation

Phosphorylation of serine and threonine residues add an additional negative charge to the histones. This leads to an open chromatin structure, which is linked to transcriptional activation [23]. H3S10 and H3S28 are the most studied phosphorylation modification sites. These two sites are reported to positively regulate chromatin condensation and mitosis [24]. In *Tetrahymena*, a ciliated protozoan, phosphorylated H3S10 (S10p) has been reported to be essential for error free chromosome segregation [25]. H3S10 is phosphorylated by Aurora kinase (humans)/Ipl1 (yeast) which is an important cell cycle checkpoint protein. H3S10p is also important in modulating the association of the heterochromatin protein HP1 and methylated H3K9 (K9me) during mitosis. Phosphorylation of the adjacent H3S10 is required to displace HP1 from H3K9me in the metaphase stage of mitosis [26]. In humans, H3T3 phosphorylation by Haspin kinase is important for recruiting survivin, another checkpoint protein and a member of the chromosomal passenger complex (discussed later), to the centromere [27]. This in turn concentrates the level of Ipl1 in the centromere. Another histone kinase, Bub1, it has recently been reported to phosphorylate H2A S121 in fission yeast. This serves as a positive signal to recruit Shugoshin (a protein which senses lack of tension among sister chromatids) to the centromeres, which is important for proper chromosome segregation [28]. The level of H3 phosphorylation is balanced by the kinase/phosphatase activity of Ipl1 and Gcl7 in *Saccharomyces cerevisiae*, which is important for proper mitosis [29, 30]. Loss of phosphorylation of H3T3, H3S10, H3T11, and H3S28 by PPI (Protein Phosphate-1) marks the exit from mitosis [31].

Methylation

Histone methylation is well characterized, particularly because of the substrate specificities of the histone methyl transferase (HMT). Lysine residues of histone H3 and H4 are mono/di/tri methylated whereas the arginine residues only accept one or two methyl groups. The addition of a methyl group to specific lysine and arginine does not interfere with the charge of the histone, but it certainly increases overall 'hydrophobicity and basicity' of the histone, making it more tightly associated with DNA [32]. H3K9me is an important marker of silent chromatin [33]. It is absent in budding yeast but is present in fission yeast and higher eukaryotes like drosophila, mice and humans [34]. Both H3K9me³ and H4K20me are important for maintaining successful chromosome segregation and integrity of centromeric chromatin structure and function in human cells [35]. H3K9me³ acts as a recognition motif for the binding of heterochromatin protein HP1 [33]. H4K20me on the other hand inhibits H4K16ac, a marker for active chromatin [36]. Methylation of H3K4, H3K36 and H3K79 is usually associated with active transcription. In budding yeast, Set1 and Set2 methylate H3K4 and K36 respectively, and associate with RNA polymerase II, emphasizing their role in transcription initiation and elongation [36, 37]. Different levels of methylation serve as recognition sites for different proteins and for different cell functions. This is evident in the case of H4K20me and H4K20me², which are recognized by DNA repair proteins when there is DNA damage. In contrast, H4K20me³ is not recognized by these repair factors [38].

For many years, no demethylase was reported, implying irreversible methylation. Recent studies have reported the presence of LSD1 (Lysine specific demethylase or KDM1A) that erases the mono and di methyl mark on H3K4 but not the tri methyl mark. However, this demethylase is not seen in budding yeast. Another group of demethylases containing the

Jumonji domain (JmjC proteins) has recently been discovered, and these enzymes are able to remove the tri-methyl lysine marker. This particular family of demethylases is found in most organisms ranging from bacteria to humans [39-42]. The levels of methylation in particular histone residues are important to be maintained by methylase and demethylase activities, as deviation from normal levels are usually seen in different cancer cells [43]. Methylases and demethylase are currently being tested as new targets to treat cancer cells [44].

Ubiquitination

Ubiquitination has usually been associated with protein degradation. However, in 1975, histone mono ubiquitination on H2A K119 was first reported in higher eukaryotes (absent in budding yeast) [45], but little was known about the role of this histone modification. Later, histone H2B was observed to have a site for this modification in K120 in mammals and K123 in budding yeast. Unlike other covalent histone modifications, ubiquitin is a large protein of 76 amino acids. This bulky modification can certainly impact the nucleosome structure and chromatin conformation. The requirement of Rad6/Ubc2 ubiquitin conjugating enzyme for H2B 123Ub has linked this modification to transcription [9]. It is known that H2B K123Ub positively affects H3K4 methylation by Set1, and negatively affects H3K36 methylation by Set2 [45]. H2B K123Ub is also important for methylation of Dam1, a kinetochore protein, by Set1. Loss of H2A K119Ub affects H2A S120p by Aurora/Ipl-1 kinase, a cell cycle regulating protein [31]. These two instances show the effectiveness of ubiquitination in the control of cell cycle and proper chromosome segregation.

Ubiquitination, like other histone modifications, is reversible. Ubp8, a deubiquitinating enzyme in yeast, erases H2B 123Ub. Ubp8 is a component of the SAGA acetyltransferase

complex, a chromatin-remodeling complex well known for its regulatory effects on transcription [46, 47]. This example emphasizes the cross regulation of acetylation and ubiquitination.

Other Histone Modifications

Sumoylation, ADP ribosylation, proline isomerization and crotonylation, are modifications less explored and little is known about their functions. Sumoylation is the addition of the SUMO (small ubiquitin-related modifier) group. This modification is conserved from yeast to mammals, and histone sumoylation is primarily related to transcriptional repression [47, 48].

As the name itself suggests, ADP ribosylation is the addition of one or more adenosine di-phosphate ribose to lysine, arginine or glutamic acid from NAD [49]. This reversible modification is mainly seen during DNA repair and plays a role in open chromatin structure, making the cellular machinery more accessible to DNA [50, 51].

Prolines present in histones can be either in trans or cis isomeric form. The change is achieved by proline isomers and is important for modulating chromatin structure. This structural change regulates the modification pattern of nearby residues [52].

Recently a new modification, lysine crotonylation has been identified. This novel modification adds a crotonyl group to the lysine residues, and is not only present in the histone tails but also found in the globular domain. It is functionally associated with active chromatin structure and is found throughout eukaryotes, from yeast to humans. The exact function and association of this modification with other non-histone proteins has not yet been identified [53].

Histone code and crosstalk among histone modifications

The presence or absence of various chemical modifications on specific histone residues serves as a marker required for the recruitment of different non-histone proteins to the chromatin. This directly or indirectly affects the nucleosome stability, chromatin structure as well as cell cycle progression. For example, in mammals, Haspin kinase phosphorylates H3T3, which facilitates binding of the chromosomal passenger complex to chromatin during mitosis. Another phosphorylation marker on H2A S122/T121p by Bub1 kinase is required for centromeric localization of Sgo1 and error free chromosome segregation [54]. There are different histone residues, either in the flexible tail or in the globular domain, which in a particular combination can generate a signal that can be detected by different regulatory proteins required for proper chromatin function. In higher eukaryotes H4K8ac, H3K14ac and H3S10p together are associated with active chromatin, whereas H3K9me³ and loss of acetylation of H3 and H4 are associated with transcriptional repression [55, 56]. Sometimes the same modification in a particular residue results in different biological functions. This is possibly due to the presence of other histone markers working in concert with it. H3S10p and H3S28p signal docking of proteins essential for chromosome condensation and segregation, but H3S10p and H3S28p along with H3K14ac recruit proteins for relaxed chromatin structure and active transcription [24]. Some of the histone residues can be subjected to dual modifications like those in H3K9. This particular lysine residue can be either acetylated or methylated, so one modification cross-regulates the other at a certain time. H3K9ac is related to open chromatin, while methylation is related to silent chromatin [32, 57]. Crosstalk is not only possible between histones, but also to various non-histone proteins. H2B K123Ub activates Set1 methyltransferase to establish the H3K4me mark on chromatin. Set1 also methylates Dam1K233, an outer kinetochore protein

important for spindle-chromatin binding. The adjacent residues of Dam1S122/123 are the sites of phosphorylation by Ipl1, another checkpoint protein required for proper chromosome segregation. However, methylation opposes phosphorylation of adjacent residues, which in turn is essential to maintain a proper balance of Dam1 phosphorylation and methylation required for its normal function [31, 58, 59].

Distinct chromatin structure of the centromere

The centromere is present in the primary constriction of the chromosome. Its presence is important for maintaining the physical association of sister chromatids until anaphase, for kinetochore protein assembly and proper chromosome dynamics. In budding yeast, a single nucleosome is recognized as the 'point centromere'. It has only 125 bp of DNA wrapped around a single specialized nucleosome. This is replaced with multiple nucleosomes in higher eukaryotes and is referred to as 'regional centromere'. In the centromeric nucleosome/nucleosomes, the usually recognized H3 is replaced with its highly conserved variant Cse4 (in budding yeast), CID (in *Drosophila*) and CENP-A (in humans) [14, 60]. The centromere is generally associated with transcriptionally inactive chromatin/ heterochromatin structure. For a long time it was assumed to have histone modifications characteristic of transcriptionally repressed heterochromatin. It was later found to have unique combinations of histone marks that are present both in heterochromatin and euchromatin regions. For example, H4K9me, which is a heterochromatin marker, is absent in the centromeric histones but is present in the adjoining pericentromeric histones. In contrast, hypoacetylation of H4 tail and H3K4me², which are euchromatin markers, are seen in the centromeric histones [61-64]. These modification markers make the centromeric histones unique from any histones present in other

parts of the chromosome. This unique centromeric identity may be important for its early replication timing which gives enough time for the kinetochore to assemble on the newly formed chromatin. Moreover the distinctive modification pattern in the centromeric nucleosome is essential for the association of kinetochore and therefore its function in chromosome segregation [63, 65].

Cell cycle and chromosome segregation

In a cell division cycle the cell duplicates its chromosomes (S phase), and at the end distributes a copy of the duplicated chromosomes to each of the daughter cells (M phase) resulting in a genetically identical progeny. The S and M phases are separated by two growth or resting phases, where the cell prepares to proceed to the next step of the cell cycle [4, 66]. To achieve error free cell propagation, the whole DNA replication and the chromosome distribution machinery of the cell are very carefully monitored. Any problem the cell encounters in replication and segregation leads to a pause signal, allowing enough time for the cell to fix the problem by itself. The centromere is a special region of the DNA that is attached to a proteinaceous complex, the kinetochore. The cell surveillance machinery ensures the attachment of the centromeric DNA to the plus end of spindle microtubules from opposite poles of the cell, before anaphase of mitosis. This attachment results in equal distribution of chromosomes into the opposite poles [67, 68]. In normal cells, if the centromere is not properly attached to the spindle or there is not enough bipolar tension sensed by the kinetochore proteins, a checkpoint gets activated that prevents the cell to proceed to anaphase until the error is fixed [69]. Once the checkpoint proteins are activated, they target to inactivate the Anaphase Promoting Complex (APC), an E3 Ubiquitin ligase. If there is sufficient bipolar attachment of the kinetochore-

microtubule, the APC is activated by binding to Cdc20. This causes the ubiquitination of the securing protein (Pds1) that secures the attachment of the sister chromatids. The destruction of securin releases separase (Eps1p), which causes cleavage of cohesin. This promotes the separation of sister chromatids and the cell moves forward to the next step, anaphase [70-72]. On the contrary, if the kinetochore is not attached to the microtubule, there are different signaling pathways that ultimately sequester Cdc20 by the formation of Mad2-Cdc-20 and MCC (mitotic checkpoint complex). The MCC is composed of Mad2-Cdc20, BubR1/Mad3, and Bub3 [73, 74].

Recent studies have shown that there are many other proteins that may act to amplify the inhibitory effect of the checkpoint proteins. Bub1 kinase, Bub3 kinase, Mps1 kinase are included in this category. Bub1 (Budding uninhibited by benomyl) kinase is dispensable for checkpoint activation, but it improves the level of inhibitory signals to inactivate the APC [73, 75]. Mps1 (Monopolar spindle) kinase, on the other hand, phosphorylates Ndc80, a kinetochore protein. This phosphorylation activates the checkpoint and dephosphorylating inactivates it [73]. There is also a phosphatase, PPI (Protein Phosphate-1) homolog (Glc7 in budding yeast) that reduces the kinase activity in the attached kinetochore. This facilitates to form an active APC [76]. Therefore, a balance of phosphorylation and dephosphorylating is required to maintain the stability of the APC. If the kinetochore is properly attached to the microtubule, the checkpoint proteins Mad1-Mad2 are removed from the kinetochore to the spindle poles which in turn release unbound Cdc20 to bind and activate the APC.

What happens when the kinetochore is attached to the microtubule but does not sense enough bipolar tension? This is particularly important in correcting the synthetic attachment, where the microtubules from the same pole are attached to both sister kinetochores. The

checkpoint signal proteins are not directly activated in this case. The conserved kinase protein Ipl1/Aurora kinase senses the tensionless in the kinetochore and dissociates the kinetochore and microtubule attachment [77]. This kindles the whole signaling pathway of checkpoint protein activation and inactivation of the APC. The Aurora kinase is conserved from yeast to humans. In budding yeast, there is only one Aurora kinase member, Ipl1. Ipl1 is a serine/threonine kinase that moves from the chromosome arms at the early part of the cell cycle to the centromeric region during metaphase, and later to the spindle during anaphase. This kinase is the enzymatic component of the CPC (chromosomal passenger complex) [31, 78]. The other major members of the CPC in budding yeast are Bir1 (Baculovirus IAP repeat, IAP-Inhibitor of Apoptosis repeat) and Sli15 (Synthetically lethal with Ipl1). Both Bir1 and Sli15 are important for the Ipl1 kinase activity [78]. In recent years, another protein, Sgo1 (Shugoshin), has received plenty of attention for its role in sensing tensionless in sister chromatids. There are two Shugoshin like proteins, Sgo1 and Sgo2 in fission yeast and higher eukaryotes. Sgo1 plays a role in protection of centromeric cohesin in meiosis whereas Sgo2 is required to sense tension generated from proper attachment of kinetochore and microtubules during both mitosis and meiosis. In budding yeast, only Sgo1 is found, which is important for protecting centromeric cohesin in meiosis [79]. The exact role of Sgo1 during mitosis is still unclear. This protein, like Pds1 (securin), is expressed at the beginning of the cell cycle (G1/S), resides in the kinetochore and dissipates as the sister chromatids successfully separate and move to the opposite poles in anaphase [80]. The checkpoint protein kinase Bub1 is reported to be essential for the proper localization of Sgo1 in the centromeric region of the chromosome. A mutation in the C terminal of the Bub1 protein that impairs its kinase activity mislocalizes Sgo1. This causes missegregation due to the incapability of the cells to sense tension in the kinetochore [81]. The phosphorylation of histone

H2A S121 by Bub1 signals Sgo1 localization at the kinetochore in fission yeast [28]. Changes observed in the structure of the inner kinetochore and pericentromeric chromatin further confirm the important role played by bub1 kinase in the phosphorylation of the conserved C terminal of histone H2A, and thereby Sgo1 recruitment to the kinetochore [82]. In fission yeast and humans, Sgo2 (equivalent to Sgo1 in budding yeast) is essential to localize Aurora kinase (Ipl-1 in budding yeast) in the centromere through Survivin (Bir-1 in yeast) [83]. This clarifies the role of Sgo1 in the time of improper tension sensed in the kinetochore; Sgo1 loads Ipl1 (along with CPC proteins) in the centromere. Ipl1 then works to disassemble the kinetochore microtubule attachment and thereby signals an active checkpoint. However, according to another independent investigation, Sgo1 is not required for Ipl1 localization to the centromere, instead it works in a parallel pathway to activate the checkpoint when there is an improper tension sensed by the kinetochore proteins. This group proposes a pathway where Bub1 kinase recruits Sgo1 to the kinetochore, which requires the involvement of Mps1 [82]. In this model, Sgo1 is not responsible for proper Ipl1 localization to the centromere. In fact, when Ipl1 is inactive, Sgo1 over expression overcomes improper kinetochore microtubule attachments [84].

III. METHODS

A. Yeast strains, genetic methods and media

The yeast strains are isogenic to FY2, which is originally derived from S288C, unless indicated otherwise [85]. The strains were developed following standard procedures [86-89]. The list of yeast strains made and used for this study are indicated, along with their genotypes, in Table 1. Strain IPY283, which already has a *lac* operator array engineered very near to centromere IV, was used to prepare the parent strains IPY1008 and IPY1044. IPY1008 and IPY1044 are believed to be genotypically identical. However IPY1044 shows a better GFP signal and is selected for the characterization studies of the mutants with the mutations integrated at their genomic loci. *HHT1-HHF1*, which encodes for the first copy of histones H3 and H4, was first deleted with the kanamycin resistance gene. A plasmid pIP220 was constructed on the plasmid background pRS317 (*CEN, LYS2*) with *HHT1-HHF1* from pIP90. This newly constructed pIP220 is then inserted into the strains mentioned above whose *HHT1-HHF1* had been deleted. This step is important before deleting the second copy of the gene H3 and H4, as absence of both the copies of H3 and H4 is lethal to the cells. The construction of IPY1008 and IPY1044 was accomplished by deleting *HHT2-HHF2*, the second copy of the genes encoding H3 and H4, with the nourseothricin resistance gene (*Nat^r*). IPY1008 and IPY1004 were used to screen the H3 and H4 mutant library after counter-selecting for pIP220. This is achieved by plating the yeast cells in medium containing alpha-aminoadipate.

HHT1-HHF1 is deleted by recombination with the PCR amplification product of GHB151 (KanMX) or pAG25 (*natMX*) using primers oIP351/oIP352 or oIP393/oIP394, respectively. The list of primers is listed in Table 3. The deletions were confirmed by PCR using oIP349/oIP73 and oIP88/oIP73 or oIP88/oIP395. *HHT2-HHF2* was deleted by recombination with the PCR amplified gene product of plasmid pAG25 (*natMx*), using

oIP353/oIP354, and confirmation was done using oIP184/oIP185. *SGO1* was deleted by using the PCR amplified gene product of pAG32 containing the hygromycin B resistance gene (HphMX) using oIP391/oIP392. The above deletion was confirmed by primers oIP326/oIP327. The 13xMyc tag was added to the 3' of *SGO1* using GHB160 (13xMyc-KanMx) as template and primers oIP396/oIP397 [90]. The 13xMyc tag was added to the 3' of *PDS1* by crossing IPY1044 to IPY1005. The tagging of *SGO1* with 13xMyc-KanMx was confirmed by PCR with oIP326/oIP327, and the tagging of *PDS1* with oIP357/oIP358. Properly sized DNA amplicons were visualized by electrophoresis on 0.8% agarose gels.

All yeast media were prepared as described [91]. Benomyl plates were prepared by adding adequate amount of benomyl (Sigma, St. Louis) to hot YPD to a final concentration of 5µg/ml, 10µg/ml, and 15µg/ml of benomyl. Canavanine plates were prepared by adding 60µg/ml of canavanine (Sigma, St. Louis) to synthetic complete medium lacking arginine (SC-Arg). Hydroxyurea (HU) plates were prepared by adding hydroxyurea (US Biologicals) to YPD at a final concentration of 200 mM. Alpha-aminoadipate medium was prepared by adding alpha-aminoadipate (US Biologicals) to SD (Synthetic minimal glucose medium) as described [92].

B. Bacterial strains and plasmids

Plasmids were amplified in *Escherichia coli* DH5α and isolated using standard procedures [93]. Plasmid pIP220 was made by digesting *HHT1-HHF1* from pIP90 with restriction enzymes *SalI* and *NotI*, and cloning it into the corresponding restriction sites in pRS317 [87, 94]. High copy plasmids for suppression studies of mutants were prepared as listed in Table 2. The fragments containing *IPL1* and *BIR1* are from pIP213 and pIP114, respectively.

BUB1 was isolated from genomic DNA of IPY498 by PCR amplification with primers oIP389/oIP390 and cloned into pRS424 [94] with restriction enzymes *XhoI* and *NotI*.

C. Mutant H3 and H4 library screening

Individual plasmids were isolated by alkaline lysis [93] or Zyppy™ Plasmid Miniprep Kit (Zymo Research) from 486 *Escherichia coli* strains having synthetic histone H3 and H4 substitution and deletion mutants in the plasmid pRS414 (Thermo Scientific Open Biosystem, Catalog NoYSC5135) [95, 96]. For yeast transformations, 2 µl of the isolated plasmids were introduced into 10 µl of 2×10^7 cells/ml of IPY1008 following 96-well plate transformation, as described [97], and resuspended in 15 µl of sterile distilled water of which 6 µl was plated on SC-tryptophan (SC-Trp). The tryptophan prototrophs were inoculated into 150 µl of SC-Trp liquid medium and incubated at 30 °C overnight. 5 µl of the above cells were plated on SD + alpha-aminoadipate medium. The transformed lysine auxotrophs were plated on YPD, YPD + Benomyl (15 µg/ml), YPD + Hydroxyurea, SC-tryptophan, SC-lysine, SC-arginine/UV, SC-arginine + Canavanine/UV, and incubated at 26 °C. Two additional YPD plates were incubated at 37 °C and 13 °C for temperature sensitivity testing of the mutants.

Selected mutant plasmids from the library were digested with *Bfu1/BciV1* (Thermo Scientific) and introduced into the yeast strain IPY1044 for integration at the *HHT2-HHF2* locus. Transformants were selected on SC-uracil plates. The integrations were confirmed by PCR with oIP371/oIP185 for H3 mutants, and oIP232/oIP185 for H4 mutants. The integrated strains were plated on SD + tryptophan + alpha-aminoadipate medium to select for the cells that have lost the *HHT1-HHF1* lysine plasmid (pIP220), which carries the wild-type H3 and H4 encoding genes and covers the mutant phenotypes. All the mutants were propagated for several generations to

allow for the substitution of the wild-type histones for the H3 and H4 mutant histones in the cell. This is accomplished by passing the cells six times through consecutive 10 ml YPD cultures. In each passage 30µl of an overnight culture was inoculated into fresh 10 ml YPD and incubated at 30°C overnight. The mutants were then subjected to phenotypic analysis by spot-plating on YPD, YPD + Benomyl (15 µg/ml), YPD + Hydroxyurea, SC-Uracil, SC-Lysine, SC-Arginine/UV, SC-Arginine + Canavanine/UV and incubated at 26 °C. Two YPD plates were incubated at 37 °C and 13 °C.

D. Time point study of mutants

All the mutants were propagated for 6 passages on YPD. The 6th-passage mutants were grown until early log phase and synchronized to the G1 phase of the cell cycle by adding alpha factor to the final concentration of 0.9 µM, and grown for 3 hrs at 30 °C. The synchronized cells were washed two times with sterile distilled water and resuspended in fresh YPD. At each designated time point, the cells were collected for cell counting by a hemocytometer, flow cytometry analysis and for nuclear visualization with 4',6-diamidino-2-phenylindole (DAPI) and centromere (GFP) visualization with fluorescence microscopy.

E. Canavanine assay of ploidy

The ploidy status of a yeast cell can be determined by monitoring the *CAN1* gene copy number on chromosome V [98]. This gene encodes for plasma membrane arginine permease [99]. Canavanine is a toxic homologue of arginine. If a yeast cell has a wild-type *CAN1* gene, it can uptake canavanine and die, while a recessive *can1* gene confers resistance to canavanine. Therefore, the frequency of canavanine resistant mutants is much higher in haploid than diploid

cells mutagenized by UV irradiation, or in cells with two copies of chromosome V [1, 100]. For this essay, the yeast strains were patched or spotted on YPD plates and then replica plated onto SC-arginine + canavanine and SC-arginine. Both plates were then subjected to UV irradiation (300 ergs/mm²) with a UV source (Stratalinker UV cross linker, Stratagene, Agilene Technologies). The cells were then incubated in the dark for 5 days at 26 °C. Cells resistant to canavanine (haploid) grow colonies that appear as papillae on the canavanine plates. The diploid cells remain sensitive to canavanine and are unable to survive on the canavanine plates.

F. Microscopy

Cells expressing green fluorescence protein (GFP) tagged centromeres and DAPI stained nucleic acids were visualized and imaged with a fluorescent microscope Axio Imager M1 (Zeiss). At each selected time point either live cells or cells fixed with ethanol were visualized. A minimum of 200 cells per time point were counted for DAPI stained nucleic acids and GFP tagged centromeres.

G. Flow cytometry

Exponentially growing cells were fixed with ethanol, treated with proteinase K, RNase and stained with propidium iodide as described in literature [16]. The DNA content was quantified by fluorescence of a minimum of 15,000 cells per sample, using a Becton Dickinson FACSCalibur Instrument at 480 nm excitation.

H. *PDS1* stability assay

Exponentially growing cells were synchronized with 0.9 μ M alpha factor for 3 to 4 hours, depending on the doubling time of the strains, and then washed twice with water before incubating them in fresh YPD at 30 °C (with or without nocodazole (30 μ g/ml)). The cells were collected at the indicated time points. The cells are treated with protein extract buffer (0.06 M Tris HCl pH-6.8, 6 M Urea, 2% SDS, 5% β mercaptoethanol and 0.0025% bromophenol blue) and immediately transferred to a boiling water bath for 5 minutes [101]. After centrifugation, the supernatants were used as protein extracts and loaded on a Nusep 4-20% gel for SDS-PAGE. The proteins were transferred to a PVDF membrane (BioTrace PVDF, Pall) for immunoblot analysis (western) using a wet tank mini Trans-blot system (Bio-Rad). The membranes were blocked in 5% nonfat dry milk in TBST (150 mM NaCl, 100 mM TrisHCl pH-6.8, 0.5% Tween-20). The proteins were detected using anti-c-Myc (9E10, Roche) or anti-*Saccharomyces cerevisiae* phosphoglycerate kinase monoclonal antibody (Invitrogen) at a 1:10,000 dilution. The blots were developed using Immunobilon Western Chemiluminescent HRP substrate (Millipore-WBKLS0100). Images of blots were captured in a FluorChemTM 8900 instrument (Alpha Innotech).

I. Chromatin Immunoprecipitation assay

Chromatin Immunoprecipitation (ChIP) was performed on wild type, H3K42A, and H4K44Q background strains (IPY1067, IPY1068, IPY1075) with *Sgo1-13xMyc*. The antibody used for immunoprecipitation was anti-c-Myc (9E10, Roche). The protocol followed is described in Kanta et al. [19]. The PCR products were resolved in a 1.5% agarose gel with ethidium bromide and imaged in a FluorChemTM 8900 instrument (Alpha Innotech). The

presence of Sgo1 was detected by performing a PCR using centromeric primers (cen3 core) oIP142/oIP143, and pericentromeric primers (cen3 + 0.5kb left) oIP210/oIP211 on the above strains and compared with untagged strains.

J. Viability assay

Two hundred and fifty exponentially growing cells were plated on YPD and incubated at 26 °C for 3 days. Viable colonies were counted in four separate replicas. Average and standard error from each strain was used to determine the percent of viability with respect to the wild-type strain.

Table 1: Yeast strains used or made for this study

	Alternate Name	
IPY167		<i>MATα ura3-52 trp1Δ63 his3Δ200 leu2Δ1 lys2Δ202</i>
IPY283		<i>MATα ura3-52 trp1Δ63 (hta2-htb2)Δ::TRP1 his3-205::HIS3-GFP-LacI leu2Δ1::lacO-LEU2</i>
IPY1008		<i>MATα ura3-52 trp1Δ63 his3-205::HIS3-GFP-LacI leu2Δ1::lacO-LEU2 lys202 (hht1-hhf1)Δ::KanMX(hht2-hhf2)Δ::natMX <pIP220></i>
IPY1044		<i>MATα ura3-52 trp1Δ63 his3-205::HIS3-GFP-LacI leu2Δ1::lacO-LEU2 lys202 (hht1-hhf1)Δ::KanMX (hht2-hhf2)Δ::natMX <pIP220></i>
PCYH3-0	IPY1067	<i>MATα ura3-52 trp1Δ63 his3-205::HIS3-GFP-LacI leu2Δ1::lacO-LEU2 lys202 (hht1-hhf1)Δ::KanMX (hht2-hhf2)Δ::HHT-hhfs-URA3 <pIP220></i>
PCYH3-1	IPY1068	<i>MATα ura3-52 trp1Δ63 his3-205::HIS3-GFP-LacI leu2Δ1::lacO-LEU2 lys202 (hht1-hhf1)Δ::KanMX (hht2-hhf2)Δ::hhfsK42A-hhfs-URA3 <pIP220></i>
PCYH3-2	IPY1069	<i>MATα ura3-52 trp1Δ63 his3-205::HIS3-GFP-LacI leu2Δ1::lacO-LEU2 lys202 (hht1-hhf1)Δ::KanMX (hht2-hhf2)Δ::hhfsK42Q-hhfs-URA3 <pIP220></i>
PCYH3-3	IPY1070	<i>MATα ura3-52 trp1Δ63 his3-205::HIS3-GFP-LacI leu2Δ1::lacO-LEU2 lys202 (hht1-hhf1)Δ::KanMX (hht2-hhf2)Δ::hhfsK42R-hhfs-URA3 <pIP220></i>
PCYH3-4	IPY1071	<i>MATα ura3-52 trp1Δ63 his3-205::HIS3-GFP-LacI leu2Δ1::lacO-LEU2 lys202 (hht1-hhf1)Δ::KanMX (hht2-hhf2)Δ::hhfsG44S-hhfs-URA3 <pIP220></i>
PCYH4-0	IPY1072	<i>MATα ura3-52 trp1Δ63 his3-205::HIS3-GFP-LacI leu2Δ1::lacO-LEU2 lys202 (hht1-hhf1)Δ::KanMX (hht2-hhf2)Δ::hhfs-HHF2-URA3 <pIP220></i>

PCYH4-1	IPY1073	<i>MATa ura3-52 trp1Δ63 his3-205::HIS3-GFP-LacI leu2Δ1::lacO-LEU2 lys202 (hht1-hhf1)Δ::KanMX (hht2-hhf2)Δ::hhts-hhfsK44A-URA3 <pIP220></i>
PCYH4-2	IPY1074	<i>MATa ura3-52 trp1Δ63 his3-205::HIS3-GFP-LacI leu2Δ1::lacO-LEU2 lys202 (hht1-hhf1)Δ::KanMX (hht2-hhf2)Δ::hhts-hhfsK44R-URA3 <pIP220></i>
PCYH4-3	IPY1075	<i>MATa ura3-52 trp1Δ63 his3-205::HIS3-GFP-LacI leu2Δ1::lacO-LEU2 lys202 (hht1-hhf1)Δ::KanMX (hht2-hhf2)Δ::hhts-hhfsK44Q-URA3 <pIP220></i>
PCYH3-5	IPY1076	<i>MATa ura3-52 trp1Δ63 his3-205::HIS3-GFP-LacI leu2Δ1::lacO-LEU2 lys202 (hht1-hhf1)Δ::KanMX (hht2-hhf2)Δ::hhtsK56A-hhfs-URA3 <pIP220></i>
PCYH3-7	IPY1077	<i>MATa ura3-52 trp1Δ63 his3-205::HIS3-GFP-LacI leu2Δ1::lacO-LEU2 lys202 (hht1-hhf1)Δ::KanMX (hht2-hhf2)Δ::hhtsK56Q-hhfs-URA3 <pIP220></i>
PCYH4-14	IPY1078	<i>MATa ura3-52 trp1Δ63 his3-205::HIS3-GFP-LacI leu2Δ1::lacO-LEU2 lys202 (hht1-hhf1)Δ::KanMX (hht2-hhf2)Δ::hhts-hhfsK91A-URA3 <pIP220></i>
PCYH4-15	IPY1079	<i>MATa ura3-52 trp1Δ63 his3-205::HIS3-GFP-LacI leu2Δ1::lacO-LEU2 lys202 (hht1-hhf1)Δ::KanMX (hht2-hhf2)Δ::hhts-hhfsK91R-URA3 <pIP220></i>
PCYH4-16	IPY1080	<i>MATa ura3-52 trp1Δ63 his3-205::HIS3-GFP-LacI leu2Δ1::lacO-LEU2 lys202 (hht1-hhf1)Δ::KanMX (hht2-hhf2)Δ::hhts-hhfsK91Q-URA3 <pIP220></i>
PCYH4-17	IPY1081	<i>MATa ura3-52 trp1Δ63 his3-205::HIS3-GFP-LacI leu2Δ1::lacO-LEU2 lys202 (hht1-hhf1)Δ::KanMX (hht2-hhf2)Δ::hhts-hhfsR92A-URA3 <pIP220></i>
PCYH4-18	IPY1082	<i>MATa ura3-52 trp1Δ63 his3-205::HIS3-GFP-LacI leu2Δ1::lacO-LEU2 lys202 (hht1-hhf1)Δ::KanMX (hht2-hhf2)Δ::hhts-hhfsR92K-URA3 <pIP220></i>
PCYH4-22	IPY1083	<i>MATa ura3-52 trp1Δ63 his3-205::HIS3-GFP-LacI leu2Δ1::lacO-LEU2 lys202 (hht1-hhf1)Δ::KanMX (hht2-hhf2)Δ::hhts-hhfsL97A-URA3 <pIP220></i>
PCYH4-23	IPY1084	<i>MATa ura3-52 trp1Δ63 his3-205::HIS3-GFP-LacI leu2Δ1::lacO-LEU2 lys202 (hht1-hhf1)Δ::KanMX (hht2-hhf2)Δ::hhts-hhfsG99A-URA3 <pIP220></i>

PCY1	IPY1085	<i>MATa ura3-52 trp1Δ63 his3-205::HIS3-GFP-LacI leu2Δ1::lacO-LEU2 lys202 (hht1-hhf1)Δ::KanMX (hht2-hhf2)Δ::hhts-HHF2-URA3 <pIP209> <pIP220></i>
PCY2	IPY1086	<i>MATa ura3-52 trp1Δ63 his3-205::HIS3-GFP-LacI leu2Δ1::lacO-LEU2 lys202 (hht1-hhf1)Δ::KanMX (hht2-hhf2)Δ::hhtsK42A-hhfs-URA3 <pIP209> <pIP220></i>
PCY3	IPY1087	<i>MATa ura3-52 trp1Δ63 his3-205::HIS3-GFP-LacI leu2Δ1::lacO-LEU2 lys202 (hht1-hhf1)Δ::KanMX (hht2-hhf2)Δ::hhtsK42Q-hhfs-URA3 <pIP209> <pIP220></i>
PCY4	IPY1088	<i>MATa ura3-52 trp1Δ63 his3-205::HIS3-GFP-LacI leu2Δ1::lacO-LEU2 lys202 (hht1-hhf1)Δ::KanMX (hht2-hhf2)Δ::hhtsG44S-hhfs-URA3 <pIP209> <pIP220></i>
PCY5	IPY1089	<i>MATa ura3-52 trp1Δ63 his3-205::HIS3-GFP-LacI leu2Δ1::lacO-LEU2 lys202 (hht1-hhf1)Δ::KanMX (hht2-hhf2)Δ::hhts-hhfsK44Q-URA3 <pIP209> <pIP220></i>
PCY6	IPY1090	<i>MATa ura3-52 trp1Δ63 his3-205::HIS3-GFP-LacI leu2Δ1::lacO-LEU2 lys202 (hht1-hhf1)Δ::KanMX (hht2-hhf2)Δ::hhts-hhfsL97A-URA3 <pIP209> <pIP220></i>
PCY61	IPY1091	<i>MATa ura3-52 trp1Δ63 his3-205::HIS3-GFP-LacI leu2Δ1::lacO-LEU2 lys202 (hht1-hhf1)Δ::KanMX (hht2-hhf2)Δ::hhts-hhfsK91Q-URA3 <pIP209> <pIP220></i>
PCY7	IPY1092	<i>MATa ura3-52 trp1Δ63 his3-205::HIS3-GFP-LacI leu2Δ1::lacO-LEU2 lys202 (hht1-hhf1)Δ::KanMX (hht2-hhf2)Δ::hhts-hhfsG99A-URA3 <pIP209> <pIP220></i>
PCY8	IPY1093	<i>MATa ura3-52 trp1Δ63 his3-205::HIS3-GFP-LacI leu2Δ1::lacO-LEU2 lys202 (hht1-hhf1)Δ::KanMX (hht2-hhf2)Δ::hhts-HHF2-URA3 <YEplac112></i>
PCY9	IPY1094	<i>MATa ura3-52 trp1Δ63 his3-205::HIS3-GFP-LacI leu2Δ1::lacO-LEU2 lys202 (hht1-hhf1)Δ::KanMX (hht2-hhf2)Δ::hhtsK42A-hhfs-URA3 <YEplac112></i>
PCY10	IPY1095	<i>MATa ura3-52 trp1Δ63 his3-205::HIS3-GFP-LacI leu2Δ1::lacO-LEU2 lys202 (hht1-hhf1)Δ::KanMX (hht2-hhf2)Δ::hhtsK42Q-hhfs-URA3 <YEplac112></i>

PCY11	IPY1096	<i>MATa ura3-52 trp1Δ63 his3-205::HIS3-GFP-LacI leu2Δ1::lacO-LEU2 lys202 (hht1-hhf1)Δ::KanMX (hht2-hhf2)Δ::hhtsG44S-hhfs-URA3 <YEplac112></i>
PCY12	IPY1097	<i>MATa ura3-52 trp1Δ63 his3-205::HIS3-GFP-LacI leu2Δ1::lacO-LEU2 lys202 (hht1-hhf1)Δ::KanMX (hht2-hhf2)Δ::hhts-hhfsK44Q-URA3 <YEplac112></i>
PCY13	IPY1098	<i>MATa ura3-52 trp1Δ63 his3-205::HIS3-GFP-LacI leu2Δ1::lacO-LEU2 lys202 (hht1-hhf1)Δ::KanMX (hht2-hhf2)Δ::hhts-hhfsL97A-URA3 <YEplac112></i>
PCY14	IPY1099	<i>MATa ura3-52 trp1Δ63 his3-205::HIS3-GFP-LacI leu2Δ1::lacO-LEU2 lys202 (hht1-hhf1)Δ::KanMX (hht2-hhf2)Δ::hhts-hhfsG99A-URA3 <YEplac112></i>
IPY1046	IPY1100	<i>MATa his3Δ200 leu2Δ0 lys202 ura3Δ0 /ura3-52 PDS1-13xMyc::KanMX</i>
PCY15	IPY1101	<i>MATa trp1Δ63 his3-205::HIS3-GFP-LacI leu2Δ1::lacO-LEU2 lys202 (hht1-hhf1)Δ::KanMX (hht2-hhf2)Δ::hhts-HHF2-URA3 PDS1-13xMyc::KanMX</i>
PCY16	IPY1102	<i>MATa trp1Δ63 his3-205::HIS3-GFP-LacI leu2Δ1::lacO-LEU2 lys202 (hht1-hhf1)Δ::KanMX (hht2-hhf2)Δ::hhtsK42A-hhfs-URA3 PDS1-13xMyc::KanMX</i>
PCY17	IPY1103	<i>MATa ura3-52 trp1Δ63 leu2Δ0 lys202 (hht1-hhf1)Δ::KanMX (hht2-hhf2)Δ::hhtsK42Q-hhfs-URA3 PDS1-13xMyc::KanMX</i>
PCY18	IPY1104	<i>MATa trp1Δ63 his3-205::HIS3-GFP-LacI leu2Δ1::lacO-LEU2 lys202 (hht1-hhf1)Δ::KanMX (hht2-hhf2)Δ::hhtsG44S-hhfs-URA3 PDS1-13xMyc::KanMX</i>
PCY19	IPY1105	<i>MATa trp1Δ63 his3-205::HIS3-GFP-LacI leu2Δ1::lacO-LEU2 lys202 (hht1-hhf1)Δ::KanMX (hht2-hhf2)Δ::hhts-hhfsK44R-URA3 PDS1-13xMyc::KanMX</i>
PCY20	IPY1106	<i>MATa his3-205::HIS3-GFP-LacI leu2Δ1::lacO-LEU2 lys202 (hht1-hhf1)Δ::KanMX (hht2-hhf2)Δ::hhts-hhfsK44Q-URA3 PDS1-13xMyc::KanMX</i>
PCY21	IPY1107	<i>MATa trp1Δ63 his3-205::HIS3-GFP-LacI leu2Δ1::lacO-leu2 lys202 (hht1-hhf1)Δ::KanMX (hht2-hhf2)Δ::hhts-hhfsL97A-URA3 PDS1-13xMyc::KanMX</i>

PCY60	IPY1108	<i>MATa trp1Δ63 his3Δ200 his3-205::HIS3-GFP-LacI leu2Δ0 lys202 (hht1-hhf1)Δ::KanMX (hht2-hhf2)Δ::hhfs-hhfsG99A-URA3 PDS1-13xMyc::KanMX</i>
PCY22	IPY1109	<i>MATa ura3-52 trp1Δ63 his3-205::HIS3-GFP-LacI leu2Δ1::lacO-LEU2 lys202 (hht1-hhf1)Δ::KanMX (hht2-hhf2)Δ::hhfs-HHF2-URA3 sgo1Δ::HphMX <pIP220></i>
PCY23	IPY1110	<i>MATa ura3-52 trp1Δ63 his3-205::HIS3-GFP-LacI leu2Δ1::lacO-LEU2 lys202 (hht1-hhf1)Δ::KanMX (hht2-hhf2)Δ::hhfsK42A-hhfs-URA3 sgo1Δ::HphMX <pIP220></i>
PCY24	IPY1111	<i>MATa ura3-52 trp1Δ63 his3-205::HIS3-GFP-LacI leu2Δ1::lacO-LEU2 lys202 (hht1-hhf1)Δ::KanMX (hht2-hhf2)Δ::hhfsK42Q-hhfs-URA3 sgo1Δ::HphMX <pIP220></i>
PCY25	IPY1112	<i>MATa ura3-52 trp1Δ63 his3-205::HIS3-GFP-LacI leu2Δ1::lacO-LEU2 lys202 (hht1-hhf1)Δ::KanMX (hht2-hhf2)Δ::hhfsG44S-hhfs-URA3 sgo1Δ::HphMX <pIP220></i>
PCY26	IPY1113	<i>MATa ura3-52 trp1Δ63 his3-205::HIS3-GFP-LacI leu2Δ1::lacO-LEU2 lys202 (hht1-hhf1)Δ::KanMX (hht2-hhf2)Δ::hhfs-hhfsK44Q-URA3 sgo1Δ::HphMX <pIP220></i>
PCY27	IPY1114	<i>MATa ura3-52 trp1Δ63 his3-205::HIS3-GFP-LacI leu2Δ1::lacO-LEU2 lys202 (hht1-hhf1)Δ::KanMX (hht2-hhf2)Δ::hhfs-hhfsK91Q-URA3 sgo1Δ::HphMX<pIP220></i>
PCY28	IPY1115	<i>MATa ura3-52 trp1Δ63 his3-205::HIS3-GFP-LacI leu2Δ1::lacO-LEU2 lys202 (hht1-hhf1)Δ::KanMX (hht2-hhf2)Δ::hhfs-HHF2-URA3 <pIP211> <pIP220></i>
PCY29	IPY1116	<i>MATa ura3-52 trp1Δ63 his3-205::HIS3-GFP-LacI leu2Δ1::lacO-LEU2 lys202 (hht1-hhf1)Δ::KanMX (hht2-hhf2)Δ::hhfsK42A-hhfs-URA3 <pIP211> <pIP220></i>
PCY30	IPY1117	<i>MATa ura3-52 trp1Δ63 his3-205::HIS3-GFP-LacI leu2Δ1::lacO-LEU2 lys202 (hht1-hhf1)Δ::KanMX (hht2-hhf2)Δ::hhfsK42Q-hhfs-URA3 <pIP211> <pIP220></i>
PCY31	IPY1118	<i>MATa ura3-52 trp1Δ63 his3-205::HIS3-GFP-LacI leu2Δ1::lacO-LEU2 lys202 (hht1-hhf1)Δ::KanMX (hht2-hhf2)Δ::hhfsG44S-hhfs-URA3 <pIP211> <pIP220></i>

PCY32	IPY1119	<i>MATa ura3-52 trp1Δ63 his3-205::HIS3-GFP-LacI leu2Δ1::lacO-LEU2 lys202 (hht1-hhf1)Δ::KanMX (hht2-hhf2)Δ::hhts-hhfsK44Q-URA3 <pIP211> <pIP220></i>
PCY33	IPY1120	<i>MATa ura3-52 trp1Δ63 his3-205::HIS3-GFP-LacI leu2Δ1::lacO-LEU2 lys202 (hht1-hhf1)Δ::KanMX (hht2-hhf2)Δ::hhts-hhfsL97A-URA3 <pIP211> <pIP220></i>
PCY34	IPY1121	<i>MATa ura3-52 trp1Δ63 his3-205::HIS3-GFP-LacI leu2Δ1::lacO-LEU2 lys202 (hht1-hhf1)Δ::KanMX (hht2-hhf2)Δ::hhts-hhfsG99A-URA3 <pIP211> <pIP220></i>
PCY35	IPY1122	<i>MATa ura3-52 trp1Δ63 his3-205::HIS3-GFP-LacI leu2Δ1::lacO-LEU2 lys202 (hht1-hhf1)Δ::KanMX (hht2-hhf2)Δ::hhts-hhfsK91Q-URA3 <pIP211> <pIP220></i>
PCY36	IPY1123	<i>MATa ura3-52 trp1Δ63 his3-205::HIS3-GFP-LacI leu2Δ1::lacO-LEU2 lys202 (hht1-hhf1)Δ::KanMX (hht2-hhf2)Δ::hhts-HHF2-URA3 <pIP214> <pIP220></i>
PCY37	IPY1124	<i>MATa ura3-52 trp1Δ63 his3-205::HIS3-GFP-LacI leu2Δ1::lacO-LEU2 lys202 (hht1-hhf1)Δ::KanMX (hht2-hhf2)Δ::hhtsK42A-hhfs-URA3 <pIP214> <pIP220></i>
PCY38	IPY1125	<i>MATa ura3-52 trp1Δ63 his3-205::HIS3-GFP-LacI leu2Δ1::lacO-LEU2 lys202 (hht1-hhf1)Δ::KanMX (hht2-hhf2)Δ::hhtsK42Q-hhfs-URA3 <pIP214> <pIP220></i>
PCY39	IPY1126	<i>MATa ura3-52 trp1Δ63 his3-205::HIS3-GFP-LacI leu2Δ1::lacO-LEU2 lys202 (hht1-hhf1)Δ::KanMX (hht2-hhf2)Δ::hhtsG44S-hhfs-URA3 <pIP214> <pIP220></i>
PCY40	IPY1127	<i>MATa ura3-52 trp1Δ63 his3-205::HIS3-GFP-LacI leu2Δ1::lacO-LEU2 lys202 (hht1-hhf1)Δ::KanMX (hht2-hhf2)Δ::hhts-hhfsK44Q-URA3 <pIP214> <pIP220></i>
PCY41	IPY1128	<i>MATa ura3-52 trp1Δ63 his3-205::HIS3-GFP-LacI leu2Δ1::lacO-LEU2 lys202 (hht1-hhf1)Δ::KanMX (hht2-hhf2)Δ::hhts-hhfsL97A-URA3 <pIP214> <pIP220></i>
PCY42	IPY1129	<i>MATa ura3-52 trp1Δ63 his3-205::HIS3-GFP-LacI leu2Δ1::lacO-LEU2 lys202 (hht1-hhf1)Δ::KanMX (hht2-hhf2)Δ::hhts-hhfsG99A-URA3 <pIP214> <pIP220></i>

PCY43	IPY1130	<i>MATa ura3-52 trp1Δ63 his3-205::HIS3-GFP-LacI leu2Δ1::lacO-LEU2 lys202 (hht1-hhf1)Δ::KanMX (hht2-hhf2)Δ::hhts-hhfsK91Q-URA3 <pIP214> <pIP220></i>
PCY44	IPY1131	<i>MATa ura3-52 trp1Δ63 his3-205::HIS3-GFP-LacI leu2Δ1::lacO-LEU2 lys202 (hht1-hhf1)Δ::KanMX (hht2-hhf2)Δ::hhts-HHF2-URA3 <pIP424> <pIP220></i>
PCY45	IPY1132	<i>MATa ura3-52 trp1Δ63 his3-205::HIS3-GFP-LacI leu2Δ1::lacO-LEU2 lys202 (hht1-hhf1)Δ::KanMX (hht2-hhf2)Δ::hhtsK42A-hhfs-URA3 <pIP424> <pIP220></i>
PCY46	IPY1133	<i>MATa ura3-52 trp1Δ63 his3-205::HIS3-GFP-LacI leu2Δ1::lacO-LEU2 lys202 (hht1-hhf1)Δ::KanMX (hht2-hhf2)Δ::hhtsK42Q-hhfs-URA3 <pIP424> <pIP220></i>
PCY47	IPY1134	<i>MATa ura3-52 trp1Δ63 his3-205::HIS3-GFP-LacI leu2Δ1::lacO-LEU2 lys202 (hht1-hhf1)Δ::KanMX (hht2-hhf2)Δ::hhtsG44S-hhfs-URA3 <pIP424> <pIP220></i>
PCY48	IPY1135	<i>MATa ura3-52 trp1Δ63 his3-205::HIS3-GFP-LacI leu2Δ1::lacO-LEU2 lys202 (hht1-hhf1)Δ::KanMX (hht2-hhf2)Δ::hhts-hhfsK44Q-URA3 <pIP424> <pIP220></i>
PCY49	IPY1136	<i>MATa ura3-52 trp1Δ63 his3-205::HIS3-GFP-LacI leu2Δ1::lacO-LEU2 lys202 (hht1-hhf1)Δ::KanMX (hht2-hhf2)Δ::hhts-hhfsL97A-URA3 <pIP424> <pIP220></i>
PCY50	IPY1137	<i>MATa ura3-52 trp1Δ63 his3-205::HIS3-GFP-LacI leu2Δ1::lacO-LEU2 lys202 (hht1-hhf1)Δ::KanMX (hht2-hhf2)Δ::hhts-hhfsG99A-URA3 <pIP424> <pIP220></i>
PCY51	IPY1138	<i>MATa ura3-52 trp1Δ63 his3-205::HIS3-GFP-LacI leu2Δ1::lacO-LEU2 lys202 (hht1-hhf1)Δ::KanMX (hht2-hhf2)Δ::hhts-hhfsK91Q-URA3 <pIP424> <pIP220></i>
PCY52	IPY1139	<i>MATa ura3-52 trp1Δ63 his3-205::HIS3-GFP-LacI leu2Δ1::lacO-LEU2 lys202 (hht1-hhf1)Δ::KanMX (hht2-hhf2)Δ::hhts-HHF2-URA3 <pIP215> <pIP220></i>
PCY53	IPY1140	<i>MATa ura3-52 trp1Δ63 his3-205::HIS3-GFP-LacI leu2Δ1::lacO-LEU2 lys202 (hht1-hhf1)Δ::KanMX (hht2-hhf2)Δ::hhtsK42A-hhfs-URA3 <pIP215> <pIP220></i>

PCY54	IPY1141	<i>MATa ura3-52 trp1Δ63 his3-205::HIS3-GFP-LacI leu2Δ1::lacO-LEU2 lys202 (hht1-hhf1)Δ::KanMX (hht2-hhf2)Δ::hhfsK42Q-hhfs-URA3 <pIP215> <pIP220></i>
PCY55	IPY1142	<i>MATa ura3-52 trp1Δ63 his3-205::HIS3-GFP-LacI leu2Δ1::lacO-LEU2 lys202 (hht1-hhf1)Δ::KanMX (hht2-hhf2)Δ::hhfsG44S-hhfs-URA3 <pIP215> <pIP220></i>
PCY56	IPY1143	<i>MATa ura3-52 trp1Δ63 his3-205::HIS3-GFP-LacI leu2Δ1::lacO-LEU2 lys202 (hht1-hhf1)Δ::KanMX (hht2-hhf2)Δ::hhfs-hhfsK44Q-URA3 <pIP215> <pIP220></i>
PCY57	IPY1144	<i>MATa ura3-52 trp1Δ63 his3-205::HIS3-GFP-LacI leu2Δ1::lacO-LEU2 lys202 (hht1-hhf1)Δ::KanMX (hht2-hhf2)Δ::hhfs-hhfsL97A-URA3 <pIP215> <pIP220></i>
PCY58	IPY1145	<i>MATa ura3-52 trp1Δ63 his3-205::HIS3-GFP-LacI leu2Δ1::lacO-LEU2 lys202 (hht1-hhf1)Δ::KanMX (hht2-hhf2)Δ::hhfs-hhfsG99A-URA3 <pIP215> <pIP220></i>
PCY59	IPY1146	<i>MATa ura3-52 trp1Δ63 his3-205::HIS3-GFP-LacI leu2Δ1::lacO-LEU2 lys202 (hht1-hhf1)Δ::KanMX (hht2-hhf2)Δ::hhfs-hhfsK91Q-URA3 <pIP215> <pIP220></i>
PCY62	IPY1147	<i>MATa ura3-52 trp1Δ63 his3-205::HIS3-GFP-LacI leu2Δ1::lacO-LEU2 lys202((hht1-hhf1)Δ::KanMX)Δ::natMX (hht2-hhf2)Δ::hhfsK42A-hhfs-URA3 <pIP220></i>
PCY63	IPY1148	<i>MATa ura3-52 trp1Δ63 his3-205::HIS3-GFP-LacI leu2Δ1::lacO-LEU2 lys202((hht1-hhf1)Δ::KanMX)Δ::natMX (hht2-hhf2)Δ::hhfs-hhfsK44Q-URA3 <pIP220></i>
PCY64	IPY1149	<i>MATa ura3-52 trp1Δ63 his3-205::HIS3-GFP-LacI leu2Δ1::lacO-LEU2 lys202((hht1-hhf1)Δ::KanMX)Δ::natMX (hht2-hhf2)Δ::hhfs-HHF2-URA3 <pIP220></i>
PCY65	IPY1150	<i>MATa ura3-52 trp1Δ63 his3-205::HIS3-GFP-LacI leu2Δ1::lacO-LEU2 lys202((hht1-hhf1)Δ::KanMX)Δ::natMX (hht2-hhf2)Δ::hhfs-HHF2-URA3 SGO1-13xMyc::KanMX <pIP220></i>
PCY66	IPY1151	<i>MATa ura3-52 trp1Δ63 his3-205::HIS3-GFP-LacI leu2Δ1::lacO-LEU2 lys202((hht1-hhf1)Δ::KanMX)Δ::natMX (hht2-hhf2)Δ::hhfsK42A-hhfs-URA3 SGO1-13xMyc::KanMX <pIP220></i>

PCY67	IPY1152	<i>MATa ura3-52 trp1Δ63 his3-205::HIS3-GFP-LacI leu2Δ1::lacO-LEU2 lys202((hht1-hhf1)Δ::KanMX)Δ::natMX (hht2-hhf2)Δ::hhts-hhfsK44Q-URA3 SGO1-13xMyc::KanMX <pIP220></i>
PCY68	IPY1153	<i>MATa ura3-52 trp1Δ63 his3-205::HIS3-GFP-LacI leu2Δ1::lacO-LEU2 lys202((hht1-hhf1)Δ::KanMX)Δ::natMX (hht2-hhf2)Δ::hhts-HHF2-URA3 SGO1-13xMyc::KanMX <pIP220></i>

Table 2: Plasmid used or made for this study

Name	Relevant genotype	Cloning vector/Restriction site	Reference
pIP90	<i>HHT1-HHF1, LEU2, 2μ</i>	pRS425/ <i>Bam</i> HI, <i>Hind</i> III	Unpublished
pIP114	<i>BIR1, TRP, 2μ</i>	pRS425/ <i>Xho</i> I, <i>Not</i> I	Unpublished
pIP209	<i>SGO1, TRP, 2μ</i>	YEplac112/ <i>Sp</i> HI, <i>Sal</i> I	This study
pIP211	<i>IPL1, TRP, 2μ</i>	pRS424/ <i>Xho</i> I, <i>Not</i> I	This study
pIP213	<i>IPL1, LEU2, 2μ</i>	pRS425/ <i>Xho</i> I, <i>Not</i> I	Unpublished
pIP214	<i>BIR1, TRP, 2μ</i>	pRS424/ <i>Xho</i> I, <i>Not</i> I	This study
pIP215	<i>BUB1, TRP, 2μ</i>	pRS424/ <i>Xho</i> I, <i>Not</i> I	This study
pIP220	<i>HHT1-HHF1, LYS, CEN</i>	pRS317/ <i>Sal</i> I, <i>Not</i> I	This study

Table 3: Primers used for this study

oIP-231	5' CATGATGAAGCGTTCTAAACGCAC 3'
oIP-232	5' TAGCCGTGACGTTTGCGATGTCTT 3'
oIP-326	5' TACAACACTGCTAGGCGCA 3'
oIP-327	5' GTATAATTGACAGCACGAGG 3'
oIP-351	5'GCAGTTGAATACGAATCCCAAATATTTGCTTGTTGTTACGGATCCC CGGGTTAATTAA 3'
oIP-352	5'TTTGTTCGTTTTTTACTAAACTGATGACAATCAACAAAGAATTTCG AGCTC GTTTAAAC 3'
oIP-353	5'CTCCTCATGTCGTTAAAAGCATTGCGAATAGATAGATGAATATCAG GGGCATGATGTGACT 3'
oIP-354	5'CTATCTAAGACAGTTCGGAACTAGTTTCTTTTATTGAGACTTAGC TCGTTTTTCGACACTGGAT3'
oIP357	5'TTCAAAGAAGTTGCCGCCGT3'
oIP358	5'ATGGGTGAGGCCGCAGATTA3'
oIP371	5'GGATGAGGCCGGTGAAAGAGA3'
oIP389	5'GCCCTCGAGTTCTAACGCTGCCAAGATAGA3'
oIP390	5'GTTGCGGCCGCACTACCAGTAACATCCCAA3'
oIP391	GCATATATATGTTTAATTGGGTATAGAGGGGTTATTGTTTGACCATC AGGGGCATGATGTGACT
oIP392	ATAGAAATTATTAAGGAACACCAGGGCAAAAAGACTATATATCAGC TCGTTTTTCGACACTGGAT
oIP393	CGGGCAGTTGAATACGAATCCCAAATATTTGCTTGTTGTTATCAGGG GCATGATGTGACT
oIP394	GTTTTTGTTTCGTTTTTTACTAAACTGATGACAATCAACAAAGCTCG TTTTTCGACACTGGAT
oIP395	ATTCGTCGTCCGATTCGT
oIP396	AAGGCAGTGAAACATCAACCAAAAACATATCGCACCAAAAAACGG ATCCCCGGGTAAATTAA
oIP397	TTTATTATGCAAAAATATAGAAATTATTAAGGAACACCAGGGCGAA TTCGAGCTCGTTTAAC
oIP398	TTGTTGCCAAAGAAGGATGCCAAGGCTACCAAG
oIP399	TTGTTGCCAAAGAAGGAAGCCAAGGCTACCAAG
oIP-400	TTGTTGCCAAAGAAGGCTGCCAAGGCTACCAAG

IV. RESULTS

Strain construction and library screening

A yeast strain was constructed to serve as a host for screening a library of histones H3 and H4 mutants. The goal was to identify specific amino acids in H3 and H4 that would affect chromosome segregation and genome integrity, with particular emphasis in ploidy maintenance. For this purpose yeast strain IPY1008, carrying deletions of the two chromosomal copies of the genes that encode histones H3 and H4, was constructed. In addition, this strain was engineered with a GFP-tagged centromere that allowed the visualization of chromosome segregation in these cells. The strain also carries a plasmid with a wild-type copy of *HHT1-HHF1*, encoding histones H3 and H4, which makes the cell viable and allows for shuffling the wild-type copy with mutant copies of H3 and H4. Strain IPY1008 was transformed with each of the H3 and H4 486 mutants present in the synthetic library. The Trp⁺ transformants were allowed to lose the wild-type plasmid pIP220 (Figure 1). The resulting 486 mutant strains that carried an episomal copy of the synthetic histone H3 and H4 mutant library plasmids in the haploid IPY1008 strain were subjected to phenotypic screening by plating them on media at different temperatures or containing various drugs. (The library mutants that are reported to be lethal to yeast were not used for IPY1008 transformation). This screening was done in 96 well plates and in 3 replicates. Ninety mutants that were sensitive to benomyl (15 µg/ml), hydroxyurea, canavanine, 13 °C or 37°C were selected for further studies. Benomyl affects the polymerization of microtubules[102, 103]. Strains that have problems in chromosome segregation are usually more sensitive to the presence of a drug that affects the function of microtubules. Hydroxyurea inhibits the enzyme ribonucleoside diphosphate, in turn affecting the production of deoxyribonucleostides from ribonucleotides, a necessary step for DNA synthesis[104]. Any mutants that have a defect in S phase will be more sensitive to hydroxyurea than the ones that have normal DNA synthesis. In

order to analyze the ploidy status of the mutants and determine whether they have a cell cycle defect that affects their genome, the DNA content of the ninety strains was determined by flow cytometry. Most of the mutants did not show any obvious ploidy defect. About thirty-four mutants among the ninety strains tested showed clear ploidy defects or what appeared an emerging diploid phenotype. All these mutants were propagated for six passages (see Methods) and re-tested for the growth and drug sensitivity phenotypes, and by flow cytometry to clarify the ploidy phenotype. The results for the H3 mutants are shown in Figure 2, 3 and 4 and for the H4 mutants in Figure 5, 6 and 7. In addition, these mutants were tested on galactose (YPGal) and glycerol (YPG) containing medium as the only source of carbon source. These are commonly used for screening mutations that may affect transcription of genes involved in carbon source utilization and respiration, respectively. In this screen, the mutants were tested on these media to assess pleiotropic phenotypes that may not relate to chromosome segregation. Strains that cannot utilize a fermentable carbon source like galactose for ATP production will be sensitive in media that have only galactose as a carbon source. Similarly, mitochondrial activity of the mutants was investigated by letting them grow on a non-fermentable carbon source like glycerol. None of the thirty-four mutants showed growth defects on YPGal or YPG (Figure 8 and 9). Based on the results of the phenotypic analysis of drug sensitivity, temperature sensitivity, ploidy, and flow cytometric analysis of the thirty-four mutants, six strains that showed consistent and severe phenotypes on benomyl plates, hydroxyurea, and ploidy maintenance were selected for further analysis. The mutations reside in two amino acids positions in histone H3, with two replacements in the same lysine at position 42; H3K42A, H3K42Q, and H3G44A, and three amino acid positions in histone H4; H4K44Q, H4L97A and H4G99A. To visualize the spatial distribution of these mutations in the nucleosome structure, they were identified in the model of

the yeast nucleosome available from crystallographic data (Figure 10). The location of the amino acid replacements of the mutants in the nucleosome model showed an interesting pattern. The histone H3 and H4 mutations are clustered in two regions of the nucleosome, suggesting that the nucleosome has structurally defined areas that are especially susceptible to chromosome segregation defects. One region is near the DNA entry/exit point (H3K42, H3G44, H4K44), and close to the surrounding DNA (H3K56), and the other region is located toward the center of the nucleosome (H4K91, H4R92, H4L97, H4G99).

To characterize these mutants, the episomal alleles were integrated into the chromosomal locus of the *hht1-hhf1* genes in the haploid IPY1044 strain. The integrated alleles were then re-tested for their initial phenotypes and used for further characterization of their chromosome segregation phenotypes. All six mutants carrying the integrated alleles retained their phenotypes, as seen in Figures 11, 12 and 13.

Characterization of the H3 and H4 mutants

The six histone H3 and H4 mutants were studied extensively throughout a cell cycle to understand the cause of the phenotypes observed. The strains were synchronized in G1 with alpha mating factor and at each designated time the growth, cell morphology, centromere localization, and DNA content of the cells were analyzed. The wild type strain cycles normally in 93 minutes (Figure 14), but both substitution mutants H3K42A and H3K42Q were delayed at the G₂/M phase of the cell cycle, reflected in the number of cells with large buds and undivided nucleus, shown by DAPI staining (Figure 18, 20 and 27). It is also interesting to note that some of the synchronized cells at time zero started as a diploid and progressed throughout the cycle as

such. At the end of three hours, many three to four GFP-centromere dots were seen, representing diploid cells and chromosome missegregation (Figure 18, 20). This is consistent with the canavanine assay and flow cytometry data, indicating that this mutant has completely diploidized. Although H3K42 has been reported as a site of histone methylation [105], the absence of this modification does not appear to be the cause for the increase in ploidy problem of the strains, since it is not seen in the H3K42R mutant, which still retains the positive charge of the lysine residue with no chance of methylation. H3K42R behaves perfectly normal like the wild type strain (Figure 19). The Pds1 stability assay was used to determine the response of the mutants to the spindle assembly checkpoint proteins. When the cells exit from metaphase, checkpoint proteins allow the cell to move to anaphase only when chromosomes are properly attached to the centromere and there is enough bipolar tension. The Pds1p protein dissipates when the cells move from metaphase to anaphase, the details of this mechanism has been described in the Literature Review section. The time of disappearance of Pds1p reflects the status of the G₂/M checkpoint in the cell. The abnormally long stability of Pds1p in H3K42A indicates that some defects in the cell have activated the checkpoint (Figure 28). The chromosomes either are not attached to the spindle properly or there is not enough tension sensed by the kinetochore proteins. The checkpoint machinery has halted the cell cycle to allow the cell time to repair the problem. This usually results in large budded cells that do not distribute the chromosomes to the daughter cells. Although H3K42Q is cycling, there is no complete dissipation of Pds1p. This reflects the incapability of H3K42Q cells to detect the chromosome segregation problem. Nocodazole, a drug that interferes with microtubule polymerization, usually halts the cells at the G₂/M checkpoint. Absence of that stop signal indicates faulty checkpoint proteins that are unable to activate a surveillance system even in the case of a

problem. In the presence of nocodazole treatment both mutants, H3K42A and H3K42Q, show a stable Pds1p, indicating that the checkpoint is functional in both strains (Figure 28).

Only two amino acid residues apart, the H3G44A replacement also has an increase-in-ploidy phenotype. This mutation also causes a slow growth rate like the mutants discussed above. Even though it has a mixed population of haploids and diploids from the beginning of the cell cycle study, unlike others it seems to have no G2/M checkpoint halt as seen in the Pds1p stability assay (Figure 21, 27 and 28). This result would indicate a faulty tension sensing system in this mutant. The checkpoint proteins are functional, seen as the cells halting at metaphase with the nocodazole treatment.

The next amino acid replacement that was studied is histone H4K44, which when placed in the nucleosome model, is in close proximity to the H3 mutants described above, at the DNA entry/exit point of the nucleosome. The H4K44Q has the slowest growth of all the mutants studied. This mutant appears to have become a stable diploid, as seen by the two GFP dots at the beginning of the cycle (Figure 23). In the Pds1p stability assay, it showed a checkpoint arrest both with and without nocodazole treatment (Figure 28). This amino acid position with other substitutions, like H4K44A, did not show any delay in growth or problem in chromosome number. On the other hand, H4K44R had some minor problems as seen in Figure 24, where it showed minor sensitivity at 13 °C and in presence of benomyl and hydroxyurea (Note: The GFP tagged centromere study of H4K44R did not work well. After 180 minutes the cells gave some blurred GFP images making it difficult to distinguish the signal, and is not included in this study). H4K44 is a site of methylation, which in turn affects methylation of H3K36 by Set1p [106, 107]. H4K44R mimics the non-methylated state of this residue, suggesting that the modification is not essential for the role of H4 in cell division. The viability assay of all the

mutants showed in Figure 16 indicates a large amount of dead cells in H4K44Q, compared to the wild type and other mutants.

In the central region of the nucleosome, H4L97A is the other mutant that had a slow growth phenotype and had many cells with large buds and undivided chromosomes (Figure 15, 25). There is an evident ploidy problem in the cells at the end of the cell cycle (three or four GFP tagged signal at centromeres), showing higher ploidy (2C and 4C) as well as aneuploidy (Figure 27). Pds1p is stable throughout the time period of assay, showing the same profile with and without treatment with nocodazole, indicating that the checkpoint has been activated in this mutant and remains active throughout the cycle.

H4G99A has a growth rate similar to the normal wild type cells (Figure 15). The strain did show an obvious ploidy defect by flow cytometry and centromere visualization with GFP. It also showed aneuploidy and some minor ploidy increase (Figure 26, 27). This mutant displays a strong sensitivity to benomyl as well hydroxyurea, and the flow cytometry data indicate some delay in S phase, which is in agreement with the hydroxyurea sensitivity. Thus, it appears that this mutant may start with defects during DNA replication that extend to mitosis, but is not delaying anaphase, based on the dissipation of Pds1 (Figure 28). Therefore, the defects are not relayed to the G₂/M checkpoint, or the cell senses that most of the problem is fixed and continues with the cycle.

Interaction of histone H3 and H4 mutants with Sgo1.

Recently, it was reported that H3G44S has an impaired tension sensing ability, most likely due to improper recruitment of Sgo1p to the kinetochore, and when Sgo1 was expressed in high dosage, it was able to suppress its mutant phenotype [108]. Sgo1p is an important member

of the checkpoint proteins that sense tension at the kinetochore during chromosome segregation. The mutants H3K42 (A/Q), H3G44 (A) and H4K44 (Q) that we are studying are either at the same position in H3 (H3G44A) or near to that position in the nucleosome (H3K42 and H4K44). Therefore, we reasoned that overexpression of Sgo1 may also suppress the mutations we are studying in this region. We tested this possibility by introducing a plasmid that expresses *SGO1* in high copy, from a yeast 2 μ m plasmid, into each of the mutant strains, including H4L97A and H4G99A, located toward the center of the nucleosome. The transformants were tested for their phenotypes on plates as well as their DNA content by flow cytometry. When Sgo1p was overexpressed in H3K42A, H3K42Q, H4G44A and H4K44Q, it completely suppressed the benomyl sensitivity (Figure 29, 30 and 31), as well as the ploidy increase, as shown by flow cytometry. However, the same over expression of Sgo1p in H4L97A and H4G99A had no suppressor effect on these mutants, differentiating them functionally from the above group (Figure 29, 30 and 31). These results not only confirm the relevance of the H3G44 position but also expand it to include H3K42 and H4K44 in their functional interaction with Sgo1. Moreover, they emphasize the unique requirement of the structure of nucleosome at the DNA entry/exit point (where H3K42, H3G44 and H4K44 reside), which is necessary for error free tension sensing during chromosome segregation.

To better understand the interaction between Sgo1p and the H3K42A/Q, H4G44A and H4K44Q mutants, strains that carried both, the H3 or H4 mutations and a deletion of *SGO1* were created. If Sgo1p were solely responsible for the inability of the mutants for erroneous chromosome distribution, then removal of this protein would be fatal for the strains carrying the histone mutations in combination with an *sgo1* deletion. Analysis of these mutants showed no

exacerbation of their phenotypes, indicating no direct effect of removing Sgo1p on these mutants (Figure 32, 33 and 34).

Previous investigations on H3G44S revealed a reduced level of Sgo1p at the pericentromeric region in this mutant [108]. To understand the effect that not only this particular residue (H3G44), but the whole region of DNA entry/exit play in establishing the association of Sgo1p with the pericentromere, a ChIP analysis was performed on the H3K42A and H4K44Q mutants from this particular region of the nucleosome. Both mutants showed a pronounced decrease of Sgo1p in the centromeric as well as pericentromeric region of chromosome III (Figure 35).

Interaction of H3 and H4 mutants with Ipl1 and Bub1 kinases.

Ipl1 kinase is an important protein for the proper distribution of chromosomes during cell division, and is necessary for the survival of the cell [100, 109]. This protein is particularly important during chromosome segregation when there is improper tension between sister chromatids [69, 77, 110]. There is also a report on the role of Sgo1p in recruiting this kinase to the centromere in human and fission yeast [83]. To investigate whether this protein can compensate for the defects caused by the histone H3 and H4 mutants, an over expression study of both Ipl1p and Bir1p (a component of chromosomal passenger complex, along with Ipl1 and Sli15) was separately conducted on all the above H3 and H4 mutants (Figure 36, 37 and 38). No striking effect was seen on the mutants, however, it cannot be ruled out that even if Ipl1 is overexpressed, it may not be functionally active as a kinase in the absence of overexpression of all the other members of the chromosomal passenger complex.

The H3K42, H3G44, H4K44 mutants seem to have a defect in tension sensing during mitosis. Bub1 kinase is a spindle checkpoint protein that is not only required to form a functional mitotic checkpoint complex but also reported to phosphorylate histone H2A S121[28, 73, 74]. The phosphorylation by Bub1 kinase regulates the pericentromeric localization of Sgo1p. Analysis of the location of the H3K42, H3G44, and H4K44 on the nucleosome model revealed that these residues are very close to H2A S121 (Figure 39). To understand the role that Bub1 may play on these mutants, and to assess whether the mutants may cause decreased phosphorylation of H2A S121, an overexpression study was done by expressing *BUB1* in a yeast 2 μ m plasmid. The data showed no striking effects on the mutants, assessed by benomyl and hydroxyurea sensitivity as well as flow cytometric analysis (Figure 40, 41 and 42). These results can be interpreted in two different ways. On one side, the structural changes in the structure of the nucleosome caused by the H3 and H4 mutations may render the H2A S121 abnormally positioned to serve as a substrate for Bub1. On the other hand, Bub1 is known to interact with other proteins, which may also need to be overexpressed to become a functional kinase.

A closer look at the nucleosome structure revealed potential interactions between the mutated residues and the neighboring environment that may lead to the structural perturbations responsible for the observed phenotypes. H3K42 forms hydrogen bonds with H3G44, H3T45 and to the surrounding DNA. Although H3K42A and H3K42Q can form hydrogen bonds with H3G44 and H3T45, they may distort the association with DNA. This distortion becomes even more apparent for H3K42Q, which shows the potential formation of an additional hydrogen bond with the DNA (Figure 43). The H3K44 residue does not normally form hydrogen bonds with the surrounding amino acids, however, H4K44Q, unlike the wild type H4K44, may form hydrogen bonds with both H3 and H2A residues, deforming the normal nucleosome structure especially at

the critical DNA entry/exit point (Figure 44). In the case of H4L97, its position in the center of the nucleosome flanked by H4T96 and H4Y98, which form hydrogen bonds with H3, must have a strong influence in the association and stability of the four histones (Figure 45). Thus, the H4L97A replacement may result in an overall shift in the structure of the nucleosome, with specific and negative consequences in the interactions needed for normal chromosome segregation.

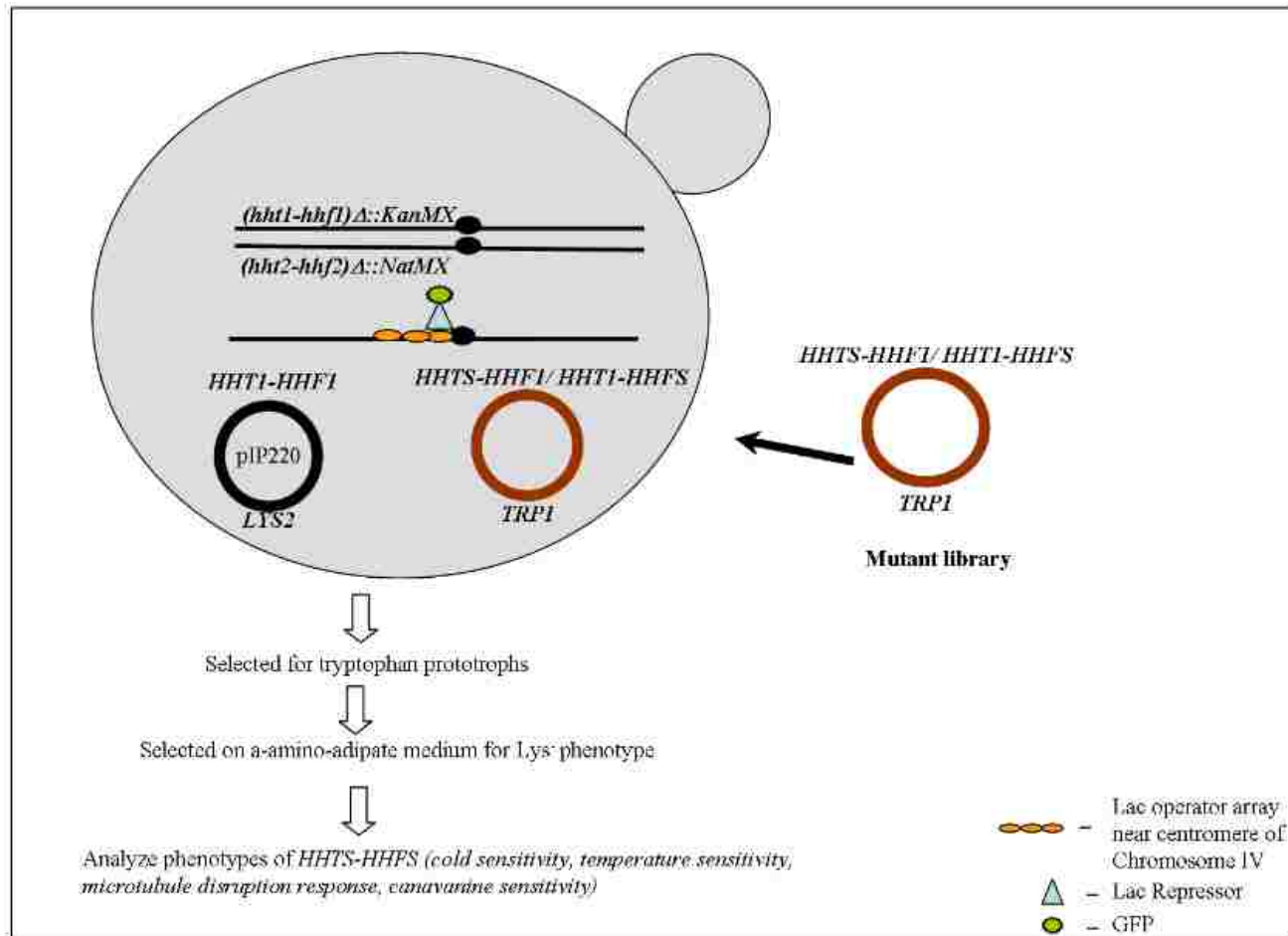


Figure 1: Library screen. *HHT1-HHF1* and *HHT2-HHF2* were first deleted from the chromosome. Viability is maintained with a plasmid carrying a wild type copy of histones H3 and H4 encoding genes (*HHT1-HHF1*) on a *LYS2* plasmid (pIP220). The diagram shows the steps followed to screen the mutant H3 and H4 histone library. *HHTS* and *HHFS* denote the synthetic H3 and H4 genes that constitute the library.

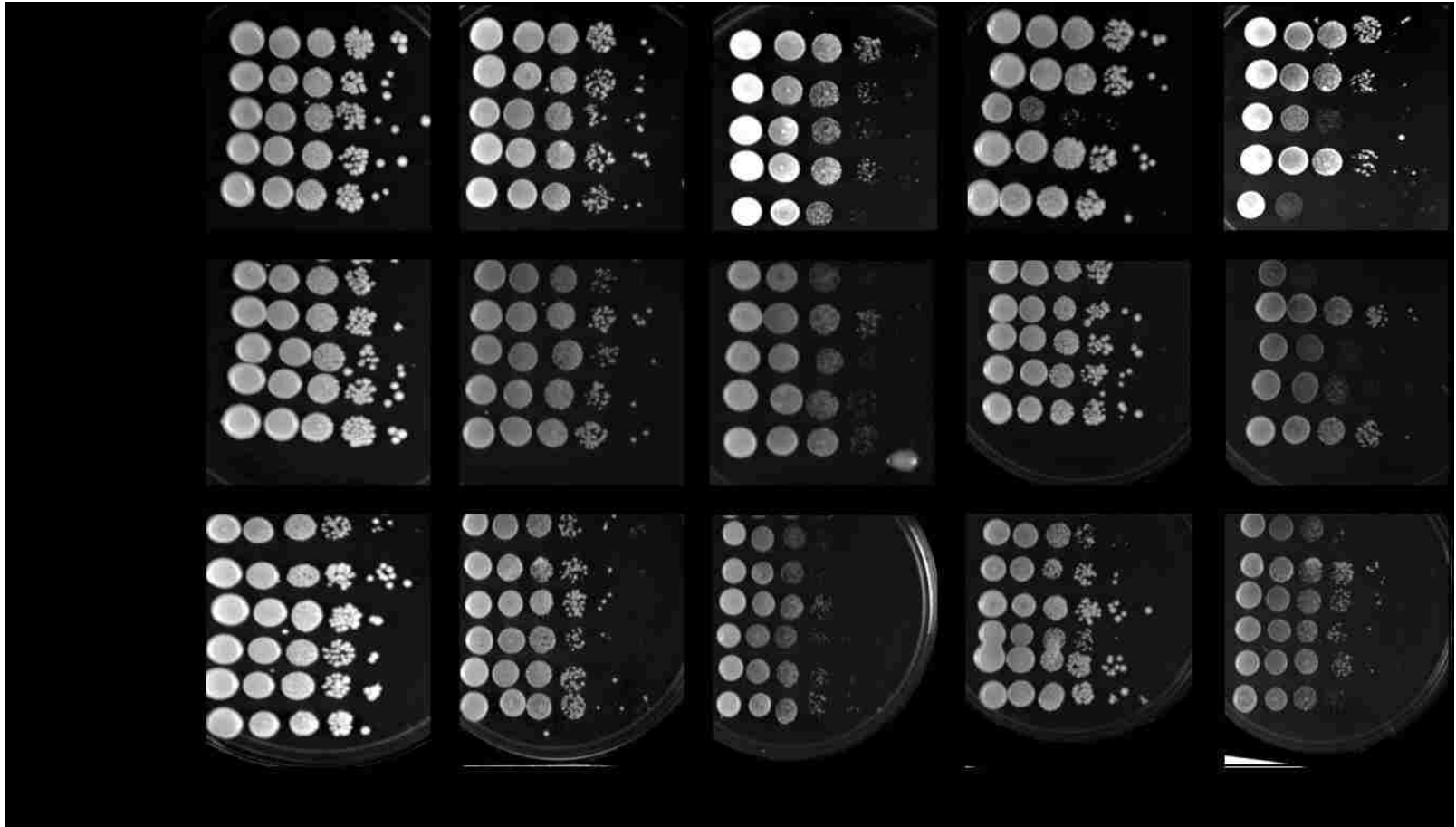


Figure 2: Sensitivity tests on plasmid expressing H3 mutants. A tenfold serial dilution of the H3 mutants was spotted on various plates starting with 10^8 cells/ml. H3K42Q and H3G44A are very sensitive to Benomyl (Ben) and Hydroxyurea (HU). Unless otherwise stated the cells were grown on YPD and the temperature was 26 °C.

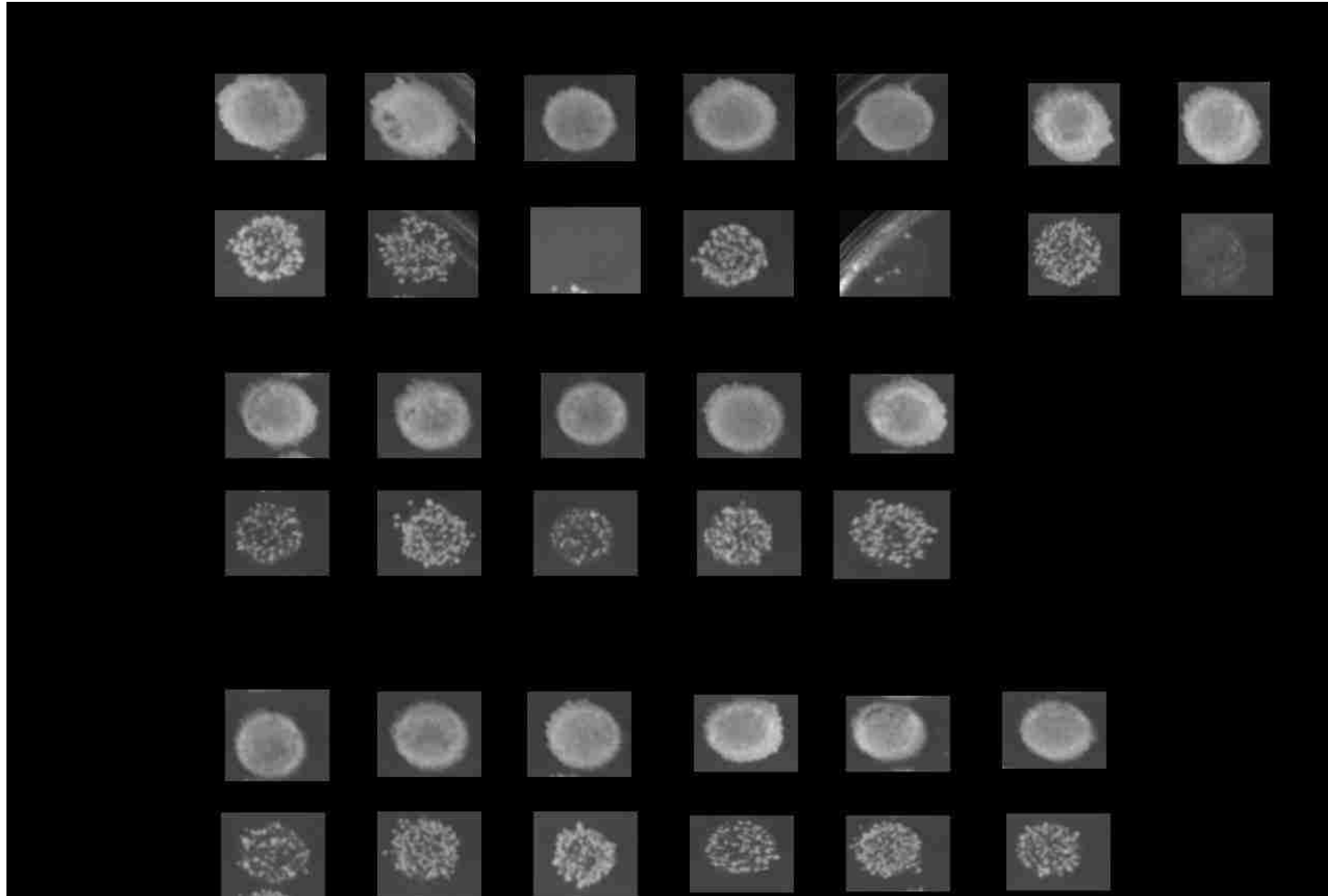


Figure 3: Canavanine assay of strains with plasmids expressing H3 mutants. Overnight grown cultures of the indicated mutants were plated on both SC-Arg (arginine) plates with or without canavanine, irradiated with UV, and incubated for 5 days at 26 °C. H3K42Q and H3G44A behave as the diploid strain, suggesting an increase in ploidy phenotype.

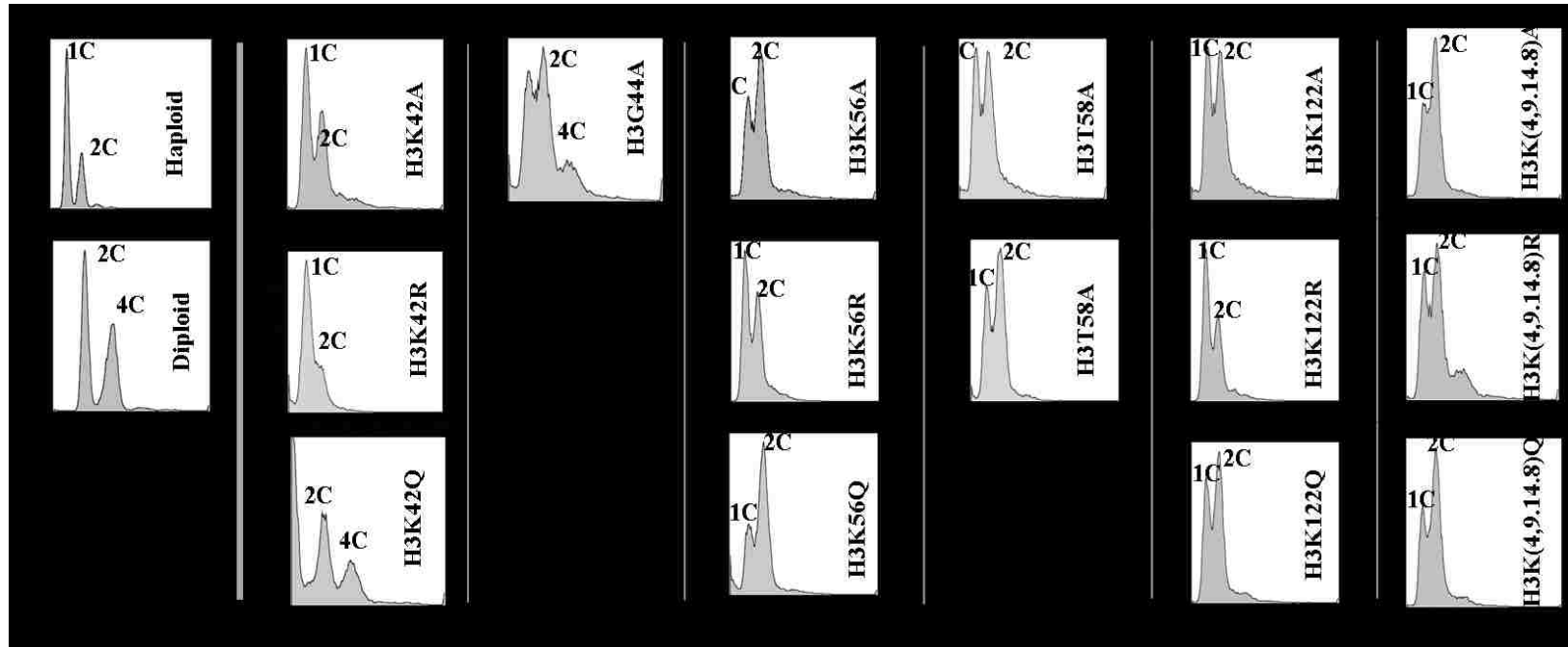


Figure 4: DNA content analysis by flow cytometry of the strains carrying the plasmids expressing H3 mutants. Only H3K42Q and, H3G44A show increase in ploidy.

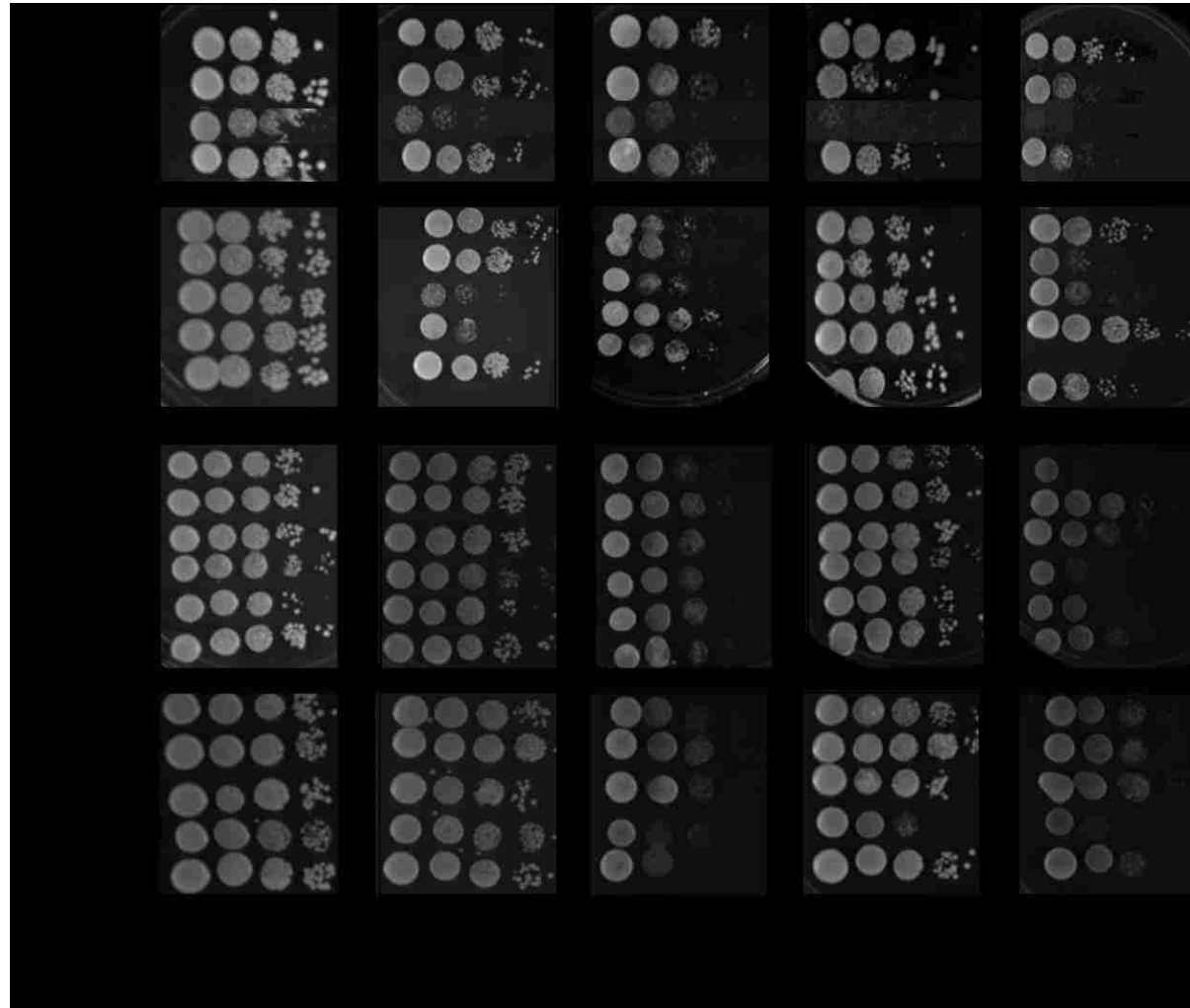


Figure 5: Sensitivity tests on plasmids expressing H4 mutants. A tenfold serial dilution of the H4 mutants was spotted on various plates starting with 10^8 cells/ml. H4K44Q and H4L97A are sensitive to Benomyl (Ben) and Hydroxyurea (HU). H4D85A/N, H4V88A and H4K91Q are sensitive to Hydroxyurea only. Unless otherwise stated the cells were grown on YPD and the temperature was 26 °C.

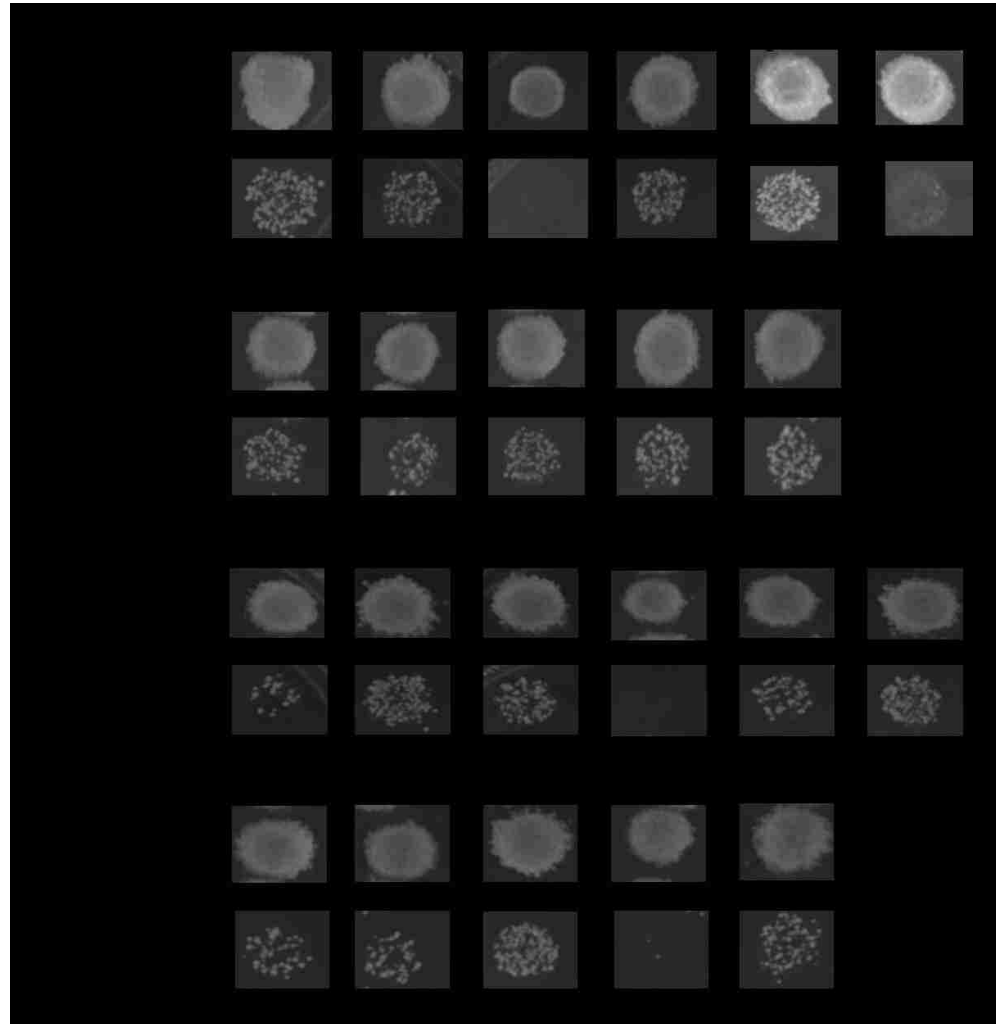


Figure 6: Canavanine assay of strains with plasmids expressing H4 mutants. Overnight grown cultures of the indicated mutants were plated on both SC-Arg (arginine) plates with or without canavanine, irradiated with UV, and incubated for 5 days at 26 °C. H4K44Q, H4K91Q, and H4L97A behave as the diploid strain, suggesting an increase in ploidy phenotype.

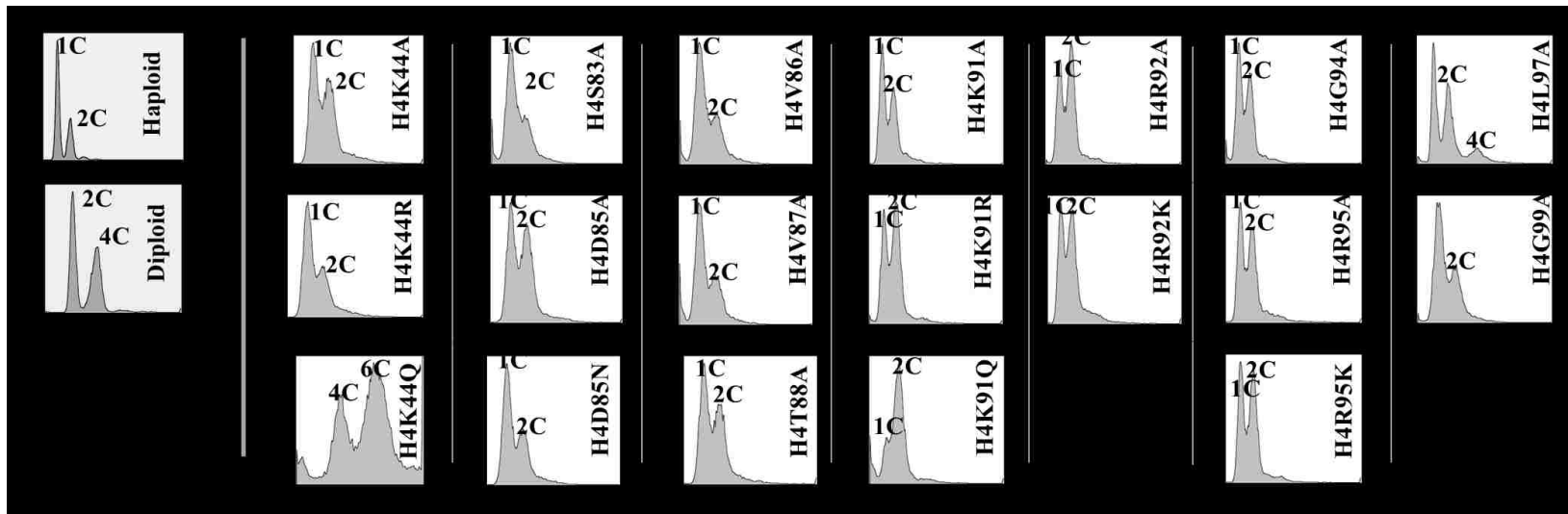


Figure 7: DNA content analysis by flow cytometry of the strains carrying the plasmids expressing H4 mutants. H4K44Q and H4L97A show an increase in ploidy.

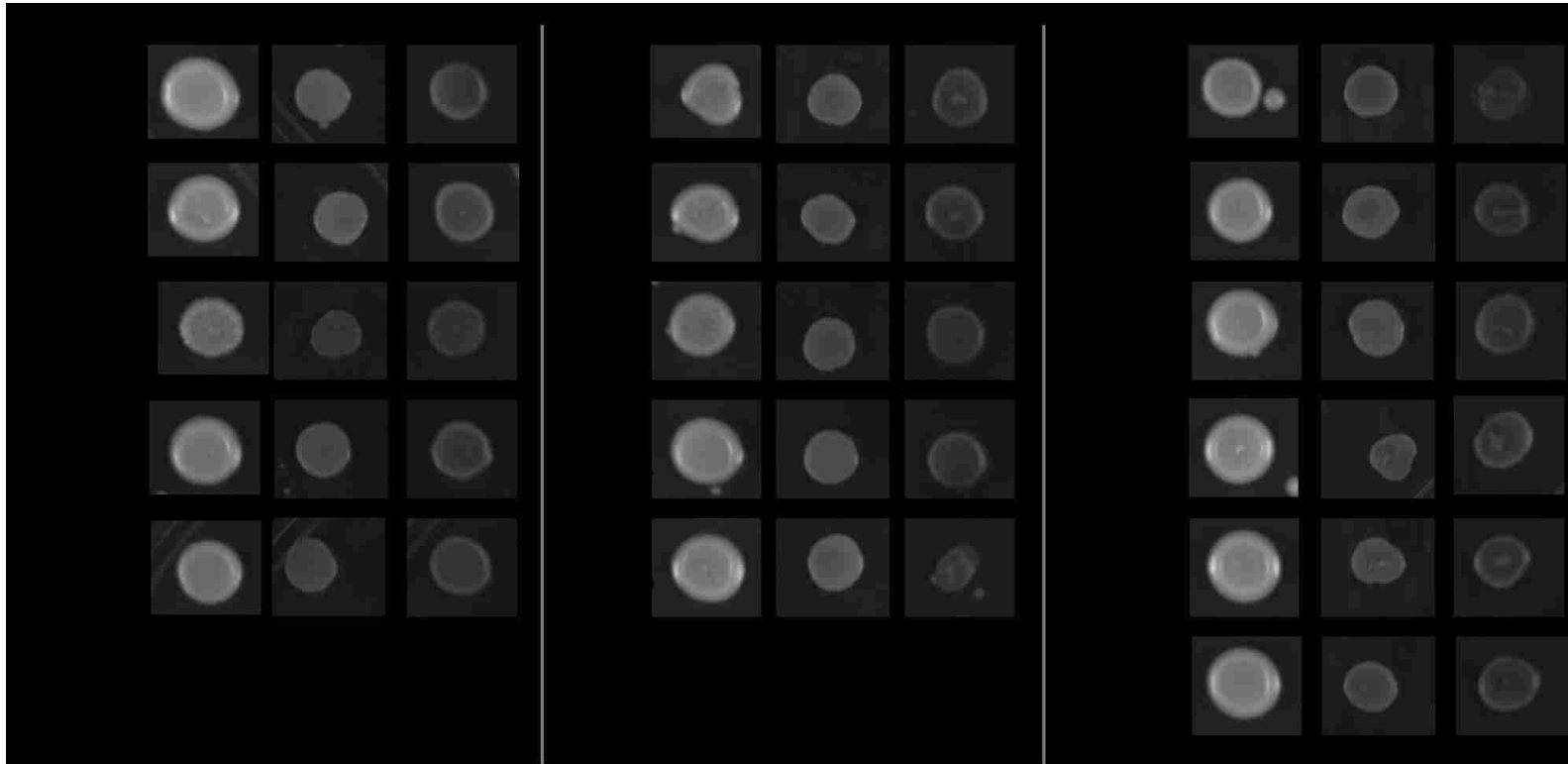


Figure 8: Carbon source assay of strains with plasmids expressing H3 mutants. Overnight grown cultures of the mutant strains were plated on YPD, YP+Glycerol and YP+Galactose plates. Picture was taken after 3 days of incubation at 26 °C. None of the mutants display growth problems on fermentable and non-fermentable carbon source.

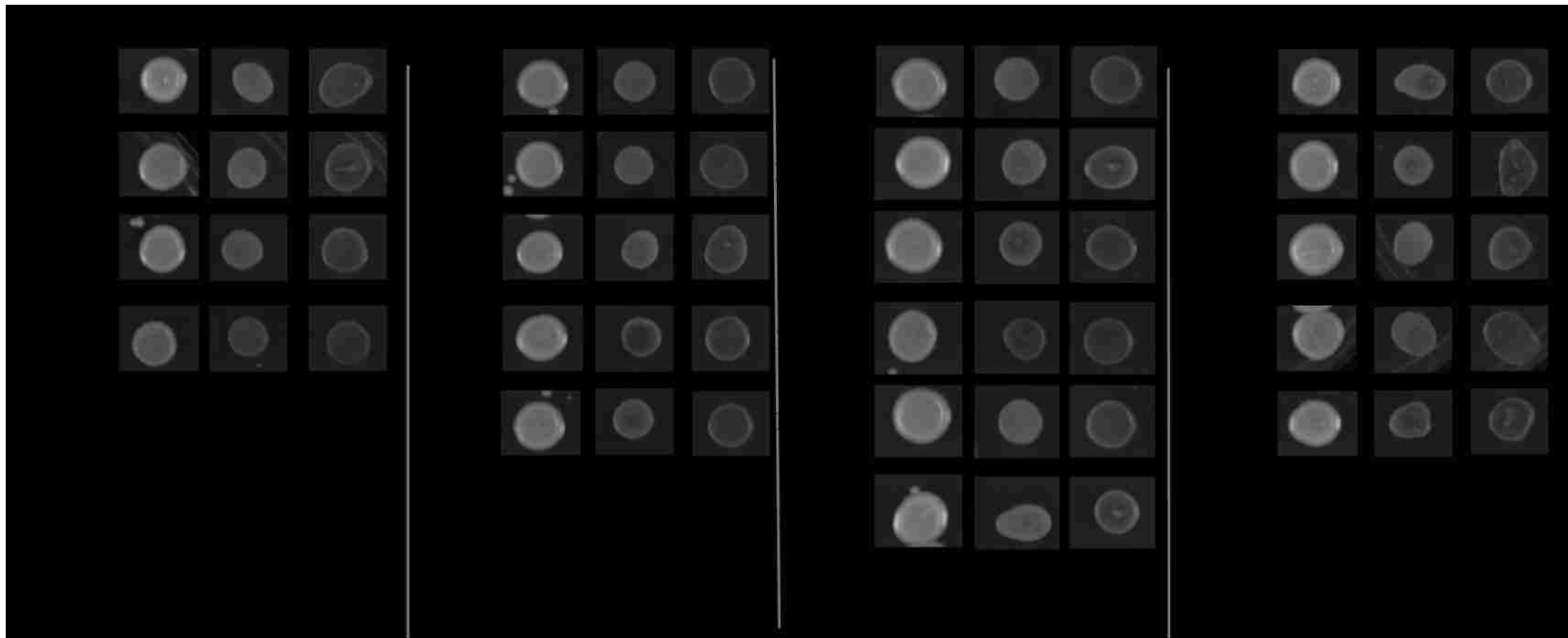


Figure 9: Carbon source assay of strains with plasmids expressing H4 mutants. Overnight grown cultures of the mutant strains were plated on YPD, YP+Glycerol and YP+Galactose plates. Picture was taken after 3 days of incubation at 26 °C. None of the mutants display growth problems on fermentable and non-fermentable carbon source.

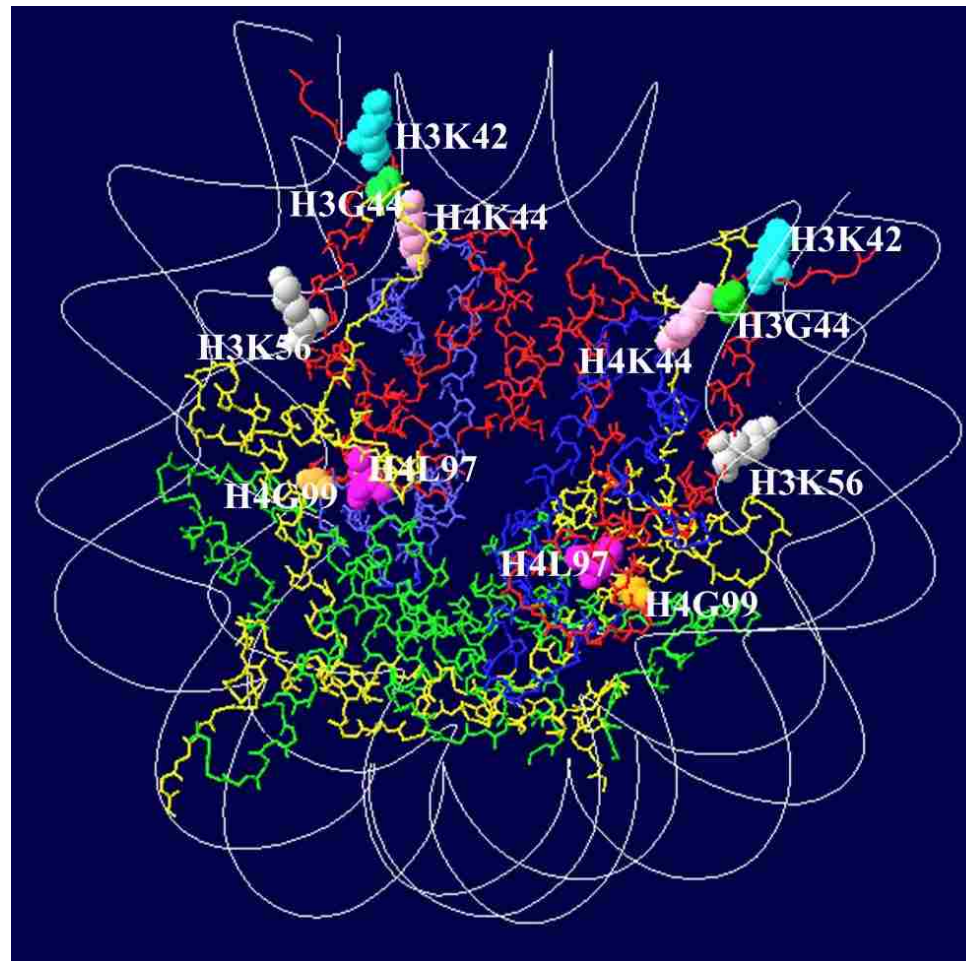


Figure 10: Nucleosome structure based on yeast crystallographic data. The location of the different H3 and H4 amino acid mutations selected from the initial plasmid expression study are highlighted. The four histone proteins are shown as wires: H4, blue; H3, red; H2B, green; and H2A, yellow. The nucleosome model was developed in Swiss PDB viewer 4.04V.

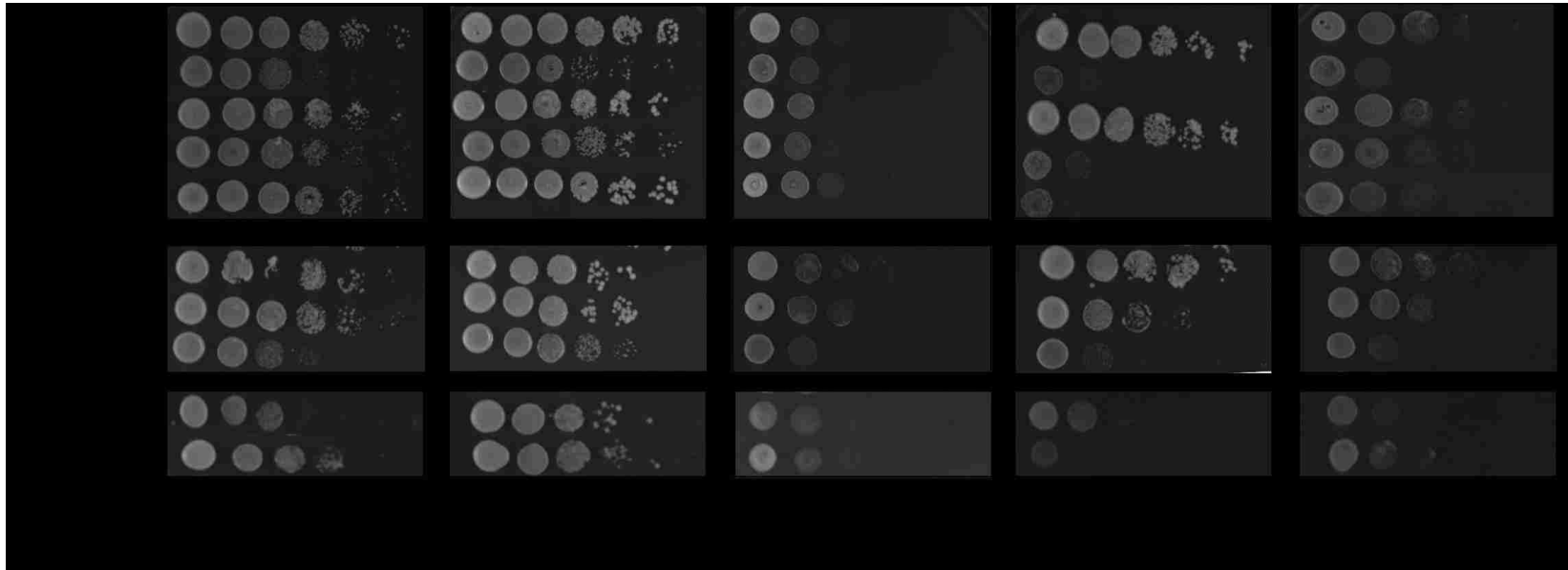


Figure 11: Sensitivity tests on integrated H3 and H4 mutants. Tenfold serial dilution of the above mutants was spotted on various plates starting with 10^8 cells/ml. H3K42Q, H3G44A, H4K44Q, and H4L97A, consistent with the plasmid expression studies, show sensitivity to Benomyl (Ben) and Hydroxyurea (HU). In addition, H3K42A and H4G99A integrated strains also show sensitivity to Benomyl and Hydroxyurea. Unless otherwise stated the cells were grown on YPD and the temperature was 26 °C.

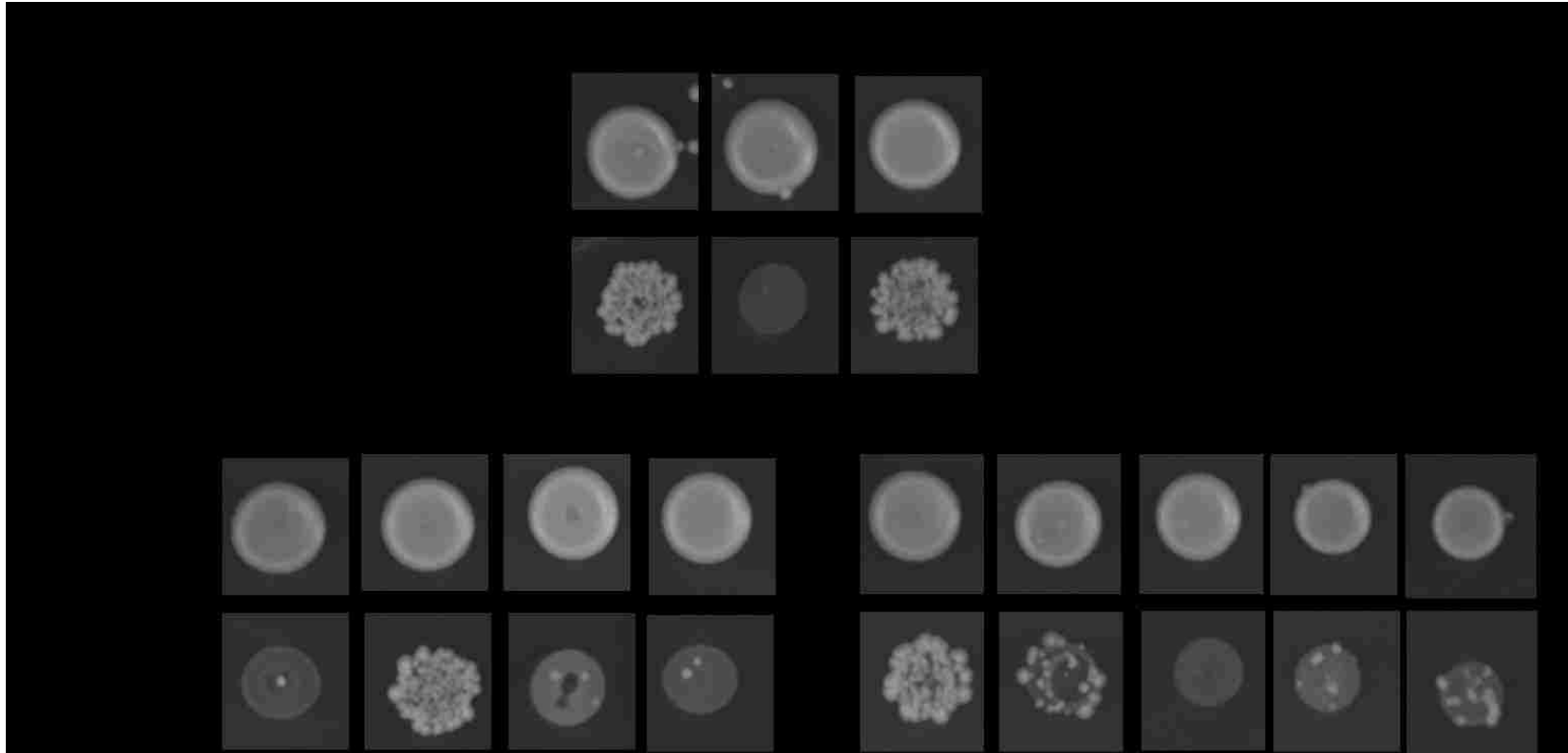


Figure 12: Canavanine assay of integrated H3 and H4 mutants. Overnight grown cultures of the indicated mutants were plated on both SC-Arg (arginine) plates with or without canavanine, irradiated with UV, and incubated for 5 days at 26 °C. H4K44Q, H4K91Q and H4L97A behave as diploid indicating an increase in ploidy phenotype.

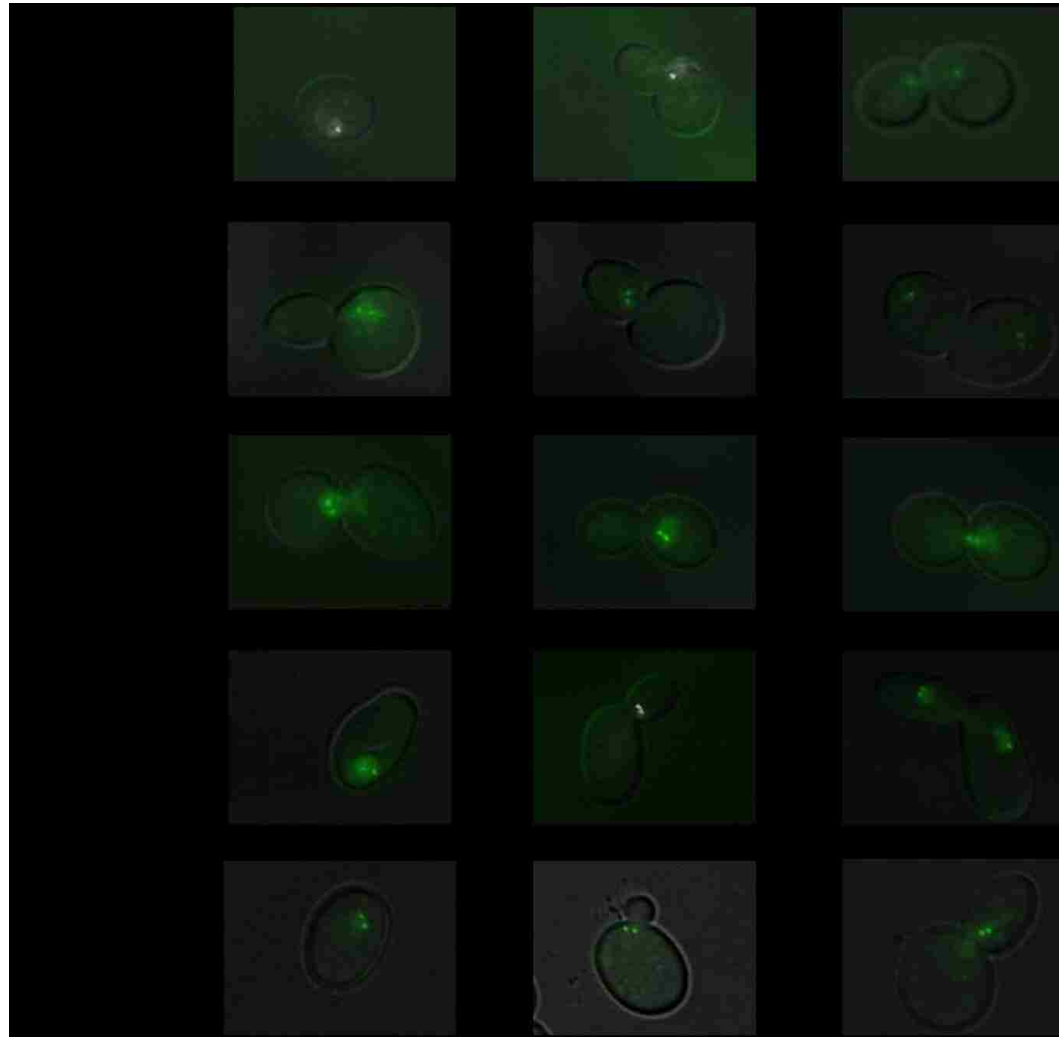


Figure 13: Analysis of GFP-tagged centromeres of the H3 and H4 mutants. Exponentially growing cells on YPD were imaged with a fluorescent microscope Axio Imager M1 (Zeiss). Images were merged with the whole cell image visualized with differential interference contrast (DIC).

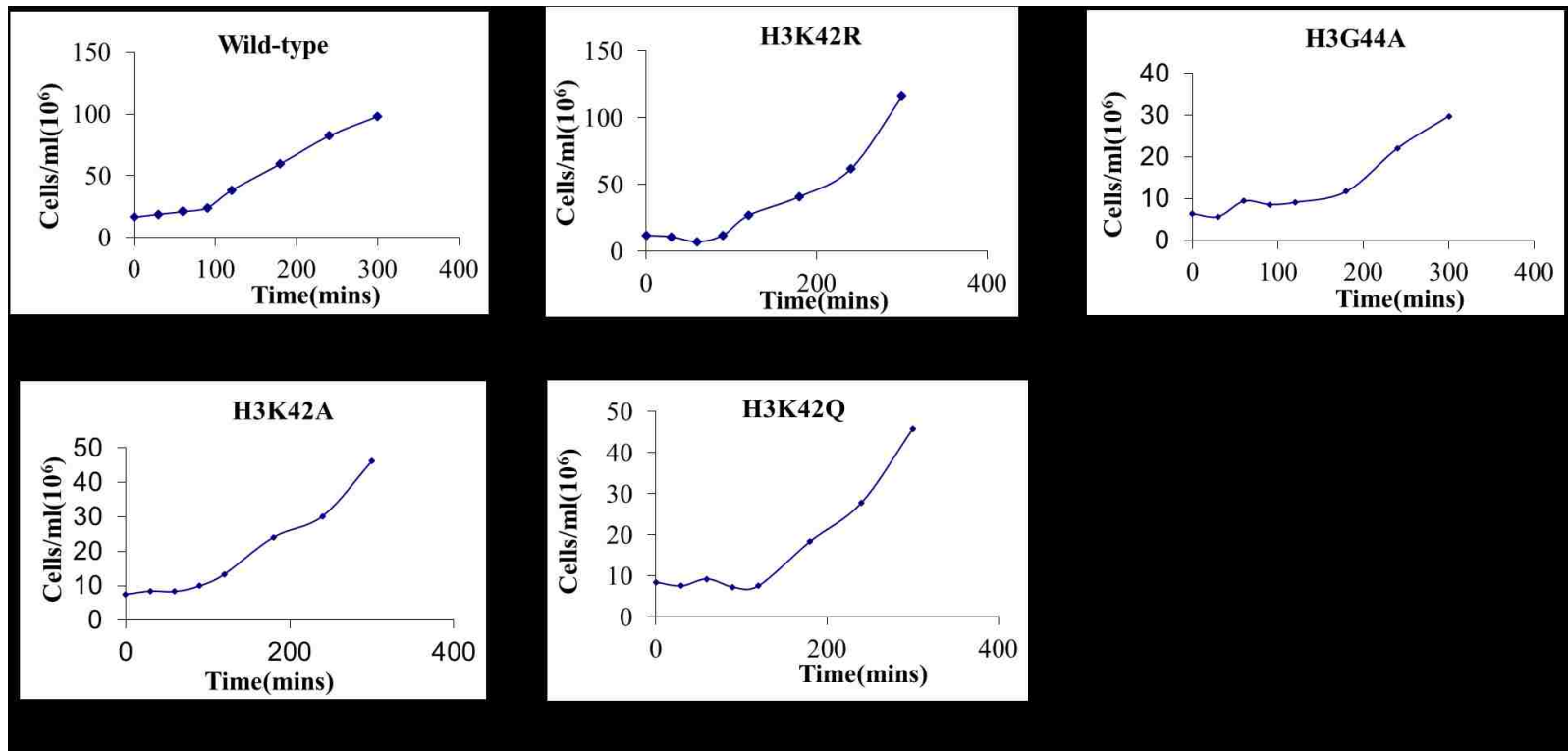


Figure 14: Growth rate of wild type and H3 mutant strains. Exponentially growing cells were synchronized with the mating pheromone alpha-factor and cells were counted with a hemocytometer at the indicated time points. Doubling time is calculated based on their growth rate. DT-Doubling Time.

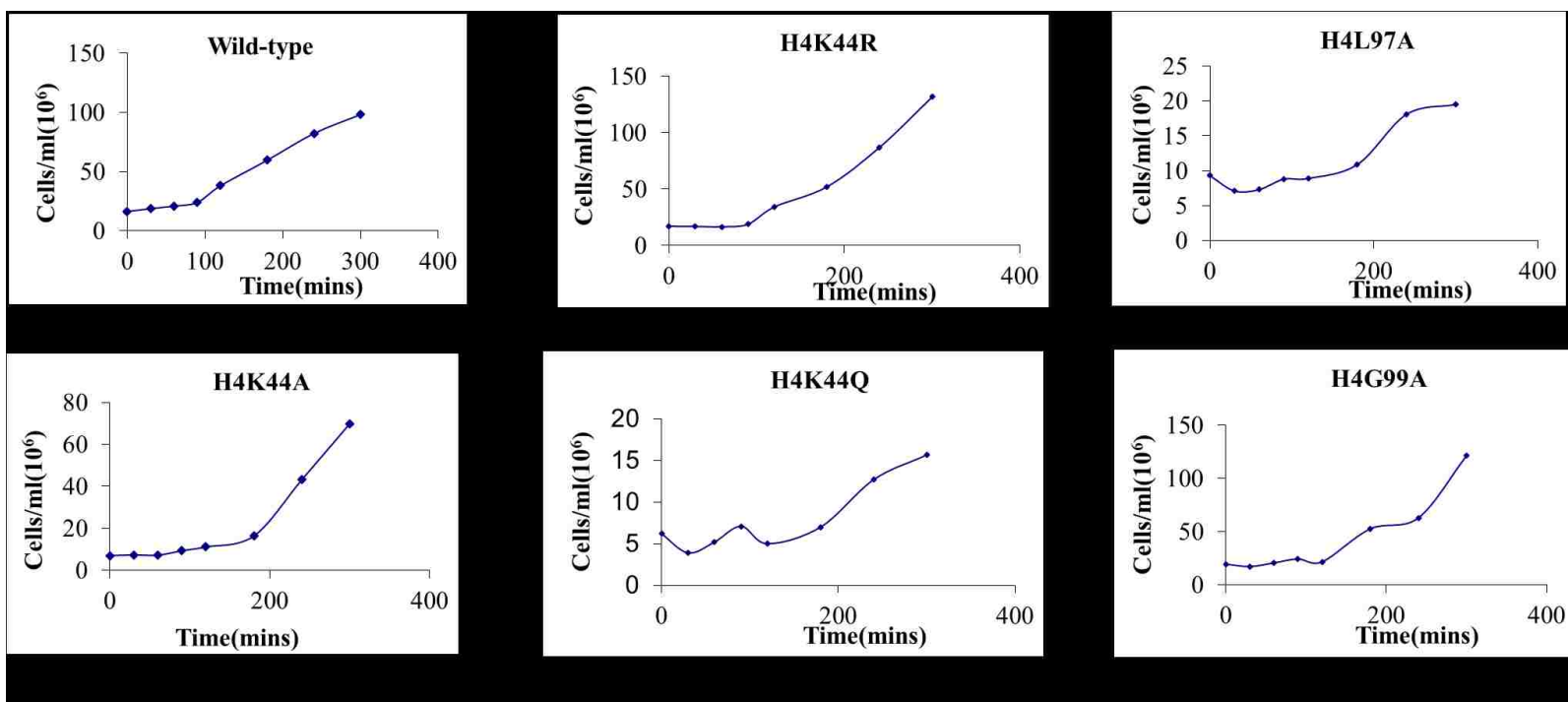
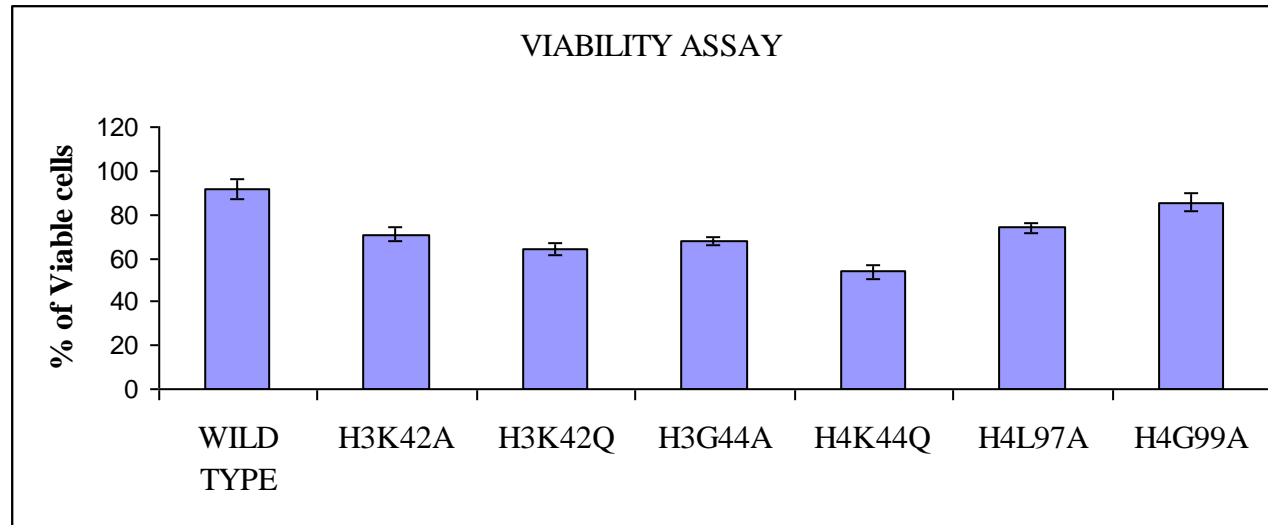













Figure 15: Growth rate of wild type and H4 mutant strains. Exponentially growing cells were synchronized with the mating pheromone alpha-factor and cells were counted with a hemocytometer at the indicated time points. Doubling time is calculated based on their growth rate. DT-Doubling Time.



62

Figure 16: Viability assay of mutants. Cell viability of wild type and mutant strains shown as percent of wild type. Two hundred and fifty cells were plated on YPD and kept at 26 °C. Viable colonies were counted after 3 days. Error bars indicate standard error from four independent experiments.

Time after α factor release	UNBUDED		BUDED								
			Small Bud	Small Bud	Small Bud	Large Bud					
											
1. 0 min	82	0	10	8	0	0	0	0	0	0	0
2. 30mins	98	0	2	0	0	0	0	0	0	0	0
3. 60 mins	3	0	51	45	0	1	0	0	0	0	0
4. 90 mins	27	0	36	36	0	1	0	0	0	0	0
5. 120 mins	5	0	45	48	0	2	0	0	0	0	0
6. 180mins	23	0	45	32	0	0	0	0	0	0	0
7. 240 mins	13	0	22	64	0	1	0	0	0	0	0
8. 300 mins	20	0	33	46	0	0	1	0	0	0	0
















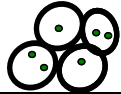

Time after α factor release	UNBUDED	BUDED					
		Small Bud	Large Bud				
							
1. 0 min	98	2	0	0	0	0	0
2. 30 mins	98	2	0	0	0	0	0
3. 60 mins	2	98	0	0	0	0	0
4. 90 mins	25	75	0	0	0	0	0
5. 120 mins	3	97	0	0	0	0	0
6. 180 mins	10	90	0	0	0	0	0
7. 240 mins	33	67	0	0	0	0	0
8. 300 mins	28	72	0	0	0	0	0

Figure 17: GFP and DAPI counts of wild type cells. Exponentially growing wild type cells were synchronized with α mating factor and released on fresh medium. GFP-tagged centromeres (green) and DAPI stained DNA (blue) denoting nuclei were visualized with fluorescence microscopy and counted based on the indicated morphologies drawn on top of each column. At least 200 cells were counted for each time point. Data is shown in percent.

Time after α factor release	UNBUDDED		BUDDED							
										
1. 0 min	60	35	0	0	0	1	0	1	2	0
2. 30 mins	22	14	0	5	38	15	6	0	0	0
3. 60 mins	12	5	9	0	47	19	5	0	3	2
4. 90 mins	8	9	4	6	21	37	3	0	10	3
5. 120 mins	0	0	31	23	0	30	10	0	4	2
6. 180 mins	18	13	21	14	4	18	8	0	1	3
7. 240 mins	4	6	15	29	4	23	12	0	5	2
8. 300 mins	12	9	30	22	14	5	1	1	5	1





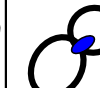
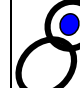
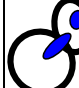











Time after α factor release	UNBUDDED	BUDDED						
								
1. 0 min	96	4	0	0	0	0	0	0
2. 30 mins	35	41	0	0	11	13	0	0
3. 60 mins	13	23	0	0	17	47	0	0
4. 90 mins	6	9	41	0	18	15	11	0
5. 120 mins	0	46	18	0	17	18	1	0
6. 180 mins	14	18	22	0	20	19	5	2
7. 240 mins	8	8	21	0	34	28	1	0
8. 300 mins	13	23	23	0	20	20	1	0

Figure 18: GFP and DAPI counts of H3K42A. Exponentially growing mutant cells were synchronized with α mating factor and released on fresh medium. GFP-tagged centromeres (green) and DAPI stained DNA (blue) denoting nuclei were visualized with fluorescence microscopy and counted based on the indicated morphologies drawn on top of each column. At least 200 cells were counted for each time point. Data is shown in percent.

Time after α factor release	UNBUDED		BUDED								
											
1. 0 min	100	0	0	0	0	0	0	0	0	0	0
2. 30 mins	100	0	0	0	0	0	0	0	0	0	0
3. 60 mins	0	0	58	38	0	3	1	0	0	0	0
4. 90 mins	0	0	42	57	0	0	1	0	0	0	0
5. 120 mins	4	0	38	45	0	12	1	0	0	0	0
6. 180 mins	4	0	56	36	0	4	0	0	0	0	0
7. 240 mins	13	2	28	49	0	7	1	0	0	0	0
8. 300 mins	39	0	23	37	0	1	0	0	0	0	0



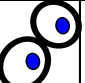
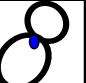

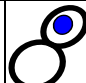












Time after α factor release	UNBUDED	BUDED						
								
1. 0 min	100	0	0	0	0	0	0	0
2. 30 mins	100	0	0	0	0	0	0	0
3. 60 mins	4	82	0	0	9	5	0	0
4. 90 mins	23	77	0	0	0	0	0	0
5. 120 mins	12	82	0	0	0	5	0	0
6. 180 mins	9	88	0	0	0	3	0	0
7. 240 mins	18	80	0	0	0	2	0	0
8. 300 mins	0	100	0	0	0	0	0	0

Figure 19: GFP and DAPI counts of H3K42R. Exponentially growing mutant cells were synchronized with α mating factor and released on fresh medium. GFP-tagged centromeres (green) and DAPI stained DNA (blue) denoting nuclei were visualized with fluorescence microscopy and counted based on the indicated morphologies drawn on top of each column. At least 200 cells were counted for each time point. Data is shown in percent.

Time after α factor release	UNBUDDED		BUDDED								
			Small Bud	Small Bud	Small Bud	Large Bud					
1. 0 min	31	66	3	0	0	0	0	0	0	0	0
2. 30 mins	10	19	0	12	10	13	34	1	0	0	0
3. 60 mins	3	5	0	1	20	46	12	4	8	0	0
4. 90 mins	17	5	0	0	10	13	6	4	24	21	0
5. 120 mins	2	6	3	25	10	12	25	9	8	1	0
6. 180 mins	8	20	14	14	7	9	19	2	4	4	0
7. 240 mins	10	18	10	5	10	12	10	0	16	9	0
8. 300 mins	8	17	14	2	8	16	18	0	12	5	0

Time after α factor release	UNBUDDED		BUDDED						
			Small Bud		Large Bud				
1. 0 min	99		1	0	0	0	0	0	0
2. 30 mins	31		60	8	0	1	0	0	0
3. 60 mins	5		22	0	40	26	7	0	0
4. 90 mins	38		19	18	19	0	6	0	0
5. 120 mins	5		30	9	28	18	9	1	0
6. 180 mins	19		33	19	13	7	5	4	0
7. 240 mins	21		24	36	11	6	2	0	0
8. 300 mins	14		35	15	19	10	6	1	0

Figure 20: GFP and DAPI counts of H3K42Q. Exponentially growing mutant cells were synchronized with α mating factor and released on fresh medium. GFP-tagged centromeres (green) and DAPI stained DNA (blue) denoting nuclei were visualized with fluorescence microscopy and counted based on the indicated morphologies drawn on top of each column. At least 200 cells were counted for each time point. Data is shown in percent.

Time after α factor release	UNBUDDED		BUDDED									
												
1. 0 min	66	33	0	0	1	0	0	0	0	0	0	0
2. 30 mins	52	26	4	0	18	0	0	0	0	0	0	0
3. 60 mins	10	4	15	0	35	29	7	0	0	0	0	0
4. 90 mins	2	2	6	0	21	38	1	0	17	13		
5. 120 mins	2	5	19	0	6	24	11	11	15	7		
6. 180 mins	5	7	6	0	23	26	7	0	21	5		
7. 240 mins	1	3	6	0	24	35	15	0	9	6		
8. 300 mins	12	12	6	0	10	32	6	9	5	6		

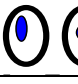

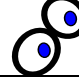
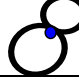
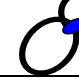
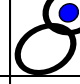











Time after α factor release	UNBUDDED	BUDDED							
									
1. 0 min	98	2	0	0	0	0	0	0	0
2. 30 mins	69	31	0	0	0	0	0	0	0
3. 60 mins	11	12	0	14	22	33	0	8	
4. 90 mins	3	4	52	5	9	25	2	0	
5. 120 mins	13	24	22	5	12	15	1	8	
6. 180 mins	40	6	21	0	2	12	0	19	
7. 240 mins	7	8	21	28	16	18	2	0	
8. 300 mins	15	17	14	0	16	23	0	15	

Figure 21: GFP and DAPI counts of H3G44A. Exponentially growing mutant cells were synchronized with α mating factor and released on fresh medium. GFP-tagged centromeres (green) and DAPI stained DNA (blue) denoting nuclei were visualized with fluorescence microscopy and counted based on the indicated morphologies drawn on top of each column. At least 200 cells were counted for each time point. Data is shown in percent.

Time after α factor release	UNBUDDED		BUDDED							
										
1. 0 min	100	0	0	0	0	0	0	0	0	0
2. 30 mins	100	0	0	0	0	0	0	0	0	0
3. 60 mins	10	0	48	42	0	0	0	0	0	0
4. 90 mins	51	0	5	44	0	0	0	0	0	0
5. 120 mins	9	0	79	12	0	0	0	0	0	0
6. 180 mins	12	0	44	39	0	5	0	0	0	0
7. 240 mins	15	1	27	56	0	0	0	0	1	0
8. 300 mins	0	1	44	55	0	0	0	0	0	0

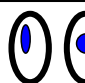

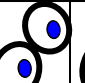
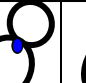
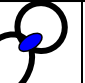
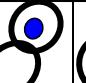
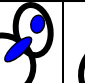
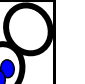











Time after α factor release	UNBUDDED	BUDDED						
								
1. 0 min	100	0	0	0	0	0	0	0
2. 30 mins	48	52	0	0	0	0	0	0
3. 60 mins	16	80	0	0	0	3	0	1
4. 90 mins	27	73	0	0	0	0	0	0
5. 120 mins	5	92	0	0	0	3	0	0
6. 180 mins	18	77	0	0	0	5	0	0
7. 240 mins	21	76	0	0	0	3	0	0
8. 300 mins	40	58	0	0	0	2	0	0

Figure 22: GFP and DAPI counts of H4K44A. Exponentially growing mutant cells were synchronized with α mating factor and released on fresh medium. GFP-tagged centromeres (green) and DAPI stained DNA (blue) denoting nuclei were visualized with fluorescence microscopy and counted based on the indicated morphologies drawn on top of each column. At least 200 cells were counted for each time point. Data is shown in percent.

Time after α factor release	UNBUDED		BUDED								
			Small Bud	Small Bud	Small Bud	Large Bud					
1. 0 min	35	65	0	0	0	0	0	0	0	0	0
2. 30 mins	42	58	0	0	0	0	0	0	0	0	0
3. 60 mins	3	11	15	0	25	31	12	0	1	2	
4. 90 mins	2	7	4	5	7	22	5	10	14	22	
5. 120 mins	1	13	5	0	22	13	11	4	12	17	
6. 180 mins	0	4	11	0	28	26	13	0	11	6	
7. 240 mins	2	7	11	0	34	25	11	0	6	5	
8. 300 mins	4	18	6	3	16	30	6	0	13	3	

Time after α factor release	UNBUDED	BUDED						
		Small Bud	Large Bud					
1. 0 min	99	1	0	0	0	0	0	0
2. 30 mins	100	0	0	0	0	0	0	0
3. 60 mins	9	20	8	5	12	46	0	0
4. 90 mins	9	9	15	6	13	44	4	0
5. 120 mins	27	18	31	1	3	18	2	0
6. 180 mins	12	8	35	19	3	22	1	0
7. 240 mins	13	17	22	12	8	28	0	0
8. 300 mins	10	14	27	14	14	20	1	0

Figure 23: GFP and DAPI counts of H4K44Q. Exponentially growing mutant cells were synchronized with α mating factor and released on fresh medium. GFP-tagged centromeres (green) and DAPI stained DNA (blue) denoting nuclei were visualized with fluorescence microscopy and counted based on the indicated morphologies drawn on top of each column. At least 200 cells were counted for each time point. Data is shown in percent.

Time after α factor release	UNBUDED		BUDED									
												
1. 0 min	97	0	3	0	0	0	0	0	0	0	0	0
2. 30 mins	99		1	0	0	0	0	0	0	0	0	0
3. 60 mins	1	0	31	25	0	36	3	3	1	0	0	0
4. 90 mins	46	17	2	14	5	8	8	0	0	0	0	0
5. 120 mins	2	1	44	10	2	26	14	1	0	0	0	0
6. 180 mins	NA	NA	NA	NA	NA	NA	NA	NA	NA	NA	NA	NA
7. 240 mins	NA	NA	NA	NA	NA	NA	NA	NA	NA	NA	NA	NA
8. 300 mins	NA	NA	NA	NA	NA	NA	NA	NA	NA	NA	NA	NA

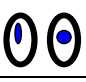
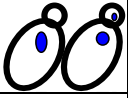

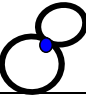

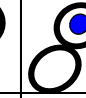

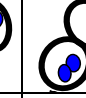






Time after α factor release	UNBUDED	BUDED						
								
1. 0 min	98	2	0	0	0	0	0	0
2. 30 mins	62	38	0	0	0	0	0	0
3. 60 mins	4	72	0	24	0	0	0	0
4. 90 mins	30	50	14	0	2	4	0	0
5. 120 mins	7	80	3	3	7	0	0	0
6. 180 mins	29	60	2	0	0	9	0	0
7. 240 mins	41	50	4	0	0	5	0	0
8. 300 mins	27	63	3	0	2	5	0	0

Figure 24: GFP and DAPI counts of H4K44R. Exponentially growing mutant cells were synchronized with α mating factor and released on fresh medium. GFP-tagged centromeres (green) and DAPI stained DNA (blue) denoting nuclei were visualized with fluorescence microscopy and counted based on the indicated morphologies drawn on top of each column. At least 200 cells were counted for each time point. Data is shown in percent. GFP-signal blurred after 180 minutes and counts could not be determined. NA-not applicable

Time after α factor release	UNBUDED		BUDED								
			Small Bud 	Small Bud 	Small Bud 	Large Bud 					
1. 0 min	23	56	14	0	7	0	0	0	0	0	0
2. 30 mins	8	17	12	0	50	4	5	0	4	0	0
3. 60 mins	1	6	3	0	15	59	10	0	4	3	0
4. 90 mins	6	6	5	3	10	23	9	13	16	9	0
5. 120 mins	3	9	8	8	24	16	15	5	6	5	0
6. 180 mins	11	8	2	2	34	18	8	11	4	3	0
7. 240 mins	6	6	8	0	9	27	29	1	10	3	0
8. 300 mins	3	2	10	7	12	19	6	0	22	18	0




















Time after α factor release	UNBUDED	BUDED						
		Small Bud 	Small Bud 	Small Bud 	Large Bud 	Large Bud 	Large Bud 	Large Bud 
1. 0 min	89	11	0	0	0	0	0	0
2. 30 mins	38	59	0	3	0	0	0	0
3. 60 mins	8	16	4	69	3	0	0	0
4. 90 mins	12	10	40	28	9	1	0	0
5. 120 mins	4	62	1	21	8	4	0	0
6. 180 mins	29	20	18	20	6	0	7	0
7. 240 mins	21	39	12	16	12	0	0	0
8. 300 mins	24	45	16	5	10	0	0	0

Figure 25: GFP and DAPI counts of H4IL97A. Exponentially growing mutant cells were synchronized with α mating factor and released on fresh medium. GFP-tagged centromeres (green) and DAPI stained DNA (blue) denoting nuclei were visualized with fluorescence microscopy and counted based on the indicated morphologies drawn on top of each column. At least 200 cells were counted for each time point. Data is shown in percent.

Time after α factor release	UNBUDED		BUDED								
			Small Bud	Small Bud	Small Bud	Large Bud					
											
1. 0 min	80	6	12	0	0	2	0	0	0	0	0
2. 30 mins	15	1	36	13	2	15	18	0	0	0	0
3. 60 mins	6	2	1	5	1	38	37	0	9	0	0
4. 90 mins	12	7	8	9	25	20	15	1	3	0	0
5. 120 mins	6	0	5	11	19	28	5	2	16	7	0
6. 180 mins	11	4	17	17	5	21	19	0	7	0	0
7. 240 mins	19	0	17	10	11	31	0	9	2	0	0
8. 300 mins	24	0	26	23	8	15	0	0	4	0	0



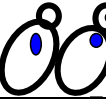


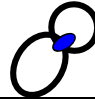
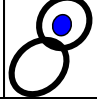
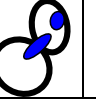

Time after α factor release	UNBUDED		BUDED						
			Small Bud	Large Bud					
									
1. 0 min	84		16	0	0	0	0	0	0
2. 30 mins	34		49	0	11	0	6	0	0
3. 60 mins	4		19	15	53	9	0	0	0
4. 90 mins	25		35	21	13	6	0	0	0
5. 120 mins	8		41	8	34	9	0	0	0
6. 180 mins	21		53	9	11	6	0	0	0
7. 240 mins	11		40	16	21	12	0	0	0
8. 300 mins	24		51	12	6	7	0	0	0

Figure 26: GFP and DAPI counts of H4G99A. Exponentially growing mutant cells were synchronized with α mating factor and released on fresh medium. GFP-tagged centromeres (green) and DAPI stained DNA (blue) denoting nuclei were visualized with fluorescence microscopy and counted based on the indicated morphologies drawn on top of each column. At least 200 cells were counted for each time point. Data is shown in percent.

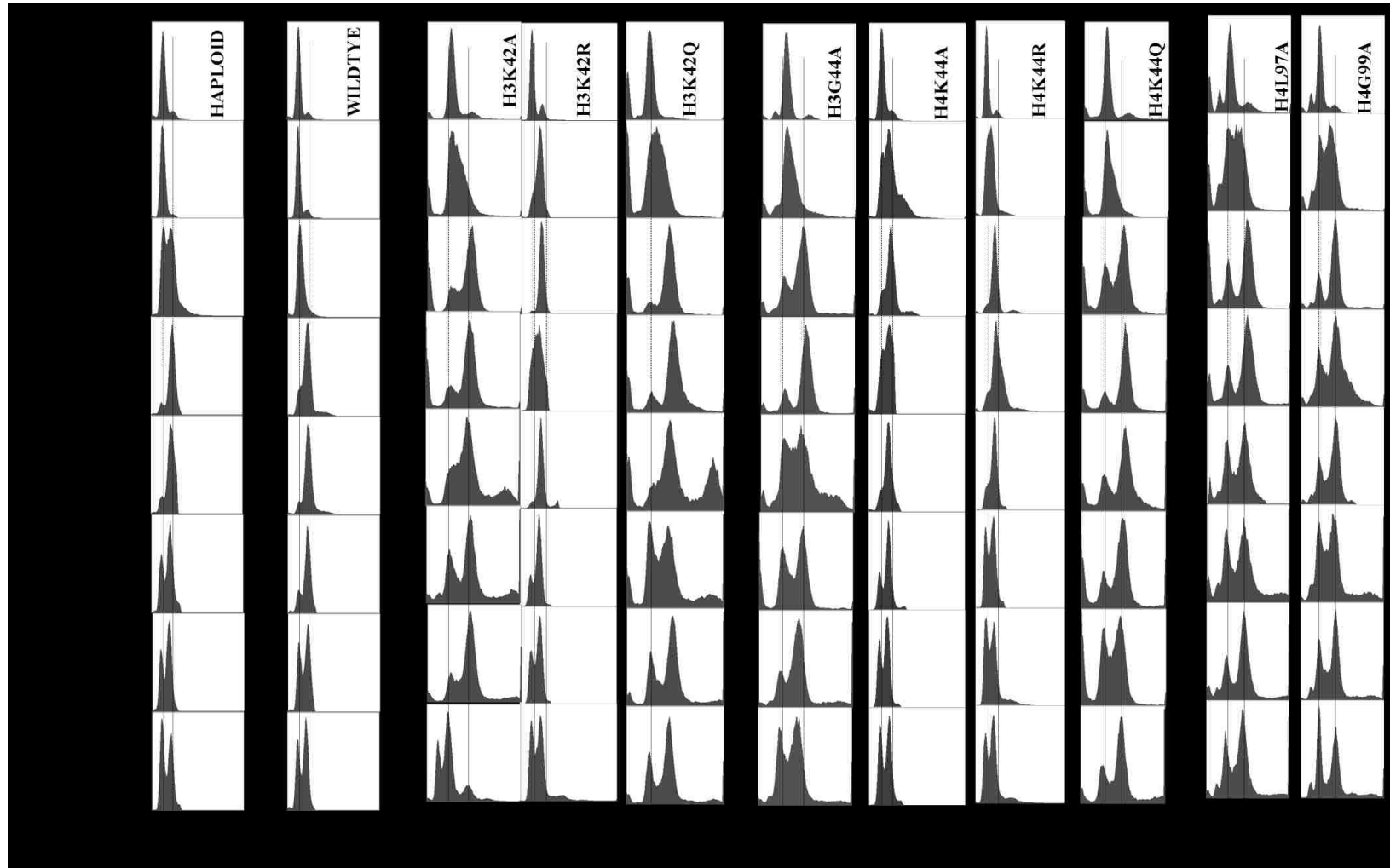


Figure 27: DNA content analysis by flow cytometry of the synchronized mutants after release from α -factor. H3K42A, H3K42Q, H3G44A, H4K44Q, H4L97A, and H4G99A show an increase in ploidy.

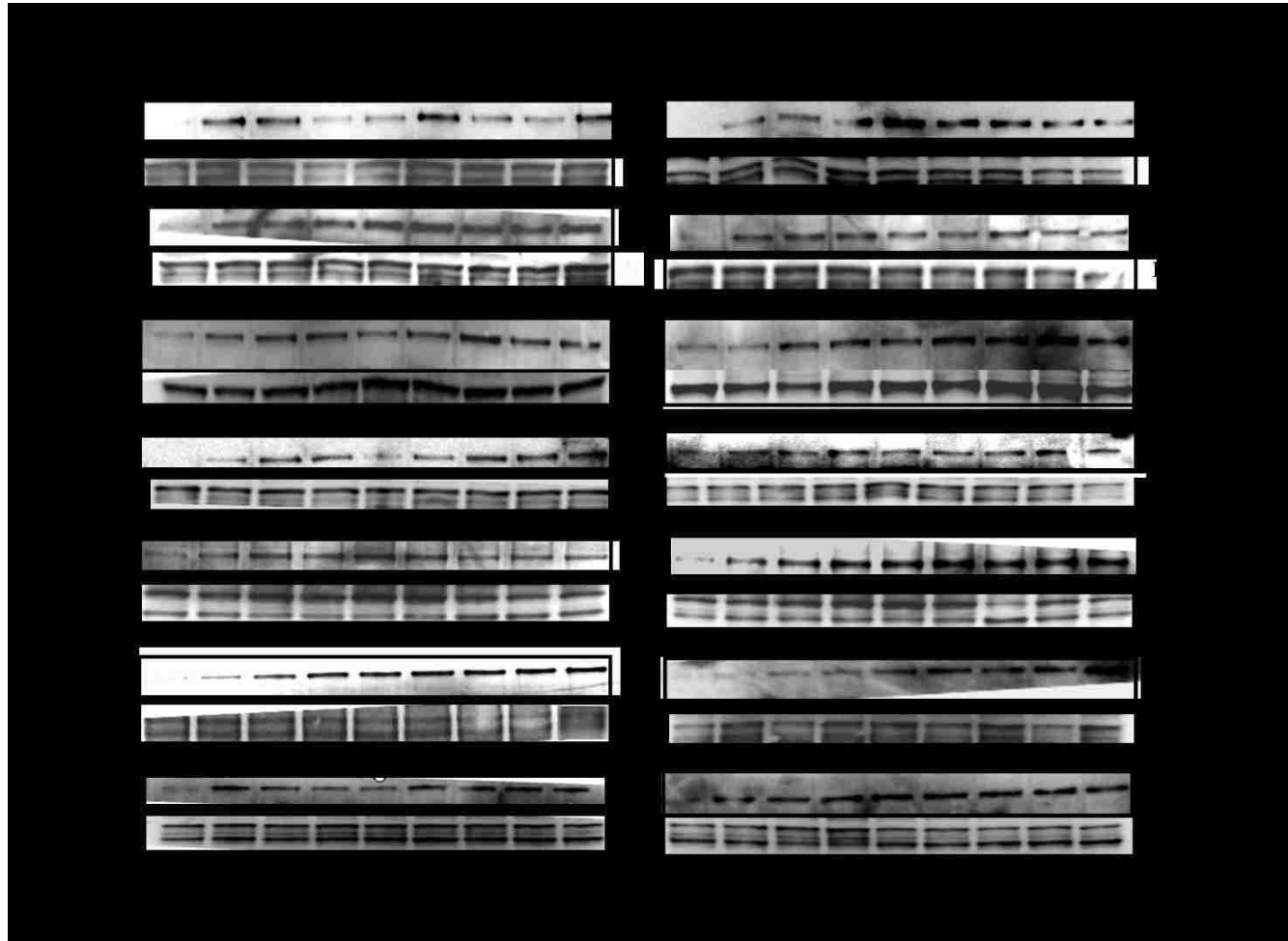


Figure 28: Pds1 stability assay of the synchronized wild type and mutant strains after release from α -factor. Immunoblot of Pds1-Myc visualized with anti-myc antibodies. Pgk1 was used as the loading control and visualized with anti-Pgk1 antibodies. Wild type, H3K42Q, H3G44A, and H4G99A cycle normally.

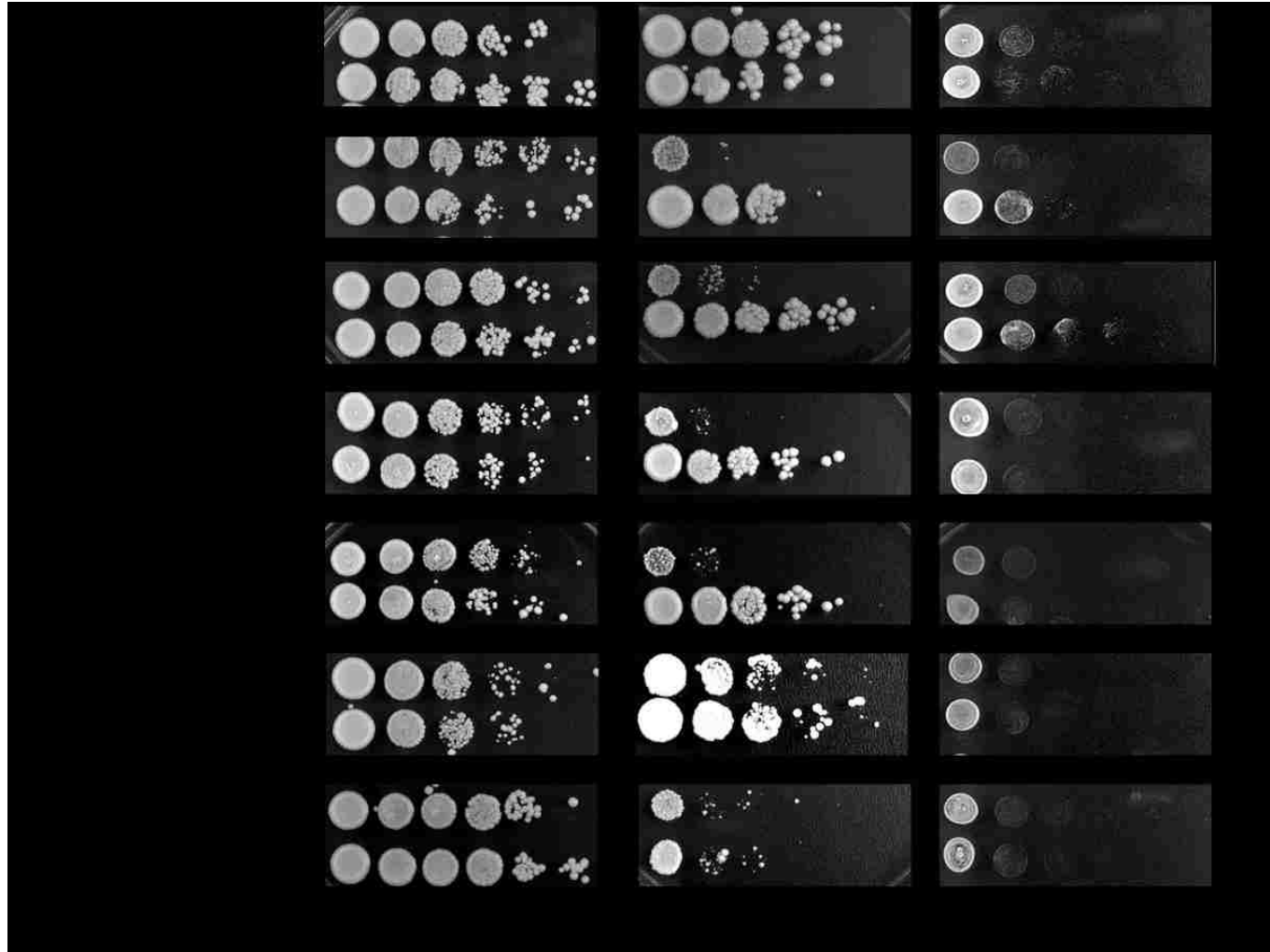


Figure 29: Sensitivity tests of the mutant strains over expressing Sgo1p. Sgo1p over expression suppresses the benomyl and hydroxyurea sensitivity of the H3K42A/Q, H3G44A, and H4K44Q strains.

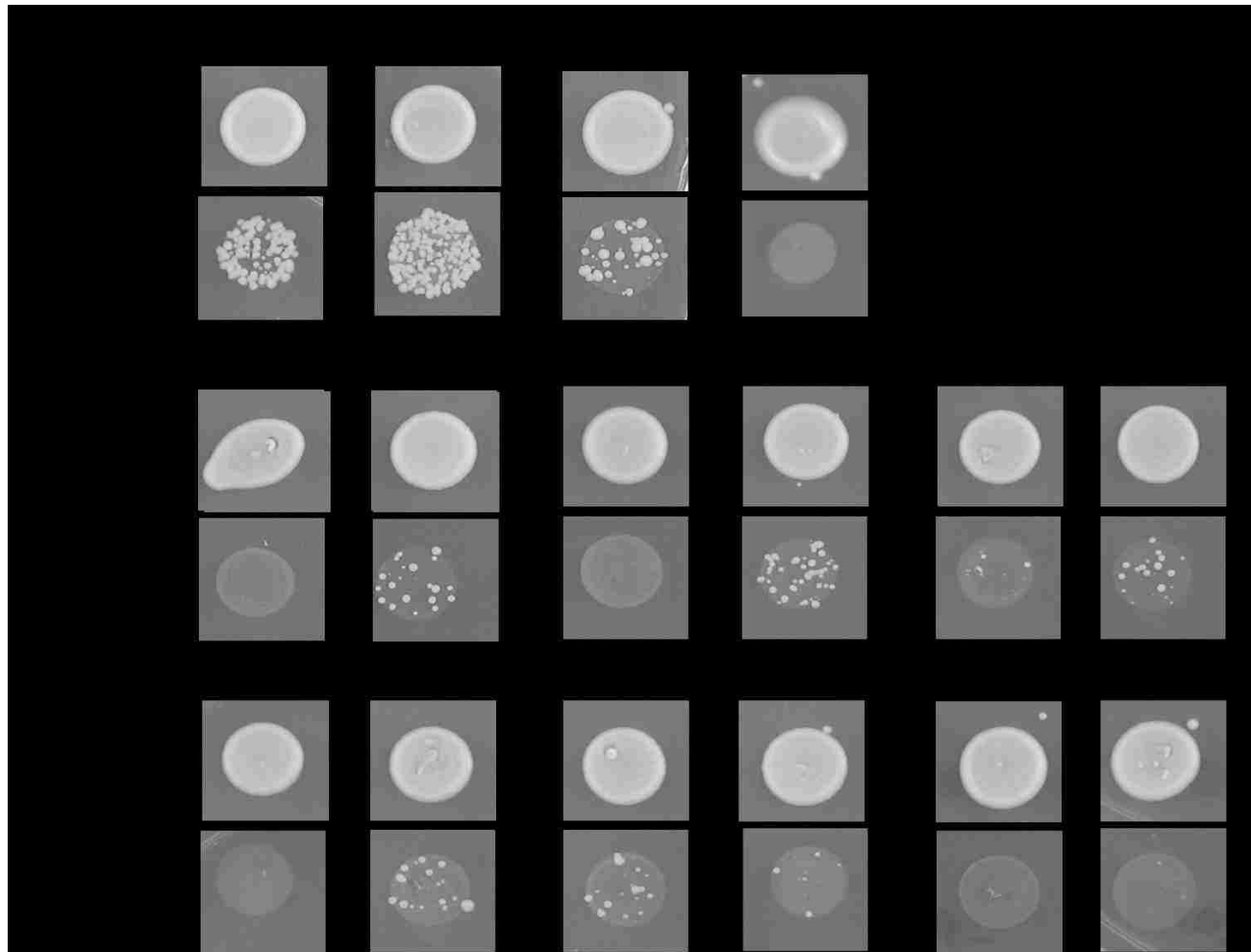


Figure 30: Canavanine assay of the mutant strains over expressing Sgo1p. Overnight grown cultures of the indicated mutants were plated on both SC-Arg (arginine) plates with or without canavanine, irradiated with UV, and incubated for 3 days at 26 °C. Sgo1p over expression in H3K42A/Q, H3G44A, and H4K44Q strains suppressed the increase in ploidy phenotype. H4L97A and H4G99A were not suppressed.

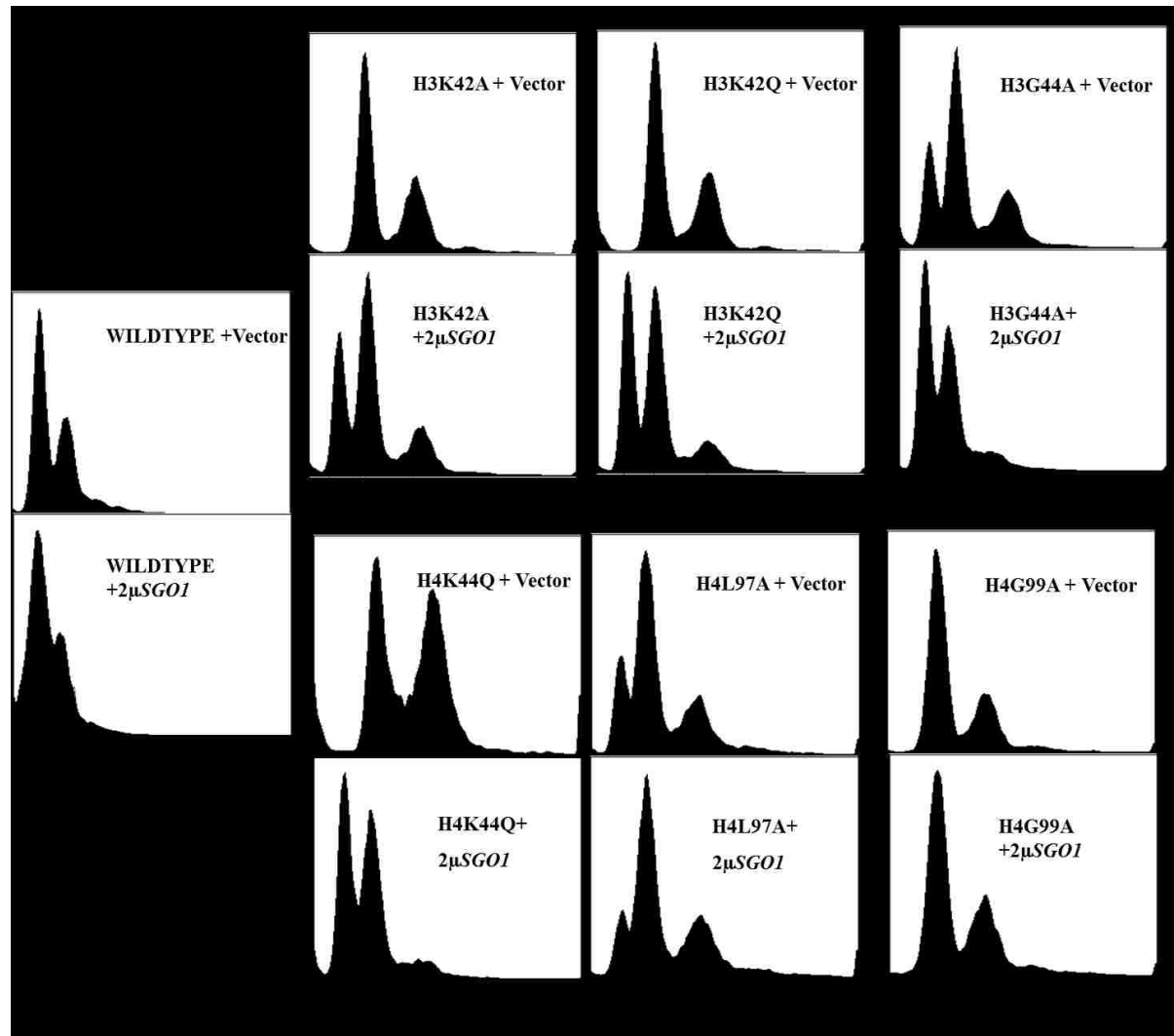
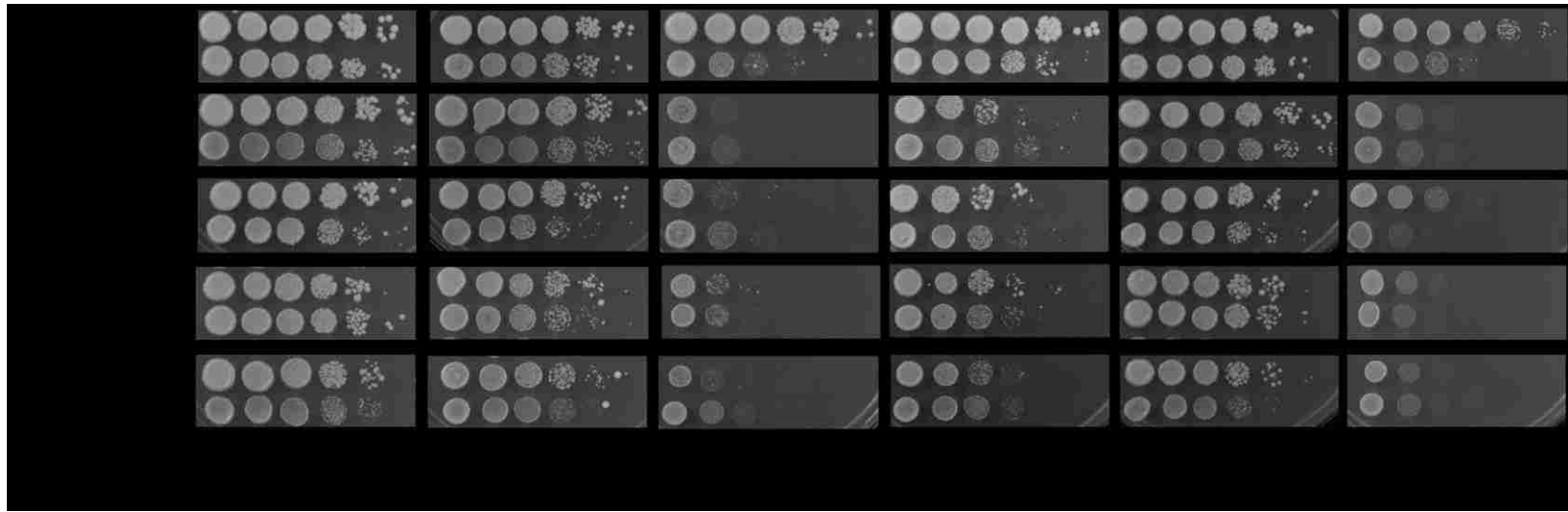


Figure 31: DNA content analysis by flow cytometry of the mutant strains over expressing Sgo1p. Sgo1p over expression in H3K42A/Q, H3G44A, and H4K44Q strains suppressed the increase in ploidy phenotype. H4L97A and H4G99A were not suppressed.



78

Figure 32: Sensitivity tests of the histone mutants carrying a *sgo1* deletion. Absence of Sgo1 in the mutants has no phenotypic effect on the sensitivity tests.

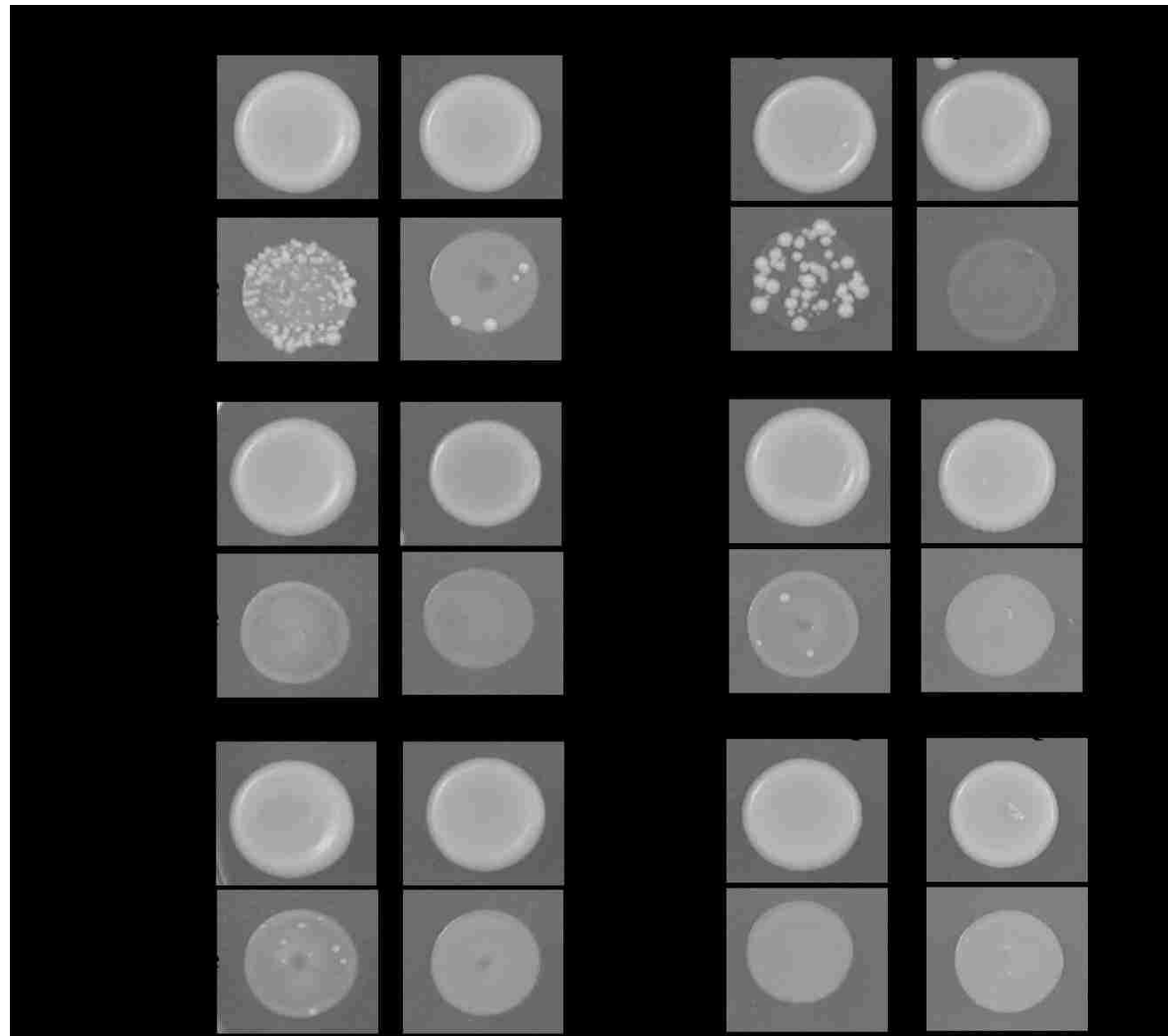
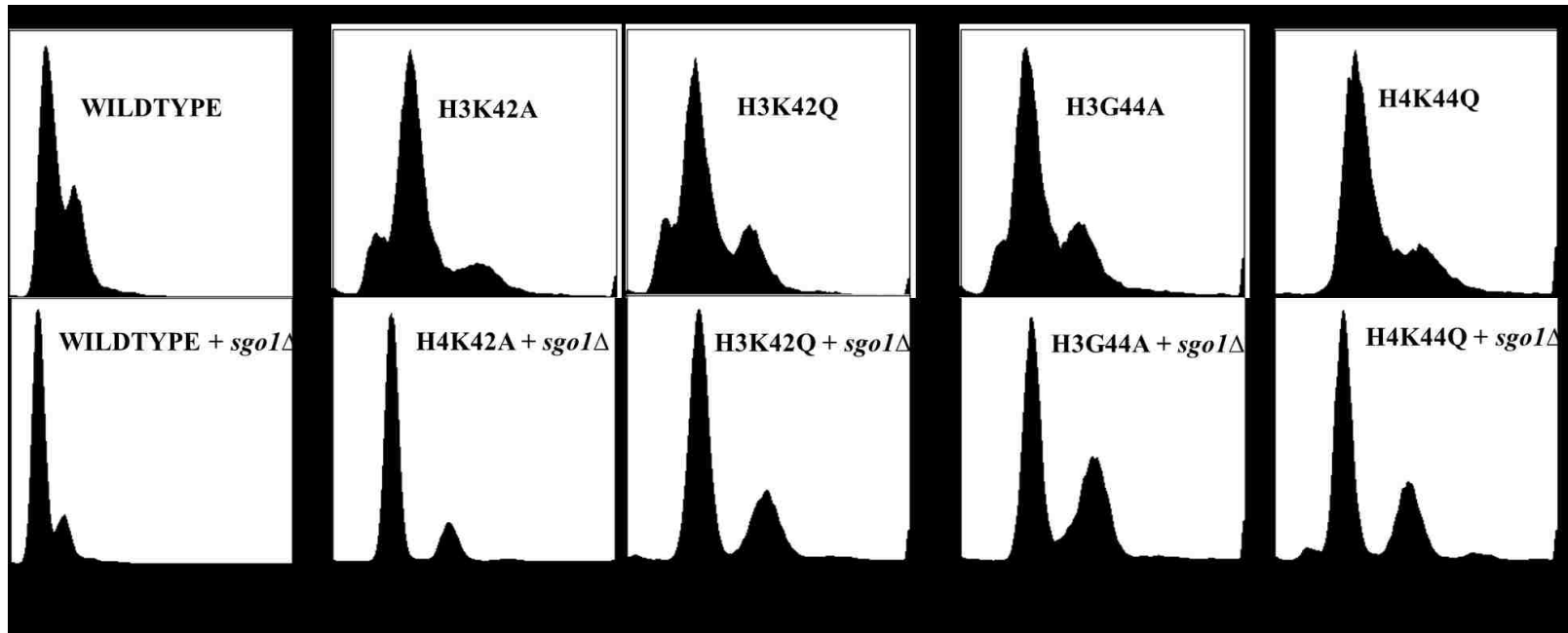


Figure 33: Canavanine assay of the histone mutants carrying a *sgo1* deletion. Overnight grown cultures of the indicated mutants were plated on both SC-Arg (arginine) plates with or without canavanine, irradiated with UV, and incubated for 3 days at 26 °C. No suppression was observed in the strains carrying a deletion of *sgo1*.



80

Figure 34: DNA content analysis by flow cytometry of the histone mutants carrying an *sgo1* deletion. Absence of Sgo1 had no effect on the histone mutants, as they retained their ploidy defect.

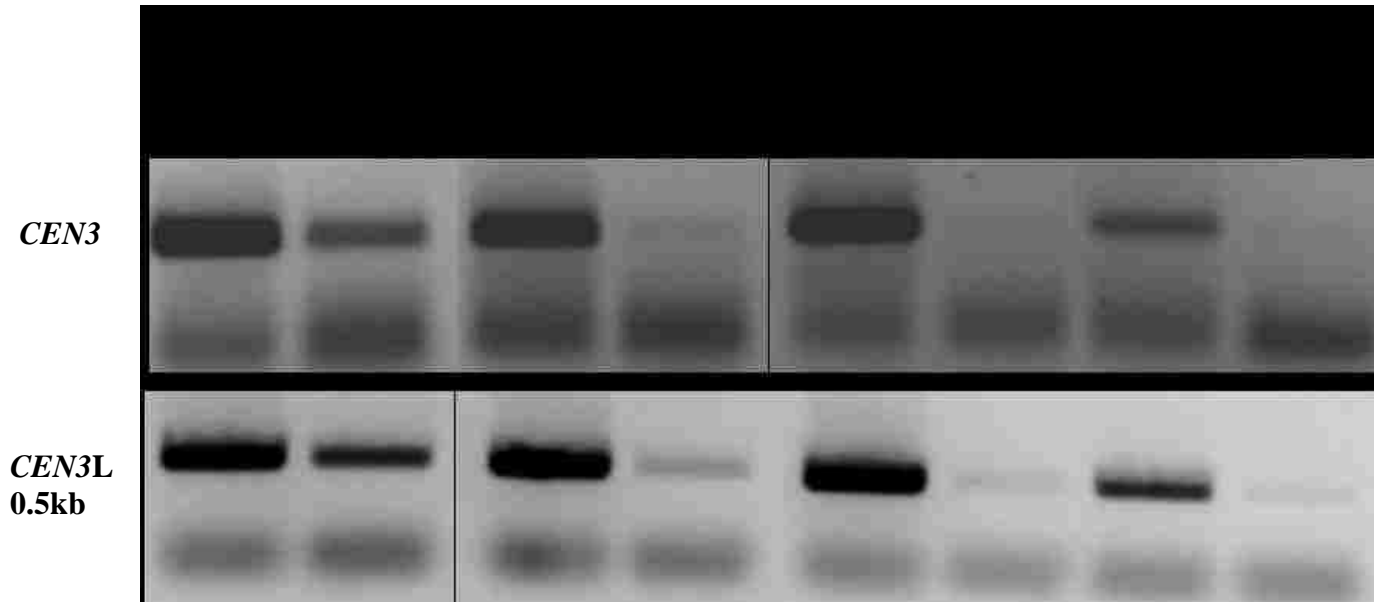


Figure 35: Chromatin Immunoprecipitation (ChIP) of Sgo1 at the centromere and pericentromeric region of chromosome III. ChIP on Sgo1-Myc was carried out with anti-myc antibodies. PCR primers used were specific for CEN3 and a pericentromeric region (CEN3+ 0.5Kb left). Sgo1 shows a decrease in association with the centromeric and pericentromeric region of chromosome III in the histone mutants located in the DNA entry/exit region of the nucleosome.

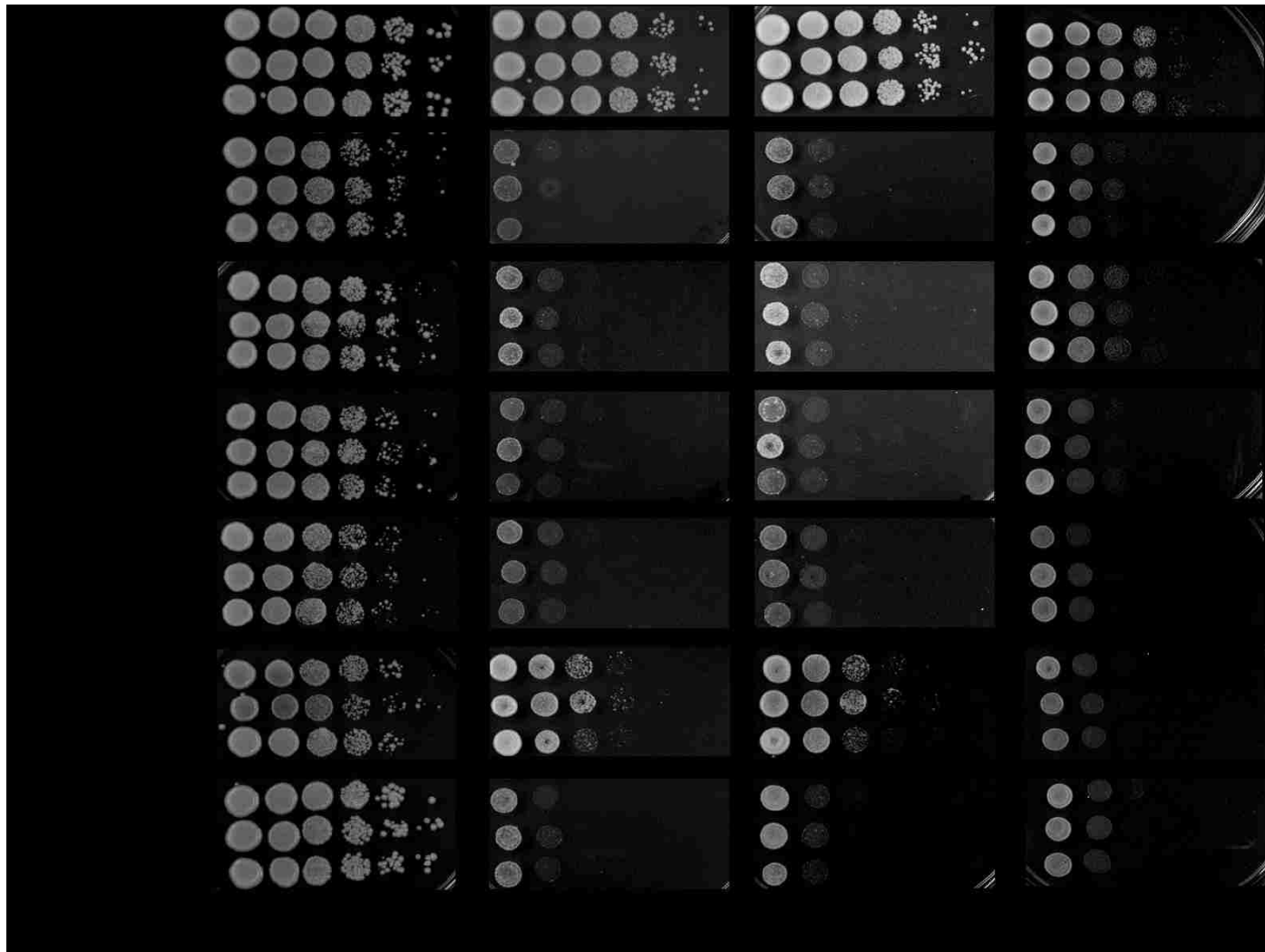


Figure 36: Sensitivity tests of the histone mutants carrying *IPL1* and *BIR1* over expressing plasmids. None of the mutant strains were affected by *IPL1* and *BIR1* overexpression.

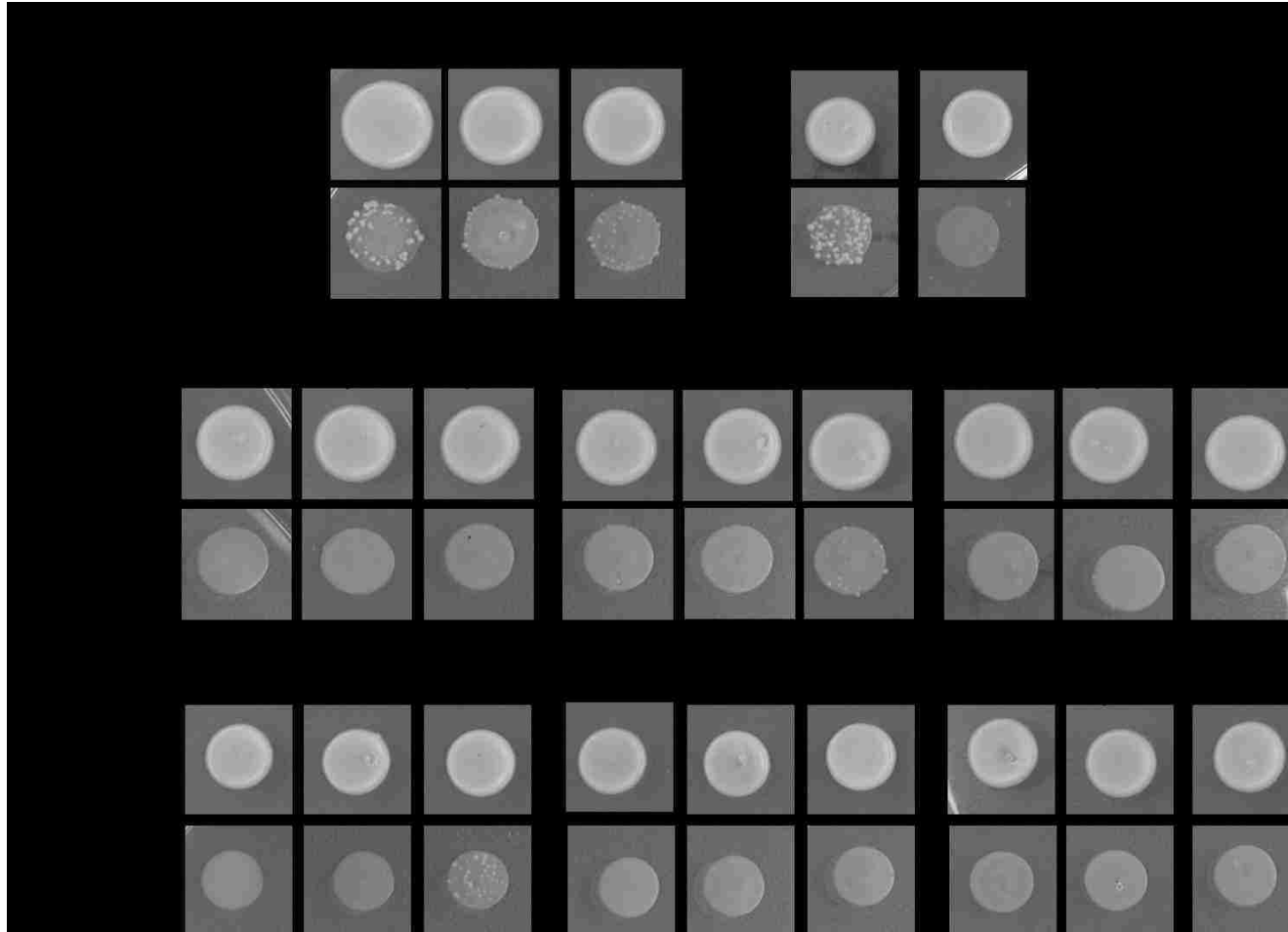


Figure 37: Canavanine assay of the histone mutants carrying *Ipl1* and *Bir1* over expressing plasmids. Overnight grown cultures of the indicated mutants were plated on both SC-Arg (arginine) plates with or without canavanine, irradiated with UV, and incubated for 3 days at 26 °C. No suppression of the increase in ploidy was observed. However, H4K44Q with overexpressing *BIR1* shows a mild suppression reflected as few papillae.

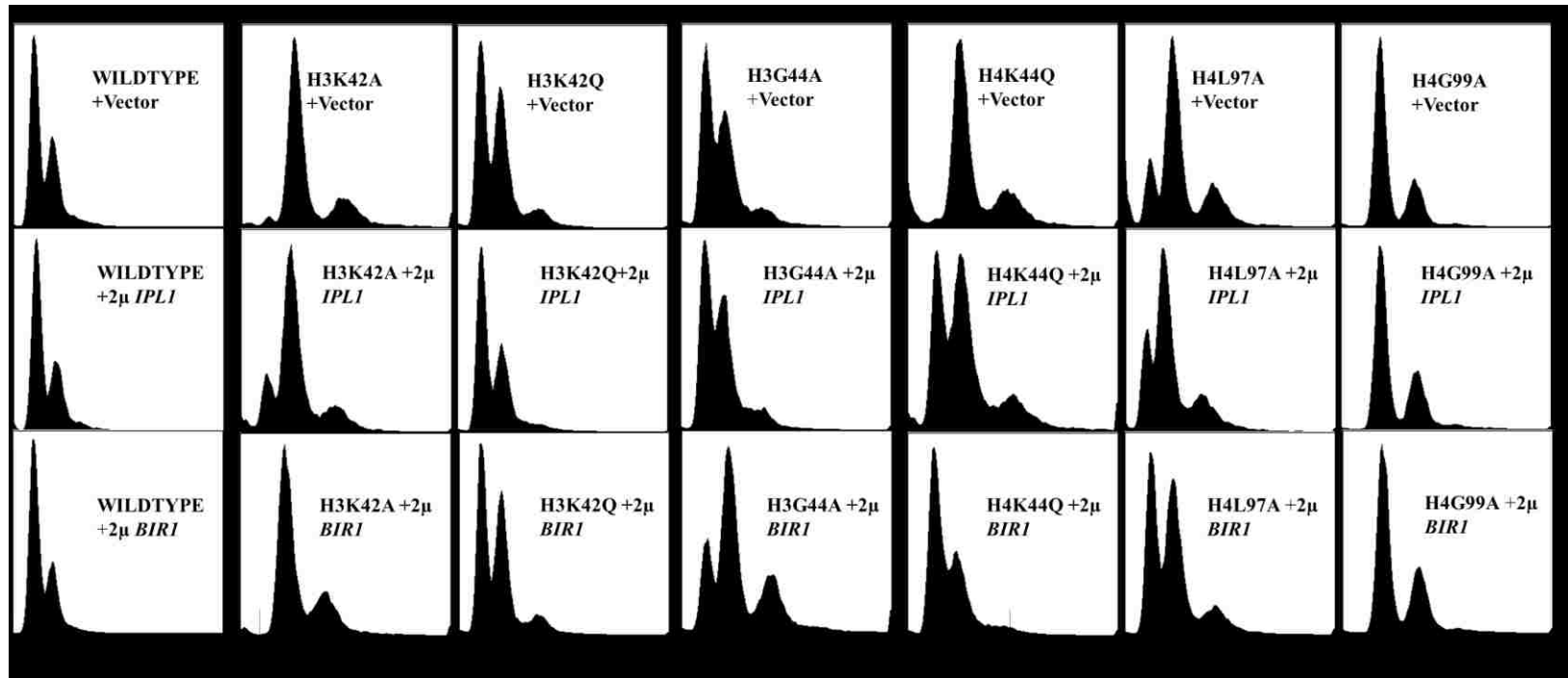


Figure 38: DNA content analysis by flow cytometry of the histone mutants carrying *Ipl1p* and *Bir1p* over expressing plasmids. *Ipl1p* and *Bir1p* over expression in most of the mutants had no effect on the ploidy level. *Bir1* overexpression appears to alleviate the ploidy defect of the H4K44Q strain.

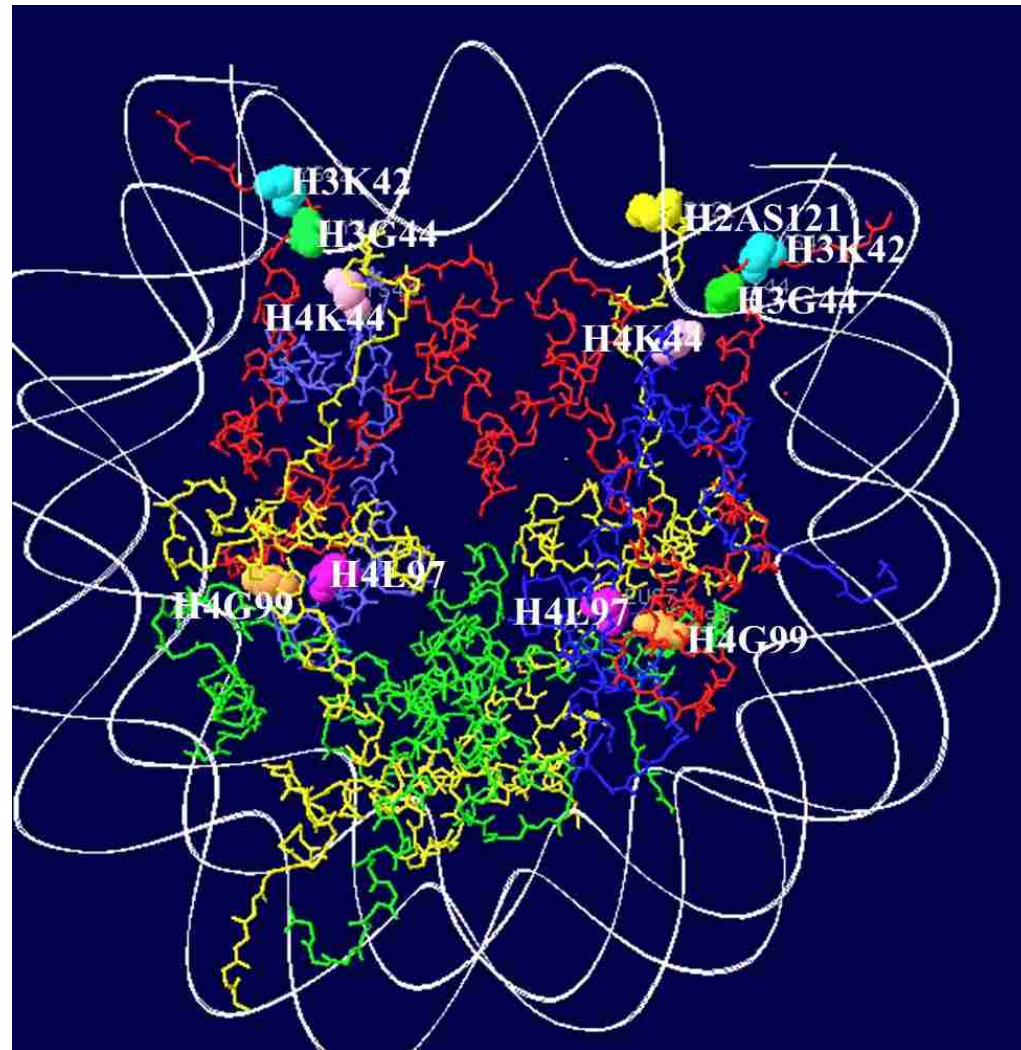


Figure 39: H2AS121 is in proximity to the histone residues H3K42, H3G44 and H4K44. The locations of the H3 and H4 mutations are highlighted, along with H2A S121. The four histone proteins are shown as wires: H4, blue; H3, red; H2B, green; and H2A, yellow. The nucleosome model was developed in Swiss PDB viewer 4.04V.

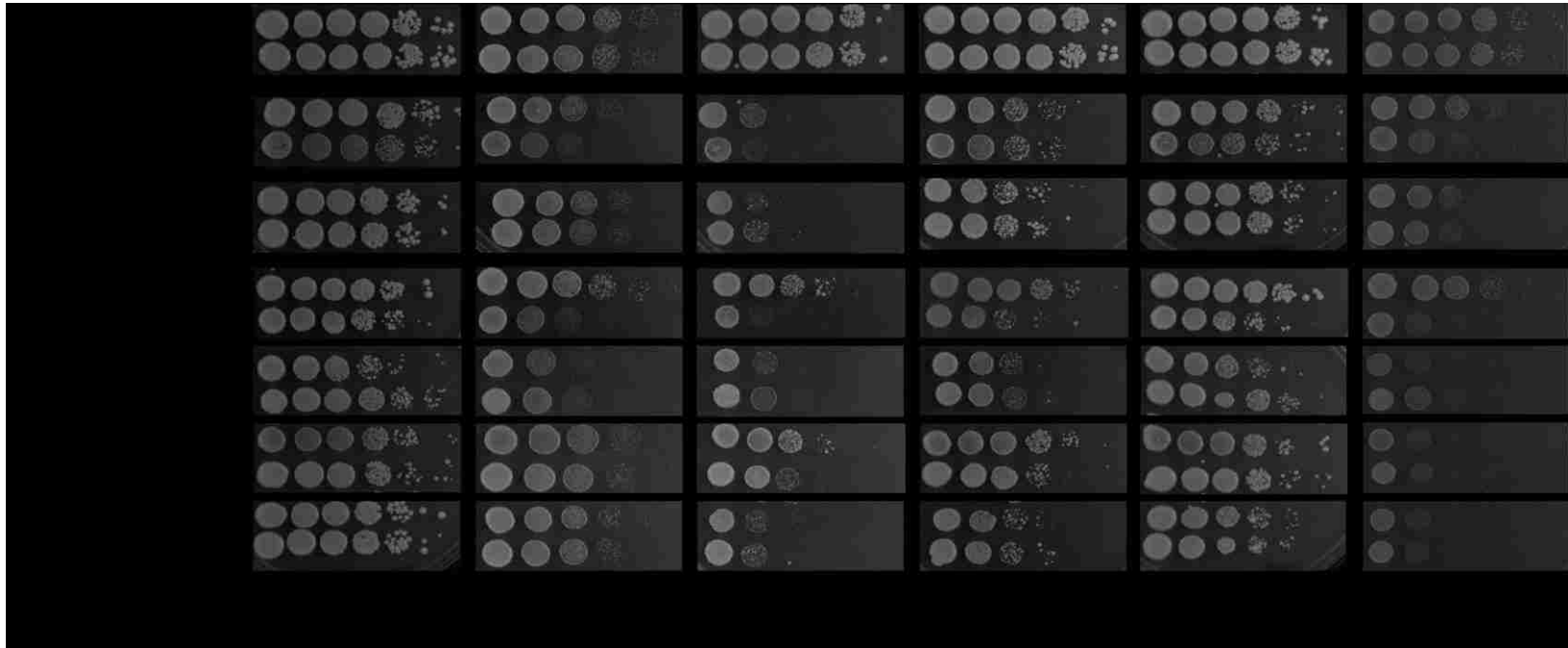


Figure 40: Sensitivity tests of the histone mutants carrying a *BUB1* over expressing plasmid. Bub1p over expression in H3G44A makes it more sensitive to benomyl and hydroxyurea.

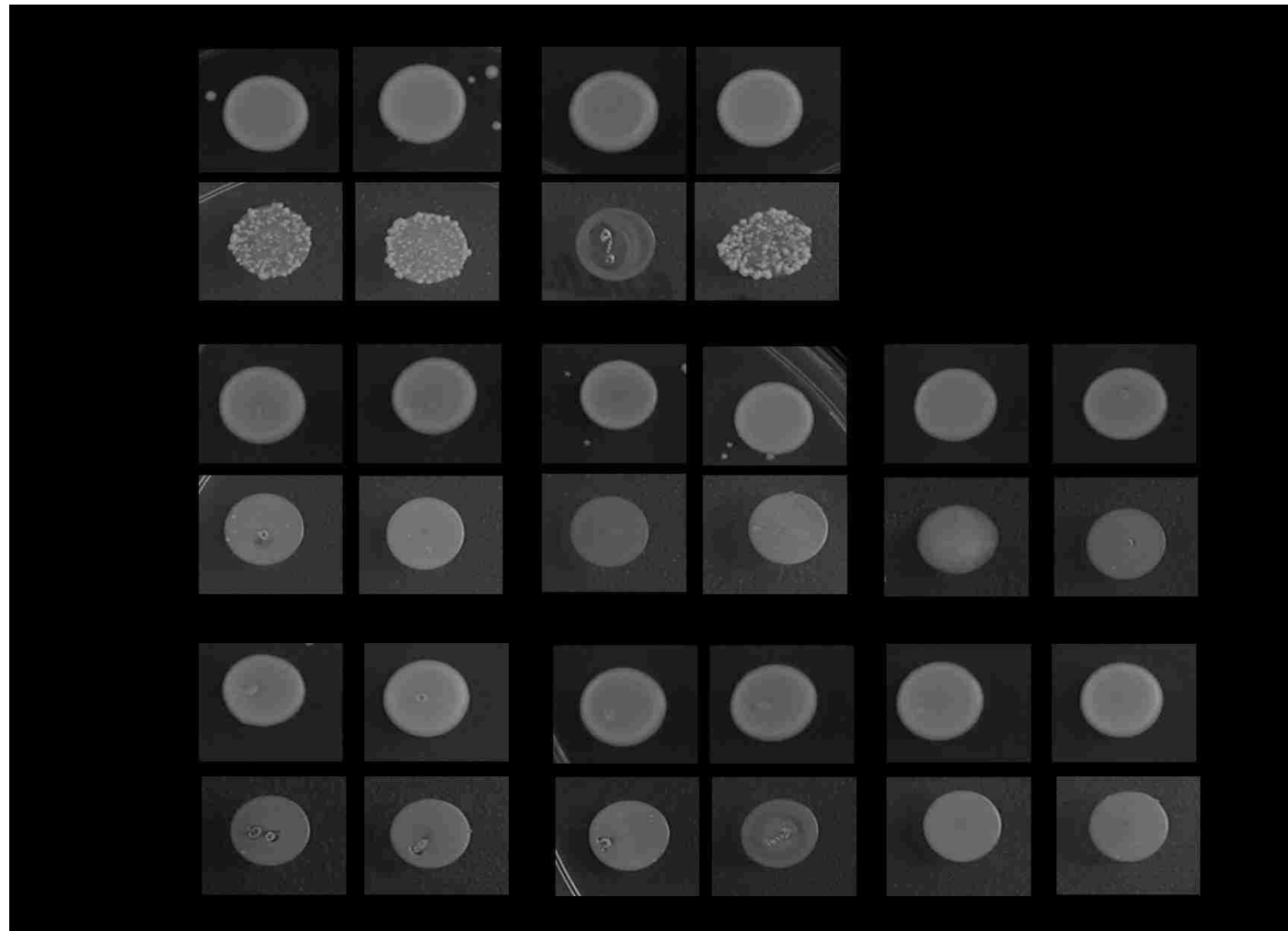


Figure 41: Canavanine assay of the histone mutants carrying a *BUB1* over expressing plasmid. Overnight grown cultures of the indicated mutants were plated on both SC-Arg (arginine) plates with or without canavanine, irradiated with UV, and incubated for 3 days at 26 °C. None of the above mutants showed suppression by over expression of *BUB1*.

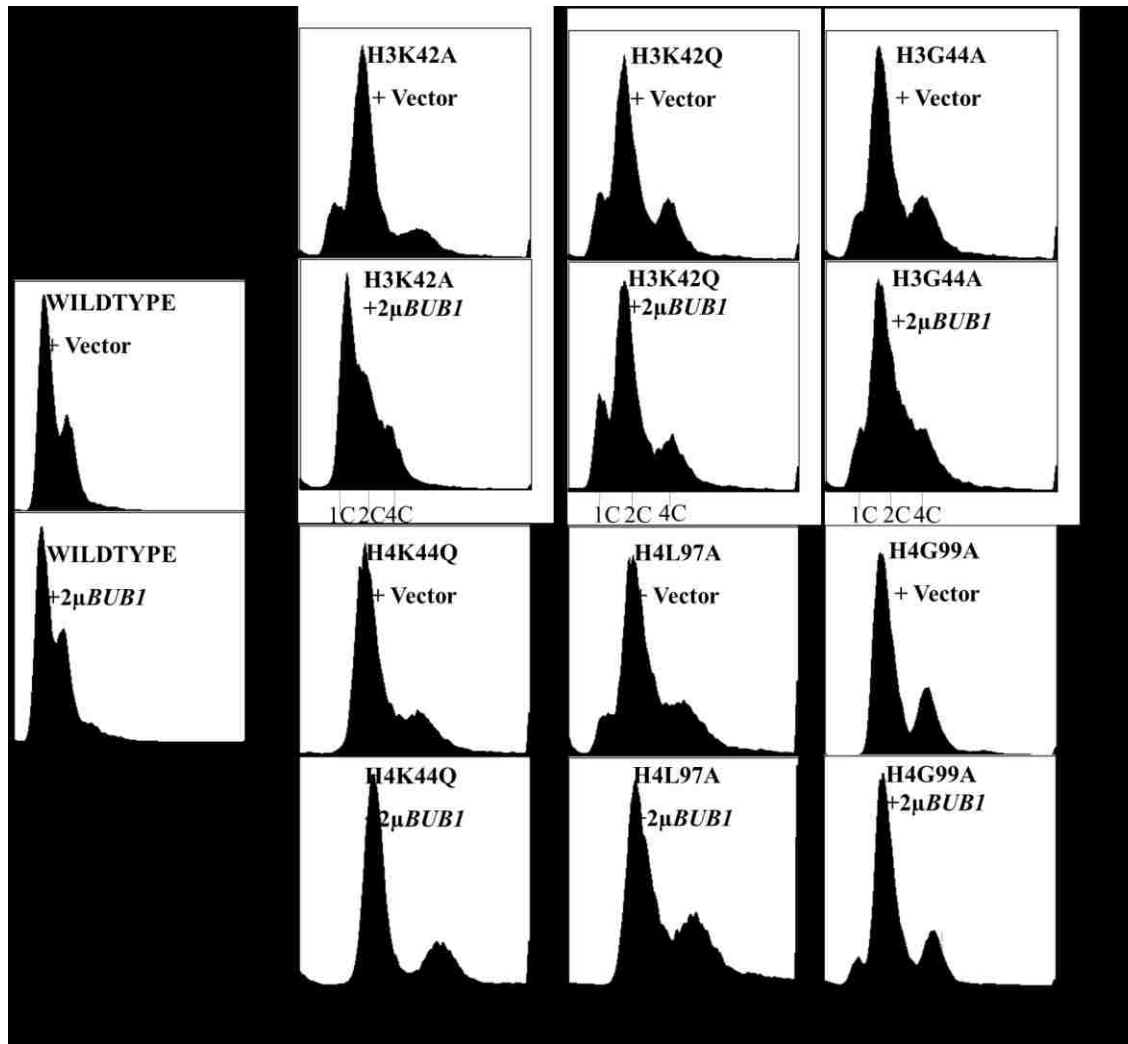


Figure 42: DNA content analysis by flow cytometry of the histone mutants carrying a *BUB1* over expressing plasmid. *BUB1* over expression had no effect on the ploidy level of the mutants.

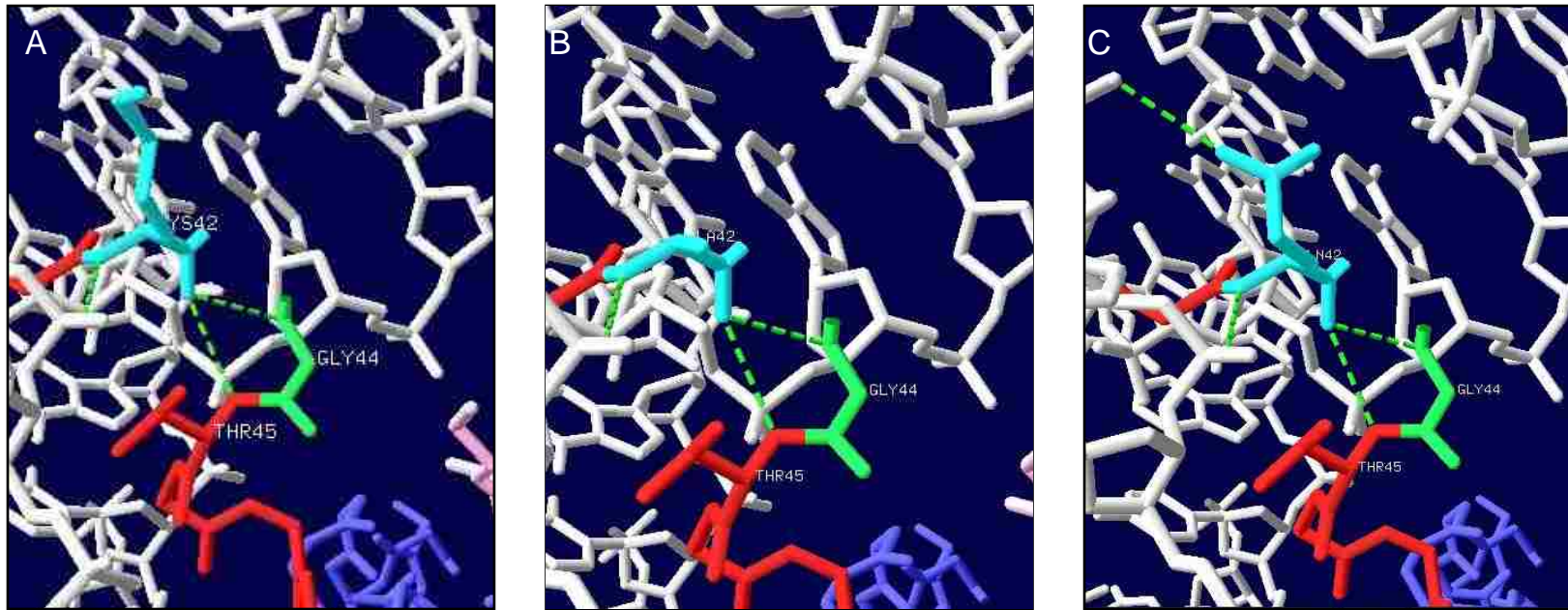


Figure 43: H3K42 and its mutations in the nucleosome structure. A. H3K42 forms hydrogen bonds with H3G44 and H3T45 and to the surrounding DNA. B. H3K42A forms hydrogen bonds with H3G44 and H3T45. C. H3K42Q forms hydrogen bonds similarly as in H3K42 and H3K42A, with an additional hydrogen bond with DNA. The four histone proteins are shown as wires: H4, blue; H3, red; H2B, green; and H2A, yellow. The surrounding DNA is shown in white. The important residues for this study are highlighted: H3K42 (cyan), H3G44 (green) and H44K44 (pink). The nucleosome model (PDB-1ID3) was imaged in Swiss PDB viewer 4.04V.

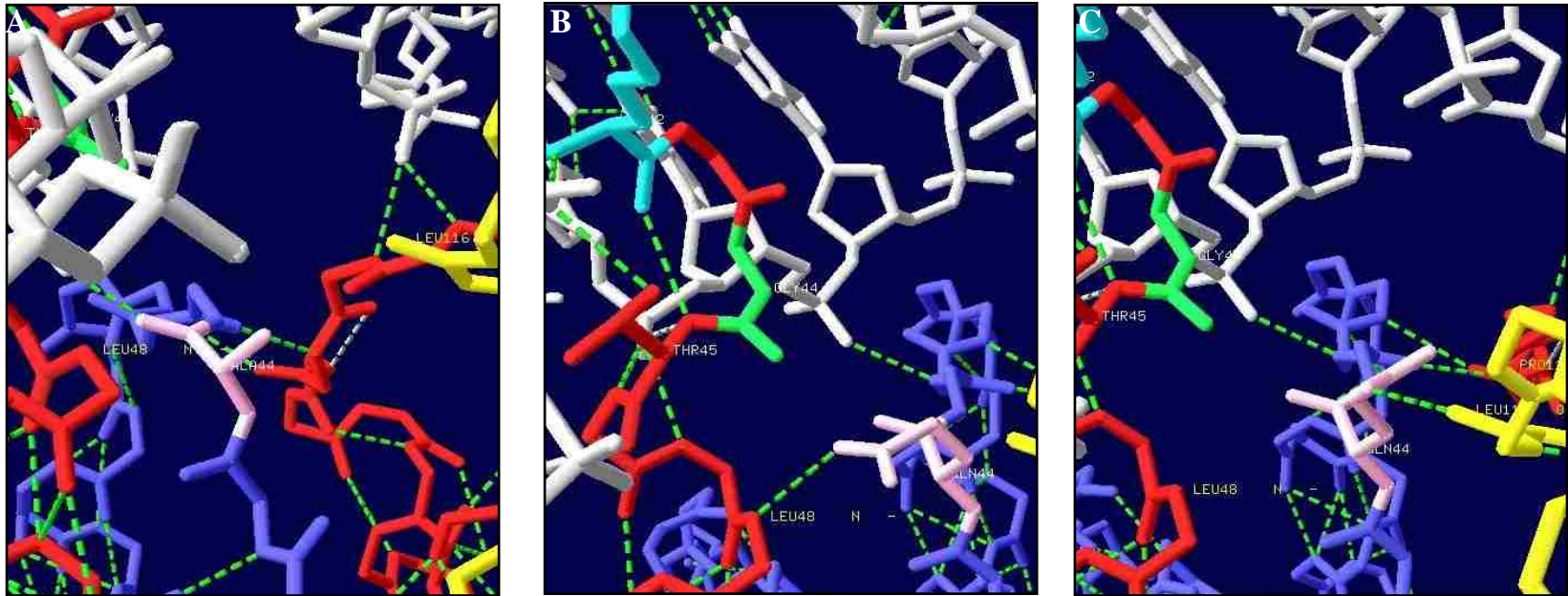


Figure 44: H4K44 and its mutations in the nucleosome structure. A. H4K44 does not form any hydrogen bond. B. H4K44Q forms hydrogen bonds with H3L48. C. H4K44Q forms hydrogen bond with H2AL116. The four histone proteins are shown as wires: H4, blue; H3, red; H2B, green; and H2A, yellow. The surrounding DNA is shown in white. The important residues for this study are highlighted: H4K44 (pink). H3K42 (cyan), and H3G44 (green). The nucleosome model (PDB-1ID3) was imaged in Swiss PDB viewer 4.04V

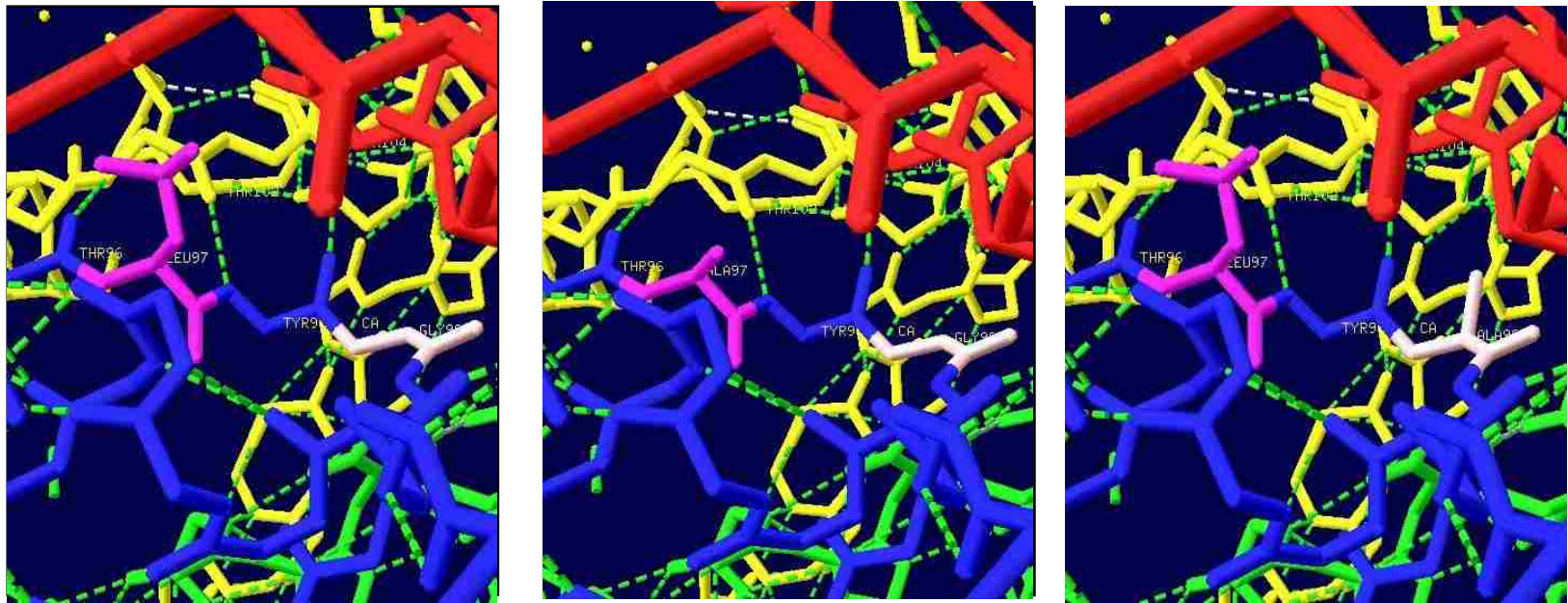


Figure 45: H4L97 in the nucleosome structure. **A** H4L97 is shown toward the center of the nucleosome, flanked by H4T96 and H4Y98, which form hydrogen bonds with H3. **B.** H4L97A still maintains the hydrogen bonds between H4T96 and H4Y98 with H3. **C.** H4G99A still maintains the hydrogen bonds between H4T96 and H4Y98 with H3. The four histone proteins are shown as wires: H4, blue; H3, red; H2B, green; and H2A, yellow. H4L97 is marked with magenta. The nucleosome model (PDB-1ID3) was imaged in Swiss PDB viewer 4.04V.

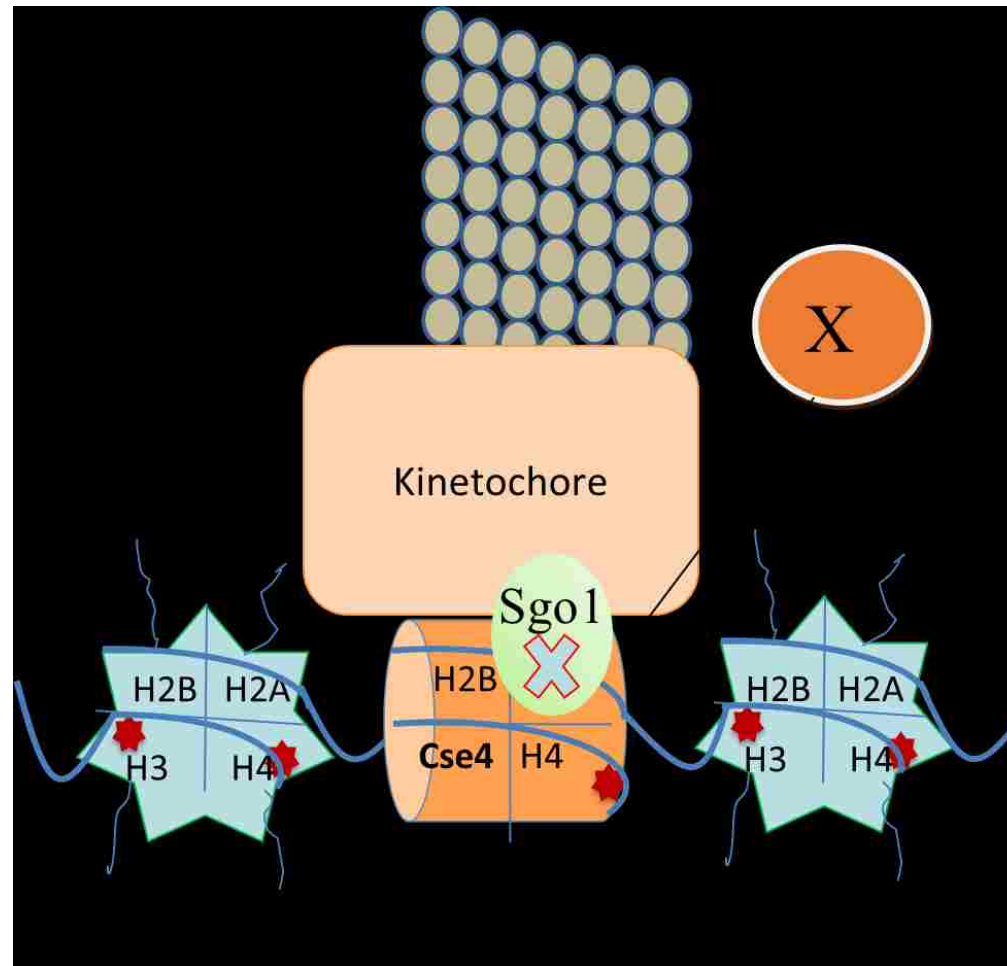


Figure 46: Model of the yeast centromere in the histone mutants. A possible change in the nucleosome structure is shown as star-shaped pericentromeric nucleosomes. The red star indicates H3 or H4 mutations in the DNA entry/exit region of the nucleosome. The mutations affect kinetochores assembly and/or microtubule attachment. Sgo1 is reduced/absent in the centromeric and pericentromeric region. X is a redundant protein that functions parallel to Sgo1 in sensing lack of tension among sister chromatids during mitosis.

V. DISCUSSION

H3 and H4 mutants define regions of the nucleosome susceptible to chromosome segregation defects.

Previous work has already demonstrated that histones play a role in maintaining proper chromosome number during the cell cycle. In a single histone protein, mutation of a single amino acid residue is sufficient to cause chromosome segregation defects [1, 111], but the precise role of each individual histone is still unclear. This is an important and still unanswered question that is necessary to better understand the whole process that controls the accurate transmission of chromosomes during cell division. This study is done to partly answer the above question. We tried to understand the contribution of each residue of histone H3 and H4 in maintaining the proper segregation of chromosomes during cell division. After screening a library encompassing 486 substitutions or deletions, six mutants were selected, because they displayed strong and consistent chromosome missegregation phenotypes. Although the library is biased towards the substitutions available for each position in H3 and H4, the screen allowed us to analyze the results in the context of the structure-function of the nucleosome. The six mutants represent five residues: H3K42, H3G44, H4K44, H4L97, and H4G99. This result indicates that histones H3 and H4 are permissive to a large number of amino acid replacements throughout the whole protein, with very few critical residues required for chromosome segregation that cannot tolerate any changes. H3K56, H3K122, H488, H4K91 are some of the residues that were initially identified in the screen, but were not selected for further studies because they have also been reported to participate in either DNA damage or transcriptional regulation [16, 112-114]. The finding that H3K42, H3G44, and H4K44 are all located in the DNA entry/exit point of the nucleosome emphasizes the role that this region has in maintaining proper chromosome segregation.

The mutations in the library were created in a way that would mimic the charge or size of the residues in its unmodified or modified state. This gives us an additional opportunity to understand the role that the particular residue is playing. In histones we see an abundance of lysine residues (the positive charge of the lysine binds tightly to the negatively charged surrounding DNA) that are mostly subjected to post translational modifications, and thus provide ample possibilities to make the protein structure more flexible in terms of charge and size. There are two lysine residues (H3K42 and H3K44) out of the five critical residues that we identified, emphasizing the probability that post translational modifications may play a role in these mutants' uncontrolled chromosome segregation. The mutation that mimics the modification required to maintain an error free cell cycle may survive the chromosome segregation phenotype testing of the mutants. On the contrary, mutations that avoid the necessary modification may succumb at non-permissive temperatures and to various drugs like benomyl or hydroxyurea. The drug sensitivity provides a connection to a pathway defective in the mutants, for example, hydroxyurea sensitivity can be associated with DNA synthesis defects, and benomyl with altered microtubule assembly and chromosome missegregation. The most abundant modifications that exist in histones are methylation, acetylation, phosphorylation and ubiquitination. These either change the charge of the residue making it more or less tightly associated with the surrounding negatively charged DNA, or the size, changing the regional conformation of the nucleosome. All these changes may affect the higher order chromatin structure of the mutants. The modification may also provide a mark required to initiate the association of other non-histone proteins required for an accurate cell cycle.

Specific H3 and H4 mutations cause chromosome segregation defects.

Characterization of the mutants as they progressed through a cell cycle allowed us to understand the deficiencies caused by the mutations. The DNA flow cytometric analysis indicated that the H3K42A strain behaved as a stable diploid, therefore it must have increased its ploidy early on after exchanging the wild type for the mutated histone H3. The cells also displayed a slow S phase and a long G₂M phase. Both of these characteristics correlate with its sensitivity to hydroxyurea and benomyl, respectively. The strain cycles very slowly, which is also confirmed by the growth rate data, with an estimate doubling time of about 130 minutes, compared to about 90 minutes in the wild type H3 and H4 strain. H3K42A has both ploidy and aneuploidy problems. The Pds1 stability assay indicated that the strain has a good tension sensing system that gets activated and arrests the cells at metaphase for an unusually long time. This reflects the strain's ability to sense the problem and an effort to repair it [115]. The GFP tagged centromere data is also consistent with these findings, reflecting a long metaphase arrest where large buds are seen but the chromosomes are not yet distributed between the mother and daughter cells [116]. The same trend is seen in H3K42Q but in this mutant the Pds1 stability assay indicated a faulty tension sensing machinery. The Pds1 protein seems to go away with time even though the DNA content in the strain shows a ploidy and aneuploidy problem. This is also supported by the growth rate of this mutant. It has a typical doubling time of 100 minutes, which is comparable to that of the wild-type strain. All these findings indicate that H3K42A and H3K42Q are defective in chromosome segregation. However, the degree of damage may differ between the two strains. Both show similar ploidy and aneuploidy problems thorough a cell cycle. It appears that H3K42A attempts to fix the problem by blocking the cells at metaphase, but H3K42Q evade the checkpoint and continues to go through the cell cycle without a halt. In

H3K42Q, the DNA content indicates that some cells can even reach the tetraploid stage. Both mutants have a functional tension sensing checkpoint proteins; they both arrest the cells for a long time under nocodazole treatment as seen in the Pds1 stability assays.

H3G44A behaves as a diploid from the beginning of the cell cycle study, similarly to H3K42A. This mutant also displays a slow S phase but does not have a very long G₂M arrest, as noticed in the flow cytometry studies. It shows a striking disappearance of Pds1, comparable to that of wild type, implying either a problem in sensing lack of tension between chromosomes, or a chromosome segregation defect that is not sensed by the spindle-assembly checkpoint.

H4K44Q is the slowest and sickest mutant of the six strains characterized in this study. This strain behaves exactly as the H3K42A mutant in terms of long cycling time, slow S and G₂M phases, and even in having problems of ploidy and aneuploidy. All these data further implies a role of the amino acid residues located at the DNA entry/exit point in maintaining a structure that is necessary to undergo a controlled cell division. Any alteration to the structure may affect the tension sensing ability of the checkpoint proteins. Alternatively, the structural defects alter the centromere-kinetochore structure in such a way that the faulty association results in poor tension, triggering the checkpoint response.

H4L97A and H4G99A behave quite differently from the above mutants. At the beginning of the cell cycle they both have a mixed haploid and diploid population. H4L97A has a long doubling time whereas H4G99A has a shorter one. H4G99A, unlike H4L97A, does not have a long metaphase arrest which is more evident through the Pds1 stability assay. Since these mutants are located in the center of the nucleosome, their defects may be related to a more general change in the overall structure of the nucleosome, perhaps by altering the association of one or more critical components of the kinetochore.

Sgo1 plays an important role in the DNA entry/exit point of the nucleosome

The mutants serve as an important tool to understand the role of the checkpoint proteins in cell cycle. Previous studies on H3G44S revealed the importance of this residue for pericentromeric localization of Sgo1, a protein known for sensing tension generated by the attachment of microtubules during chromosome segregation [80, 108, 117]. Surprisingly, we found that overexpression of Sgo1 not only suppressed the benomyl sensitivity of H3G44A but also all the other mutants that are in the DNA entry/exit point of the nucleosome. H3K42A, H3K42Q, and H4K44Q belong to this category. On the contrary, the H4L97A and H4G99A mutants, that are located in the center of the nucleosome, are not affected by the Sgo1 overexpression. This finding emphasizes the relevance of the DNA entry/exit point region in the function of Sgo1. We analyzed the localization of Sgo1 in two mutants, H3K42A and H4K44Q, both mutations located at the DNA entry/exit point of the nucleosome. There is no or very little Sgo1 in the centromeric and pericentromeric regions of chromosome III in these mutants compared to the wild-type strain, indicating that these mutations are in critical residues for the recruitment of Sgo1 to the centromere and pericentromere of chromosomes. A deletion of *SGO1* in a wild-type cell causes only a mild sensitivity to benomyl, with no obvious chromosome segregation defects. Therefore, the absence of Sgo1 at the centromere and pericentromere in the histone mutants must contribute in part, but not solely, to the chromosome segregation defects. Likely, the improper association of Sgo1 exacerbates the microtubule attachment defects that the abnormal chromatin structure of the mutants has created. Therefore, a deletion of *SGO1* would not enhance the phenotypes observed in the mutants. In fact, the strains carrying the histone mutations in conjunction with a deletion of *SGO1* showed identical phenotypes to those of the individual histone mutants. This result suggests that another redundant protein or group of

proteins may sense the lack of tension in these mutants and functions in a parallel pathway to that of Sgo1.

Ipl1 kinase is a member of the chromosome passenger protein complex that is important for sensing lack of tension in unattached or mis-attached kinetochores to microtubules [77]. In fission yeast it was reported that Sgo1 is important for Ipl1/Aurora kinase localization to the centromere [83]. Thus, if increased Sgo1 alleviates the problem of chromosome missegregation in the mutants, then overexpressing Ipl1 may increase the level of Sgo1. This in turn may help to diminish chromosome missegregation in the mutants. No effect of over-expression of Ipl1 and its partner Bir1 in the mutant strains was found. This cannot be judged completely as a negative result since the Ipl1 kinase may be over-expressed but may not be active in the absence of its partners Bir1, Nbl1 and Sli15, the components of the chromosomal passenger complex [78, 109, 118]. The same situation may apply to Bir1. Co-overexpression of all the subunits may be necessary for full activity of the individual kinases in the complex, providing more conclusive results.

The H3 and H4 mutants alter the structure of histone H2A in the nucleosome

The location of the H3K42, H3G44A and H4K44 is spatially close to H2AS121 in the nucleosome structure. Bub1 kinase has been reported to phosphorylate H2AS121, a mark that is important for Sgo1 localization to the pericentromere [28, 81, 82]. It has been shown by X-ray crystallography that in the H4K44Q mutant the H2A protein is unconventionally placed in the nucleosome [119]. All these data together suggest that Bub1 may play a role in the phenotypes observed in the H3 and H4 mutants. Although Bub1 over-expression did not show any suppression, it is possible that its kinase activity also depends on the over-expression of its

interacting partners. Moreover, the suppression seen by Sgo1 over-expression stresses the connection between these mutations and Sgo1 centromeric localization, regardless of the potential Bub1 participation in the process. The mutations may affect a direct association of Sgo1 with nucleosomes, or the interaction with an intermediate messenger that relays of information between the lack of tension along chromosomes and Sgo1 activity.

H3 and H4 mutant effects on the nucleosome structure

H3K42 is a site of methylation, which is known to be unique for Ascomycetes including *Saccharomyces cerevisiae*. This particular residue is reported to affect transcription through alteration of the chromatin structure [120]. However, this residue is partially conserved in higher eukaryotes, including humans, where the positively charged lysine is replaced by the positively charged arginine. This arginine residue is also reported to be dimethylated in both human and mouse cells [121]. Therefore, it appears relevant that this residue is methylated for proper histone function. In the nucleosome model we can see a hydrogen bond between H3K42 and the surrounding DNA in the DNA entry/exit point, suggesting implications for the nucleosome and higher order chromatin structure. Methylation of lysine or arginine residues maintains the net positive charge of the residue with increased size and hydrophobicity making a more close association with the surrounding DNA [32]. The hydrophobicity of methyl residues is usually mimicked by substituting lysine with phenylalanine, leucine, or methionine [120]. These changes were unavailable in the library. H3K42A and H3K42Q both show chromosome segregation defects whereas H3K42R does not. The positive charge of the lysine residue is only maintained when it is mutated to arginine. This correlates well with our sensitivity assays where the H3K42R behaves comparable to the wild-type strain in the presence of benomyl and

hydroxyurea. When H3K42 is mutated to either alanine (where it is unable to form a hydrogen bond with the DNA) or glutamine (where it is able to form a hydrogen bond with the surrounding DNA), it loses the positive charge of the residue. Until now we understand that the positive charge at H3K42 is important to be maintained for an accurate nucleosome structure. Methylation, which maintains the charge but adds hydrophobicity, makes the association of DNA and H3 tighter. All these interactions may be important to maintain the nucleosome structure at the DNA entry/exit point.

H3G44 is the other residue that is conserved from yeast to humans. Again this residue is located at a very critical site of the nucleosome, the DNA entry/exit point that connects the flexible tail of H3 to rest of the core H3 with a β turn. Glycine has the smallest size among all the amino acids, and is preferentially positioned in the turns of the protein between alpha helices. H3G44 forms a hydrogen bond with DNA which may also be essential for maintaining the structure of the nucleosome [7]. H3G44A may distort the turn of the H3 protein resulting in an unstable nucleosome or unfavorable chromatin structure.

H4K44 is not in the same histone protein as the above residues but shares the same position at the DNA entry/exit point of the nucleosome as the other H3 mutants discussed above. There is no confirmed report of any kind of modifications in this residue [106]. The H4K44A and H4K44R strains have similar phenotype as wild type in the presence of benomyl and hydroxyurea. But H4K44Q is a very sick strain with a severe slow growth rate and extreme sensitivity to benomyl and hydroxyurea. H4K44Q mimics the acetylated state of the lysine residue in terms of its charge and size similarity [119, 122]. Acetylation of lysine residue relieves the positive charge on the residue making it less likely associated to the surrounding DNA. The charge on H4K44 may also act as a marker to attract other non-histone proteins that

have a chromatin-related function. H4K44 is known to be important for maintaining the methylation of H3K36 by Set2 [107, 123]. Furthermore, X-ray crystallographic analysis of H4K44Q established a nucleosome structural change in this mutant relative to the wild type [119]. Whether the structural change of the nucleosome is due to the altered interaction of this residue with the surrounding DNA or to its effect on the methylation of H3K36 is still unclear.

The other residues that were selected for this study are H4L97A and H4G99A. Both residues are located in the center of the nucleosome and interact with the H2A-H2B dimer [7]. These mutations may affect the histone-histone interaction, which certainly has its consequence on nucleosome instability [10]. A previous investigation on these mutants showed altered chromatin structure with lower number of nucleosomes [124]. H4L97A is also genetically suppressed by over-expression of the histone H2A variant Htz1 [117, 125]. Further work needs to be done to understand the role of these two residues in the maintenance of a normal cell cycle.

Proposed model of the centromeric /pericentromeric chromatin structure in the histone H3 and H4 mutants

Our results clearly indicate that the nucleosome has different regions that correlate with different functions. Sgo1, which is a non-essential protein, is necessary to maintain normal chromosome segregation in strains that have problems with sensing tension. The function of Sgo1 is associated with to the nucleosome structure in the DNA entry/exit point. Based on our investigation, we believe there is a possible chromatin structural change in the cells having mutations in H3 and H4 at the DNA entry/exist point of the nucleosome (Figure 46). This change may have a particularly strong effect on the structure of the centromere, which in turn affects kinetochore assembly, chromosome attachment and proper segregation during mitosis. In

addition, the altered chromatin structure diminishes or abolishes the association of Sgo1 with the centromeric/pericentromeric region (Figure 46). When Sgo1 is present in the histone mutants, Sgo1 is not likely functional because it is not present at the centromere/pericentromeric chromatin. This is equivalent to the deletion of *SGO1*. The finding that a deletion of *SGO1* has no further chromosome segregation defects on the mutants emphasizes the fact that Sgo1 has diminished or no association to the centromeric/pericentromeric region of the chromosome in these mutants of the DNA entry/exit region. It also suggests that Sgo1 is functioning on the same pathway affected by the histone mutations. Overexpression of Sgo1 suppresses the chromosome segregation defects caused by the histone mutants, perhaps by overcoming a reduced affinity between Sgo1 and the nucleosome at the DNA entry/exit point (in a Bub1 dependent or independent manner, as indicated below). There is the probability of a redundant parallel pathway (Protein X in Figure 46) that is important to sense lack of tension during chromosome segregation. This pathway could be associated with the Ipl1 chromosome passenger complex. In the histone mutants, where there is reduced Sgo1 at the centromere, the alternate parallel pathway takes over the task of sensing proper tension among sister chromatids. Both pathways are necessary for sensing bipolar tension among sister chromatids, and one is not sufficient to overcome the severe defects caused by the histone mutations. Sgo1 is not essential, but may improve the tension-sensing checkpoint of the cell cycle.

Bub1 kinase, which is proposed to engage Sgo1, has a mild or no effect on the mutants. Correct nucleosome structure at the DNA entry/exit point must be necessary to transfer the signal between Bub1 activity and Sgo1 function. Further work can be done to understand the exact role of Bub1 in this process. Bub1, a non-essential protein kinase, not only phosphorylate H2A S121 and signals Sgo1 to the pericentromere, but it is also a component of the spindle-assembly

checkpoint protein complex. Assuming H2A S121 phosphorylation is the only signal that brings Sgo1 to the pericentromere, a mutation of H2A S121A will mimic loss of phosphorylation by Bub1, keeping its other checkpoint function intact, and interfering only with the Sgo1 function at the pericentromere. This mutation introduced in the mutants H3K42A/Q, H3G44A, or H4K44Q will help us to further understand the sequence of events between Bub1 phosphorylation on H2A S121 and Sgo1 positioning in the chromosome.

There is a great deal of debate on the activity of Sgo1 and Ipl1, or in a broader sense the chromosome passenger protein complex. Ipl1 is an essential protein while Sgo1 is not. What would happen when we make a temperature sensitive allele of Ipl1, or a kinase-dead mutant, in the strains that have problems with Sgo1 function like the H3K42A/Q, H3G44A, and H4K44Q mutants? Can Ipl1 and Sgo1 substitute for each other's function? Non-essential Sgo1 becomes essential when the Ipl1 activity is greatly reduced? The answers to these questions will help our understanding of many functions required for proper cell cycle and chromosome segregation.

In the future, we can extend this work to understanding more complex cell cycle proteins in humans. Aneuploidy, polyploidy, and tumorigenesis are closely related in terms of their appearance and cell response [126, 127]. Moreover, many of the cell cycle regulatory proteins like Ipl1/Aurora kinase and HDAC (Histone deacetylase) are currently been researched as potential targets for anticancer drug development [128, 129]. This study can be continued to reveal the mechanism of action of many of these different cell cycle proteins in both normal and tumor cells.

VI. REFERENCES

1. Pinto, I. and F. Winston, *Histone H2A is required for normal centromere function in Saccharomyces cerevisiae*. The EMBO journal, 2000. **19**(7): p. 1598-612.
2. Goffeau, A., et al., *Life with 6000 genes*. Science, 1996. **274**(5287): p. 546, 563-7.
3. Sherman, F., *Getting started with yeast*. Methods in enzymology, 2002. **350**: p. 3-41.
4. Hartwell, L., *Genetics : from genes to genomes*2000, Boston: McGraw-Hill. xxiii, 813 p.
5. Sherr, C.J., *Cancer cell cycles*. Science, 1996. **274**(5293): p. 1672-7.
6. Nasmyth, K., *At the heart of the budding yeast cell cycle*. Trends in genetics : TIG, 1996. **12**(10): p. 405-12.
7. Luger, K., et al., *Crystal structure of the nucleosome core particle at 2.8 Å resolution*. Nature, 1997. **389**(6648): p. 251-60.
8. Luger, K. and T.J. Richmond, *The histone tails of the nucleosome*. Current opinion in genetics & development, 1998. **8**(2): p. 140-6.
9. Henry, K.W. and S.L. Berger, *Trans-tail histone modifications: wedge or bridge?* Nature structural biology, 2002. **9**(8): p. 565-6.
10. White, C.L., R.K. Suto, and K. Luger, *Structure of the yeast nucleosome core particle reveals fundamental changes in internucleosome interactions*. The EMBO journal, 2001. **20**(18): p. 5207-18.
11. Thoma, F., T. Koller, and A. Klug, *Involvement of histone H1 in the organization of the nucleosome and of the salt-dependent superstructures of chromatin*. The Journal of cell biology, 1979. **83**(2 Pt 1): p. 403-27.
12. Eriksson, P.R., et al., *Regulation of histone gene expression in budding yeast*. Genetics, 2012. **191**(1): p. 7-20.
13. Griffiths, A.J.F., *An Introduction to genetic analysis*. 5th ed1993, New York: W.H. Freeman. xi, 840 p.

14. Millar, C.B. and M. Grunstein, *Genome-wide patterns of histone modifications in yeast*. Nature reviews. Molecular cell biology, 2006. **7**(9): p. 657-66.
15. Grunstein, M., *Histone acetylation in chromatin structure and transcription*. Nature, 1997. **389**(6649): p. 349-52.
16. Shahbazian, M.D. and M. Grunstein, *Functions of site-specific histone acetylation and deacetylation*. Annual review of biochemistry, 2007. **76**: p. 75-100.
17. Oppikofer, M., et al., *A dual role of H4K16 acetylation in the establishment of yeast silent chromatin*. The EMBO journal, 2011. **30**(13): p. 2610-21.
18. Cimini, D., et al., *Histone hyperacetylation in mitosis prevents sister chromatid separation and produces chromosome segregation defects*. Molecular biology of the cell, 2003. **14**(9): p. 3821-33.
19. Kanta, H., et al., *Suppressor analysis of a histone defect identifies a new function for the hda1 complex in chromosome segregation*. Genetics, 2006. **173**(1): p. 435-50.
20. Nome, R.V., et al., *Cell cycle checkpoint signaling involved in histone deacetylase inhibition and radiation-induced cell death*. Molecular cancer therapeutics, 2005. **4**(8): p. 1231-8.
21. Lee, E.J., et al., *Histone deacetylase inhibitor scriptaid induces cell cycle arrest and epigenetic change in colon cancer cells*. International journal of oncology, 2008. **33**(4): p. 767-76.
22. Kim, Y.B., et al., *Mechanism of cell cycle arrest caused by histone deacetylase inhibitors in human carcinoma cells*. The Journal of antibiotics, 2000. **53**(10): p. 1191-200.
23. Cheung, P., C.D. Allis, and P. Sassone-Corsi, *Signaling to chromatin through histone modifications*. Cell, 2000. **103**(2): p. 263-71.
24. Strahl, B.D. and C.D. Allis, *The language of covalent histone modifications*. Nature, 2000. **403**(6765): p. 41-5.
25. Wei, Y., et al., *Phosphorylation of histone H3 is required for proper chromosome condensation and segregation*. Cell, 1999. **97**(1): p. 99-109.

26. Fischle, W., et al., *Regulation of HP1-chromatin binding by histone H3 methylation and phosphorylation*. Nature, 2005. **438**(7071): p. 1116-22.
27. Kelly, A.E., et al., *Survivin reads phosphorylated histone H3 threonine 3 to activate the mitotic kinase Aurora B*. Science, 2010. **330**(6001): p. 235-9.
28. Kawashima, S.A., et al., *Phosphorylation of H2A by Bub1 prevents chromosomal instability through localizing shugoshin*. Science, 2010. **327**(5962): p. 172-7.
29. Hsu, J.Y., et al., *Mitotic phosphorylation of histone H3 is governed by Ipl1/aurora kinase and Glc7/PP1 phosphatase in budding yeast and nematodes*. Cell, 2000. **102**(3): p. 279-91.
30. Nowak, S.J. and V.G. Corces, *Phosphorylation of histone H3: a balancing act between chromosome condensation and transcriptional activation*. Trends in genetics : TIG, 2004. **20**(4): p. 214-20.
31. Wang, F. and J.M. Higgins, *Histone modifications and mitosis: countermarks, landmarks, and bookmarks*. Trends in cell biology, 2012.
32. Rice, J.C. and C.D. Allis, *Histone methylation versus histone acetylation: new insights into epigenetic regulation*. Current opinion in cell biology, 2001. **13**(3): p. 263-73.
33. Rice, J.C., et al., *Mitotic-specific methylation of histone H4 Lys 20 follows increased PR-Set7 expression and its localization to mitotic chromosomes*. Genes & development, 2002. **16**(17): p. 2225-30.
34. Rea, S., et al., *Regulation of chromatin structure by site-specific histone H3 methyltransferases*. Nature, 2000. **406**(6796): p. 593-9.
35. Heit, R., et al., *G2 histone methylation is required for the proper segregation of chromosomes*. Journal of cell science, 2009. **122**(Pt 16): p. 2957-68.
36. Sims, R.J., 3rd, K. Nishioka, and D. Reinberg, *Histone lysine methylation: a signature for chromatin function*. Trends in genetics : TIG, 2003. **19**(11): p. 629-39.
37. Santos-Rosa, H., et al., *Active genes are tri-methylated at K4 of histone H3*. Nature, 2002. **419**(6905): p. 407-11.

38. Botuyan, M.V., et al., *Structural basis for the methylation state-specific recognition of histone H4-K20 by 53BP1 and Crb2 in DNA repair*. Cell, 2006. **127**(7): p. 1361-73.
39. Fang, J., et al., *The Saccharomyces cerevisiae histone demethylase Jhd1 fine-tunes the distribution of H3K36me2*. Molecular and cellular biology, 2007. **27**(13): p. 5055-65.
40. Mosammamarast, N. and Y. Shi, *Reversal of histone methylation: biochemical and molecular mechanisms of histone demethylases*. Annual review of biochemistry, 2010. **79**: p. 155-79.
41. Cloos, P.A., et al., *Erasing the methyl mark: histone demethylases at the center of cellular differentiation and disease*. Genes & development, 2008. **22**(9): p. 1115-40.
42. Tu, S., et al., *Identification of histone demethylases in Saccharomyces cerevisiae*. The Journal of biological chemistry, 2007. **282**(19): p. 14262-71.
43. Varier, R.A. and H.T. Timmers, *Histone lysine methylation and demethylation pathways in cancer*. Biochimica et biophysica acta, 2011. **1815**(1): p. 75-89.
44. Rotili, D. and A. Mai, *Targeting Histone Demethylases: A New Avenue for the Fight against Cancer*. Genes & cancer, 2011. **2**(6): p. 663-79.
45. Zhang, Y., *Transcriptional regulation by histone ubiquitination and deubiquitination*. Genes & development, 2003. **17**(22): p. 2733-40.
46. Kouzarides, T., *Chromatin modifications and their function*. Cell, 2007. **128**(4): p. 693-705.
47. Shiiio, Y. and R.N. Eisenman, *Histone sumoylation is associated with transcriptional repression*. Proceedings of the National Academy of Sciences of the United States of America, 2003. **100**(23): p. 13225-30.
48. Nathan, D., et al., *Histone sumoylation is a negative regulator in Saccharomyces cerevisiae and shows dynamic interplay with positive-acting histone modifications*. Genes & development, 2006. **20**(8): p. 966-76.

49. Boulikas, T., *DNA strand breaks alter histone ADP-ribosylation*. Proceedings of the National Academy of Sciences of the United States of America, 1989. **86**(10): p. 3499-503.
50. Martinez-Zamudio, R. and H.C. Ha, *Histone ADP-ribosylation facilitates gene transcription by directly remodeling nucleosomes*. Molecular and cellular biology, 2012. **32**(13): p. 2490-502.
51. Realini, C.A. and F.R. Althaus, *Histone shuttling by poly(ADP-ribosylation)*. The Journal of biological chemistry, 1992. **267**(26): p. 18858-65.
52. Nelson, C.J., H. Santos-Rosa, and T. Kouzarides, *Proline isomerization of histone H3 regulates lysine methylation and gene expression*. Cell, 2006. **126**(5): p. 905-16.
53. Tan, M., et al., *Identification of 67 histone marks and histone lysine crotonylation as a new type of histone modification*. Cell, 2011. **146**(6): p. 1016-28.
54. *Monographs editors: j. Alan diehl, dale s. Haines, and serge y. Fuchs*. Genes & cancer, 2010. **1**(7): p. 677-8.
55. Peterson, C.L. and M.A. Laniel, *Histones and histone modifications*. Current biology : CB, 2004. **14**(14): p. R546-51.
56. Zhang, K., et al., *A mass spectrometric "Western blot" to evaluate the correlations between histone methylation and histone acetylation*. Proteomics, 2004. **4**(12): p. 3765-75.
57. Czermin, B. and A. Imhof, *The sounds of silence--histone deacetylation meets histone methylation*. Genetica, 2003. **117**(2-3): p. 159-64.
58. Latham, J.A. and S.Y. Dent, *Cross-regulation of histone modifications*. Nature structural & molecular biology, 2007. **14**(11): p. 1017-24.
59. Zhang, K., et al., *The Set1 methyltransferase opposes Ipl1 aurora kinase functions in chromosome segregation*. Cell, 2005. **122**(5): p. 723-34.
60. Williamson, W.D. and I. Pinto, *Histones and genome integrity*. Frontiers in bioscience, 2012. **17**: p. 984-95.

61. Verdaasdonk, J.S. and K. Bloom, *Centromeres: unique chromatin structures that drive chromosome segregation*. Nature reviews. Molecular cell biology, 2011. **12**(5): p. 320-32.
62. Stimpson, K.M. and B.A. Sullivan, *Histone H3K4 methylation keeps centromeres open for business*. The EMBO journal, 2011. **30**(2): p. 233-4.
63. Sullivan, B.A. and G.H. Karpen, *Centromeric chromatin exhibits a histone modification pattern that is distinct from both euchromatin and heterochromatin*. Nature structural & molecular biology, 2004. **11**(11): p. 1076-83.
64. Mellone, B.G., et al., *Centromere silencing and function in fission yeast is governed by the amino terminus of histone H3*. Current biology : CB, 2003. **13**(20): p. 1748-57.
65. Biggins, S., *The composition, functions, and regulation of the budding yeast kinetochore*. Genetics, 2013. **194**(4): p. 817-46.
66. Herskowitz, I., *Life cycle of the budding yeast Saccharomyces cerevisiae*. Microbiological reviews, 1988. **52**(4): p. 536-53.
67. Westermann, S., D.G. Drubin, and G. Barnes, *Structures and functions of yeast kinetochore complexes*. Annual review of biochemistry, 2007. **76**: p. 563-91.
68. Wood, A. and A. Shilatifard, *Guided by COMPASS on a journey through chromosome segregation*. Nature structural & molecular biology, 2005. **12**(10): p. 839-40.
69. Pinsky, B.A., et al., *An Mtw1 complex promotes kinetochore biorientation that is monitored by the Ipl1/Aurora protein kinase*. Developmental cell, 2003. **5**(5): p. 735-45.
70. Lew, D.J. and D.J. Burke, *The spindle assembly and spindle position checkpoints*. Annual review of genetics, 2003. **37**: p. 251-82.
71. Wasch, R. and D. Engelbert, *Anaphase-promoting complex-dependent proteolysis of cell cycle regulators and genomic instability of cancer cells*. Oncogene, 2005. **24**(1): p. 1-10.
72. Palframan, W.J., et al., *Anaphase inactivation of the spindle checkpoint*. Science, 2006. **313**(5787): p. 680-4.

73. Vanoosthuyse, V. and K.G. Hardwick, *Overcoming inhibition in the spindle checkpoint*. Genes & development, 2009. **23**(24): p. 2799-805.
74. Musacchio, A. and K.G. Hardwick, *The spindle checkpoint: structural insights into dynamic signalling*. Nature reviews. Molecular cell biology, 2002. **3**(10): p. 731-41.
75. May, K.M. and K.G. Hardwick, *The spindle checkpoint*. Journal of cell science, 2006. **119**(Pt 20): p. 4139-42.
76. Hardwick, K.G. and J.V. Shah, *Spindle checkpoint silencing: ensuring rapid and concerted anaphase onset*. F1000 biology reports, 2010. **2**: p. 55.
77. Pinsky, B.A., et al., *The Ipl1-Aurora protein kinase activates the spindle checkpoint by creating unattached kinetochores*. Nature cell biology, 2006. **8**(1): p. 78-83.
78. Ruchaud, S., M. Carmena, and W.C. Earnshaw, *Chromosomal passengers: conducting cell division*. Nature reviews. Molecular cell biology, 2007. **8**(10): p. 798-812.
79. Kiburz, B.M., A. Amon, and A.L. Marston, *Shugoshin promotes sister kinetochore biorientation in Saccharomyces cerevisiae*. Molecular biology of the cell, 2008. **19**(3): p. 1199-209.
80. Indjeian, V.B., B.M. Stern, and A.W. Murray, *The centromeric protein Sgo1 is required to sense lack of tension on mitotic chromosomes*. Science, 2005. **307**(5706): p. 130-3.
81. Fernius, J. and K.G. Hardwick, *Bub1 kinase targets Sgo1 to ensure efficient chromosome biorientation in budding yeast mitosis*. PLoS genetics, 2007. **3**(11): p. e213.
82. Haase, J., et al., *Bub1 kinase and Sgo1 modulate pericentric chromatin in response to altered microtubule dynamics*. Current biology : CB, 2012. **22**(6): p. 471-81.
83. Kawashima, S.A., et al., *Shugoshin enables tension-generating attachment of kinetochores by loading Aurora to centromeres*. Genes & development, 2007. **21**(4): p. 420-35.
84. Storchova, Z., et al., *Bub1, Sgo1, and Mps1 mediate a distinct pathway for chromosome biorientation in budding yeast*. Molecular biology of the cell, 2011. **22**(9): p. 1473-85.

85. Winston, F., C. Dollard, and S.L. RicuperoHovasse, *Construction of a Set of Convenient Saccharomyces-Cerevisiae Strains That Are Isogenic to S288c*. *Yeast*, 1995. **11**(1): p. 53-55.
86. C. Guthrie and G. Fink, E., ed. *Guide to Yeast Genetics and Molecular and Cell Biology*. *Methods of Enzymology*. Vol. 350 and 351 2001, Academic Press.
87. C. Guthrie and G. Fink, E., ed. *Guide to Yeast Genetics and Molecular Biology*. *Methods in enzymology*. Vol. 194. 1991, Academic Press.
88. Gietz, R.D., et al., *Studies on the transformation of intact yeast cells by the LiAc/SS-DNA/PEG procedure*. *Yeast*, 1995. **11**(4): p. 355-60.
89. Chen, D.C., B.C. Yang, and T.T. Kuo, *One-step transformation of yeast in stationary phase*. *Current genetics*, 1992. **21**(1): p. 83-4.
90. Longtine, M.S., et al., *Additional modules for versatile and economical PCR-based gene deletion and modification in Saccharomyces cerevisiae*. *Yeast*, 1998. **14**(10): p. 953-61.
91. Rose, M.D., Winston, F., and Hieter, P., *Methods in Yeast Genetics, A Laboratory Course Manual*. 1990.
92. Chattoo, B.B., et al., *Patterns of Genetic and Phenotypic Suppression of lys2 Mutations in the Yeast SACCHAROMYCES CEREVISIAE*. *Genetics*, 1979. **93**(1): p. 67-79.
93. Ausubel, F.M., R. Brent, R.E. Kingston, D.D. Moore, J.G. Seidman, J.A. Smith, and K. Struhl ed. *Current Protocols in Molecular Biology* 1987.
94. Sikorski, R.S. and P. Hieter, *A system of shuttle vectors and yeast host strains designed for efficient manipulation of DNA in Saccharomyces cerevisiae*. *Genetics*, 1989. **122**(1): p. 19-27.
95. Birnboim, H.C. and J. Doly, *A rapid alkaline extraction procedure for screening recombinant plasmid DNA*. *Nucleic acids research*, 1979. **7**(6): p. 1513-23.
96. Dai, J., et al., *Probing nucleosome function: a highly versatile library of synthetic histone H3 and H4 mutants*. *Cell*, 2008. **134**(6): p. 1066-78.

97. Gietz, R.D. and R.A. Woods, *Yeast transformation by the LiAc/SS Carrier DNA/PEG method*. *Methods in molecular biology*, 2006. **313**: p. 107-20.
98. Schild, D., H.N. Ananthaswamy, and R.K. Mortimer, *An endomitotic effect of a cell cycle mutation of *Saccharomyces cerevisiae**. *Genetics*, 1981. **97**(3-4): p. 551-62.
99. Ahmad, M. and H. Bussey, *Yeast arginine permease: nucleotide sequence of the CAN1 gene*. *Current genetics*, 1986. **10**(8): p. 587-92.
100. Chan, C.S. and D. Botstein, *Isolation and characterization of chromosome-gain and increase-in-ploidy mutants in yeast*. *Genetics*, 1993. **135**(3): p. 677-91.
101. Horvath, A. and H. Riezman, *Rapid protein extraction from *Saccharomyces cerevisiae**. *Yeast*, 1994. **10**(10): p. 1305-10.
102. Gupta, K., et al., *Antimitotic antifungal compound benomyl inhibits brain microtubule polymerization and dynamics and cancer cell proliferation at mitosis, by binding to a novel site in tubulin*. *Biochemistry*, 2004. **43**(21): p. 6645-55.
103. Stearns, T., M.A. Hoyt, and D. Botstein, *Yeast mutants sensitive to antimicrotubule drugs define three genes that affect microtubule function*. *Genetics*, 1990. **124**(2): p. 251-62.
104. Zala, C., D. Rouleau, and J.S. Montaner, *Role of hydroxyurea in treatment of disease due to human immunodeficiency virus infection*. *Clinical infectious diseases : an official publication of the Infectious Diseases Society of America*, 2000. **30 Suppl 2**: p. S143-50.
105. Rando, O.J. and F. Winston, *Chromatin and transcription in yeast*. *Genetics*, 2012. **190**(2): p. 351-87.
106. Li, Y., et al., *The target of the NSD family of histone lysine methyltransferases depends on the nature of the substrate*. *The Journal of biological chemistry*, 2009. **284**(49): p. 34283-95.
107. Du, H.N. and S.D. Briggs, *A nucleosome surface formed by histone H4, H2A, and H3 residues is needed for proper histone H3 Lys36 methylation, histone acetylation, and repression of cryptic transcription*. *The Journal of biological chemistry*, 2010. **285**(15): p. 11704-13.

108. Luo, J., et al., *Histone h3 exerts a key function in mitotic checkpoint control*. Molecular and cellular biology, 2010. **30**(2): p. 537-49.
109. Kim, J.H., J.S. Kang, and C.S. Chan, *Sli15 associates with the ipl1 protein kinase to promote proper chromosome segregation in Saccharomyces cerevisiae*. The Journal of cell biology, 1999. **145**(7): p. 1381-94.
110. Biggins, S. and A.W. Murray, *The budding yeast protein kinase Ipl1/Aurora allows the absence of tension to activate the spindle checkpoint*. Genes & development, 2001. **15**(23): p. 3118-29.
111. Maruyama, T., et al., *Histone H2B mutations in inner region affect ubiquitination, centromere function, silencing and chromosome segregation*. The EMBO journal, 2006. **25**(11): p. 2420-31.
112. Manohar, M., et al., *Acetylation of histone H3 at the nucleosome dyad alters DNA-histone binding*. The Journal of biological chemistry, 2009. **284**(35): p. 23312-21.
113. Schneider, J., et al., *Rtt109 is required for proper H3K56 acetylation: a chromatin mark associated with the elongating RNA polymerase II*. The Journal of biological chemistry, 2006. **281**(49): p. 37270-4.
114. Clemente-Ruiz, M., R. Gonzalez-Prieto, and F. Prado, *Histone H3K56 acetylation, CAF1, and Rtt106 coordinate nucleosome assembly and stability of advancing replication forks*. PLoS genetics, 2011. **7**(11): p. e1002376.
115. Tinker-Kulberg, R.L. and D.O. Morgan, *Pds1 and Esp1 control both anaphase and mitotic exit in normal cells and after DNA damage*. Genes & development, 1999. **13**(15): p. 1936-49.
116. Hartwell, L.H., J. Culotti, and B. Reid, *Genetic control of the cell-division cycle in yeast. I. Detection of mutants*. Proceedings of the National Academy of Sciences of the United States of America, 1970. **66**(2): p. 352-9.
117. Kawashima, S., et al., *Global analysis of core histones reveals nucleosomal surfaces required for chromosome bi-orientation*. The EMBO journal, 2011. **30**(16): p. 3353-67.
118. Sandall, S., et al., *A Bir1-Sli15 complex connects centromeres to microtubules and is required to sense kinetochore tension*. Cell, 2006. **127**(6): p. 1179-91.

119. Iwasaki, W., et al., *Comprehensive structural analysis of mutant nucleosomes containing lysine to glutamine (KQ) substitutions in the H3 and H4 histone-fold domains*. *Biochemistry*, 2011. **50**(36): p. 7822-32.
120. Hyland, E.M., et al., *An evolutionarily 'young' lysine residue in histone H3 attenuates transcriptional output in Saccharomyces cerevisiae*. *Genes & development*, 2011. **25**(12): p. 1306-19.
121. Casadio, F., et al., *H3R42me2a is a histone modification with positive transcriptional effects*. *Proceedings of the National Academy of Sciences of the United States of America*, 2013. **110**(37): p. 14894-9.
122. Wang, X. and J.J. Hayes, *Acetylation mimics within individual core histone tail domains indicate distinct roles in regulating the stability of higher-order chromatin structure*. *Molecular and cellular biology*, 2008. **28**(1): p. 227-36.
123. Du, H.N., I.M. Fingerman, and S.D. Briggs, *Histone H3 K36 methylation is mediated by a trans-histone methylation pathway involving an interaction between Set2 and histone H4*. *Genes & development*, 2008. **22**(20): p. 2786-98.
124. Yu, Y., et al., *A conserved patch near the C terminus of histone H4 is required for genome stability in budding yeast*. *Molecular and cellular biology*, 2011. **31**(11): p. 2311-25.
125. Santisteban, M.S., T. Kalashnikova, and M.M. Smith, *Histone H2A.Z regulates transcription and is partially redundant with nucleosome remodeling complexes*. *Cell*, 2000. **103**(3): p. 411-22.
126. Storchova, Z. and C. Kuffer, *The consequences of tetraploidy and aneuploidy*. *Journal of cell science*, 2008. **121**(Pt 23): p. 3859-66.
127. Fu, J., et al., *Roles of Aurora kinases in mitosis and tumorigenesis*. *Molecular cancer research : MCR*, 2007. **5**(1): p. 1-10.
128. Keen, N. and S. Taylor, *Aurora-kinase inhibitors as anticancer agents*. *Nature reviews. Cancer*, 2004. **4**(12): p. 927-36.
129. Shapiro, G.I. and J.W. Harper, *Anticancer drug targets: cell cycle and checkpoint control*. *The Journal of clinical investigation*, 1999. **104**(12): p. 1645-53.